2007

Robust and Decentralized Control of Web Winding Systems

Wankun Zhou
Cleveland State University

Robust and Decentralized Control of Web Winding Systems

WANKUN ZHOU

Bachelor of Science in Material Science and Engineering

Harbin Institute of Technology

July, 1995

Master of Science in Electrical Engineering

Gansu University of Technology

July, 1998

submitted in partial fulfillment of the requirements for the degree

DOCTOR OF ENGINEERING

at the

CLEVELAND STATE UNIVERSITY

November 2007

This thesis has been approved for the

Department of **ELECTRICAL AND COMPUTER ENGINEERING**

and the College of Graduate Studies by

Thesis Committee Chairperson, Dr. Zhiqiang Gao

Department/Date

Dr. Sally Shao

Department/Date

Dr. Dan Simon

Department/Date

Dr. Hanz Richter

Department/Date

Dr. Lili Dong

Department/Date

To my parents, and my wife...

ACKNOWLEDGMENTS

I wish to express my sincerest appreciation to my advisor Dr. Zhiqiang Gao for his intelligent supervision, constructive guidance, inspiration, and friendship.

I would like to extend my warmest thanks to my committee members: Dr. Sally Shao, Dr. Dan Simon, Dr. Hanz Richter, and Dr. Lili Dong for their time in reviewing and evaluating this dissertation.

There are a number of people I would like to acknowledge in connection with the successful completion of this work. I thank all the lab members who shared time, space, and lore with me at CACT. In particular, I thank Qing Zheng, Gang Tian, Jeffrey Csank, Aaron Radke, Robert Miklosovic and Frank J. Goforth. It is they who made my graduate days wonderful and enjoyable.

Lastly, but by no means least, my heartfelt appreciation and gratitude goes to my family, especially my wife, for their "time-invariant" support, encouragement, and patience.

Robust and Decentralized Control of Web Winding Systems

WANKUN ZHOU

ABSTRACT

This research addresses the velocity and tension regulation problems in web handling, including those found in the single element of an accumulator and those in the large-scale system settings. A continuous web winding system is a complex large-scale interconnected dynamics system with numerous tension zones to transport the web while processing it. A major challenge in controlling such systems is the unexpected disturbances that propagate through the system and affect both tension and velocity loops along the way. To solve this problem, a unique active disturbance rejection control (ADRC) strategy is proposed. Simulation results show remarkable disturbance rejection capability of the proposed control scheme in coping with large dynamic variations commonly seen in web winding systems. Another complication in web winding system stems from its large-scale and interconnected dynamics which makes control design difficult. This motivates the research in formulating a novel robust decentralized control strategy. The key idea in the proposed approach is that nonlinearities and interactions between adjunct subsystems are regarded as perturbations, to be estimated by an augmented state observer and rejected in the control loop, therefore making the local control design extremely simple. The proposed decentralized control strategy was implemented on a 3-tension-zone web winding processing

line. Simulation results show that the proposed control method leads to much better tension and velocity regulation quality than the existing controller common in industry. Finally, this research tackles the challenging problem of stability analysis. Although ADRC has demonstrated the validity and advantage in many applications, the rigorous stability study has not been fully addressed previously. To this end, stability characterization of ADRC is carried out in this work. The closed-loop system is first reformulated, resulting in a form that allows the application of the well-established singular perturbation method. Based on the decomposed subsystems by singular perturbation, the composite Lyapunov function method is used to determine the condition for exponential stability of the closed-loop system.

TABLE OF CONTENTS

LIST OF TABLES

LIST OF FIGURES

ACRONYM

ADRC Active Disturbance Rejection Control

PWM Pulse Width Modulation

MIMO Multi-input Multi-output

SISO Single-input Single-output

FLC Fuzzy Logic Controller

NN Neural Network

LQG Linear Quadratic Gaussian

NTV Nonlinear and time-varying

IMC Internal Model Control

DoB Disturbance Observer

PoB Perturbation Observer

UIO Unknown Input Observer

IMP Internal Model Principle

LTI Linear Time Variant

CHAPTER I

INTRODUCTION

In the material processing industry, long flexible sheets are usually described as web. More precisely, web refers to any object which is very long compared to its width, and very wide compared to its thickness. Many types of material are manufactured or processed in web form such as paper, plastic film, cloth fabrics, and even strip steel [2]. To produce an end product from a raw web material, web converting and web handling are the two major processes that are involved. Web converting [5] involves all those processes which are required to modify the physical properties of the web material such as coating, slitting, drying, and embossing, etc. while the web handling [6] processes consist of those processes that are associated with the web transportation.

This chapter will introduce the basic concept of web winding systems, the motivation behind this research, and finally the outline of the dissertation.

1.1 Background

Web winding systems are common in the manufacture, fabrication, and transport of any materials such as paper, metal, and photographic film. A continuous web processing line is a large-scale, complex interconnected dynamic system with numerous tension zones to transport the web while processing it. A continuous web processing line is also a multi-span web transporting system which consists of a combination of some basic mechanical/electrical elements, such as unwinder, rewinder, roller, free web span, measuring sensors, and driving motors.

A prototype web winding system is shown in Figure 1. This system consists of an unwinding roll which releases the web material, a nip roller which regulates the velocity of the web, a winding roll which rewinds the released material, and some transporting rolls which transmit the web material. These rolls are driven independently by DC or AC servo motors with their torques regulated. Between the nip roller and the rewinder/unwinder, there are a number of idle rolls which help form a desired web path and the contact rolls which push the web against the transport roll.

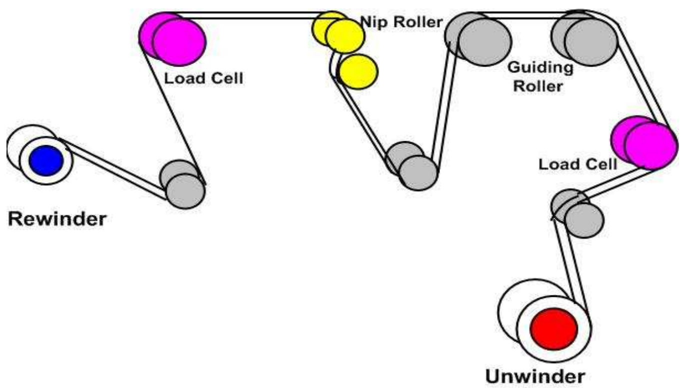

Figure 1: A prototype multi-span web transporting system

The roller in this web winding system is worthy of mention. Rollers are essential parts of a web handling machine. In any web handling system, there are two types of rollers: 1) externally torque driven rollers such as the unwinder, rewinder and the nip roller; and 2) the web driven rollers (idlers). These devices are also called "transport rollers" in industry because they are not intended to change the physical properties of the web. The traditional role of a "nipped roller" is to step the tension up or down between sections of processes and, hence, create different tension zones for different processes. In designing a controller for a web system, the nipped roller torque input and the wound roller torque inputs (rewinder and unwinder) provide multiple inputs for multivariable tension/speed control. In the control system design, these torque inputs are usually regulated by Pulse Width Modulation (PWM) drives. The torque outputs from the PWM drives can be either positive or negative and, hence, can either act as "drives" or "brakes" in web tension control. The tensions of the web system are measured by load cells. To provide real-time monitoring of time varying information such as inertia of the unwinder and rewinder, there are also diameter sensors which measure the changing diameters of the unwinder and rewinder.

The main purpose of the web handling process is to transport web with maximum throughput (speed) and with minimum damage. To achieve this, web tension control is crucial for the following reasons:

1) Web tension affects the geometry of the web, such as the apparent length and width of the web.

2) Web tension control helps reduce wrinkling. In particular, high process tension will help decrease the wrinkling caused by a misalignment of rollers. However, excessively high tension will cause more wrinkling to occur on very thin materials. Hence, appropriate web tension control is very important.

3) Web tension affects the wound-in tension and the shape of the final product roll and, hence, the roll quality.

For these reasons, it is essential in web winding systems to control the web tension at a desired value as closely as possible.

A continuous web winding system is a large-scale, complex interconnected dynamic system with numerous tension zones to transport the web while processing it. There are two control schemes for large-scale system control: the centralized scheme and the decentralized scheme. Centralized control is the traditional control method, which considers all the information about the system to be a single dynamic model and design a control system for this model. Since the system is a Multi-input Multi-output (MIMO) system, modern multivariable control theory seems to be a natural fit. However, when the dimensions of the system becomes larger, it is not practical to implement the high order controllers obtained by multivariable control. Decentralized control strategy is commonly used, because the whole system consists of many subsystems, such as driven rolls and idle rollers. The controller is designed for each subsystem, which removes the complexity of designing MIMO controllers. However, the interactions among the input signals should be estimated sufficiently to assure appropriate stability and performance of the decentralized control system.

1.2 Motivation

The ever-increasing demands on quality and efficiency in industry motivate researchers and engineers alike to explore better methods for tension and velocity control. However, the tension control problem is challenging because of the highly nonlinear dynamics and external disturbance of the system. If tension variations occur, they will result in degradation of product quality or even rupture of the material. Therefore, in order to have a high quality product and to reduce cost, it is very important to monitor and control the tension within the desired range.

Advances in web-winding system control might improve these situations in a number of ways, such as increasing transient performance or reliability, and facilitating tighter tracking of the desired velocity and tension. More advanced control schemes may also reduce costs. For instance, robust control techniques diminish the need for lengthy and costly "tuning" of controllers or expensive, highly specified hardware components. Finally, observer-based control may allow costly and complicated tension sensors to be eliminated from some systems.

Most control schemes presented in the literature aim to maneuver the system via feedback control, possibly accounting for some of the uncertainties and disturbances. All of them rely on the availability of velocity and tension measurements. A control system is described in [16], which addresses only the LTI system model and does not account for changing roller radii, friction, or any other disturbances. Other gain-scheduled or H_∞ controllers form most of the rest of the web winding system control literature [28, 29, 30, 31]. These schemes are shown to be stable at a range of steady-state operating points. However, the system cannot be assumed to be in steady-state during many maneuvers, especially when attempting to rapidly change the roller velocities. The stability of these controllers has yet to be established analytically for the whole nonlinear system (i.e., where the roller radii and moments are dynamic variables). Furthermore, gain-scheduled linear controllers have the potential disadvantage of being costly and time-consuming to tune [30]. Finally, while these schemes have proven workable in experiment and practice, a nonlinear control strategy may offer advantages in performance, intuitive clarity, and the tractability of stability analysis. It may also help reduce component and development costs and facilitate new observer-based schemes that eliminate the need for costly sensors.

Therefore, one of the purposes of this research is to implement and compare these control design methods in order to find a better control algorithm that will be used in practical applications.

Another complication in web winding control stems from its strong coupling caused by large-scale interconnected nature. Centralized control is the traditional control method, which considers all the segments and interconnections to be a single dynamic system. Since the system is a MIMO system, multivariable controllers were the reasonable choices. In multivariable industrial controller design, three approaches can be taken: 1) assume the system consists of a set of Single-input Single-output (SISO) control loops and design each control loop independently of the others using SISO methods; 2) define a mathematical model of the system using either analytical or identification methods, and then apply any of the well-known multivariable controller synthesis methods to design a multivariable controller for the system; 3) apply some type of multivariable tuning controller design. In the case of 1), this approach has the advantage of simplicity and is often used, but the disadvantage is that the resulting performance may be poor due to ignored interaction effects. In the case of 2), the main disadvantage of the method is in the effort required in the construction of a suitable mathematical model of the system, or in the difficulty in carrying out identification experiments, and in the fact that there is no guarantee that the resultant model obtained is “sufficiently accurate” for controller design. In the case of 3), when the dimension of the system becomes much larger, the tuning process becomes troublesome, and it also requires carrying out steady-state experiments on the system.

Recently, many research results have been applied to large scale decentralized control strategies to this specific problem. We have seen some research towards this direction, such as work by Pagilla [125, 126] and Knittel [84, 92]. By far, the most common control strategy used in web winding systems is the decentralized proportional-integral (PI) control scheme. Although decentralized PI control is easier, the wide variation of web winding systems requires extensive tuning by an experienced control engineer to obtain acceptable performance. Furthermore, controllers rarely remain well tuned in the process industry and require multiple tuning sessions. The tuning rules should be easier to understand by less experienced technicians who then can perform the procedure. Another purpose of this research is to find a stable decentralized control strategy that is easy for utilization in industry.

1.3 Summary

This dissertation is organized as follows: Background on web winding systems and motivation are introduced in Chapter 1. Chapter 2 presents general models of rollers and free web span separately in a typical web winding system. They are then combined to give a description of a complete coupled web winding system. Literature review of existing techniques on web tension control and decentralized control are given in Chapter 3. Chapter 4 reviews different disturbance rejection techniques and introduces a new control paradigm - Active Disturbance Rejection Control (ADRC), which is chosen to be the disturbance rejection control strategy applied throughout this dissertation. Chapter 5 presents a robust tension/velocity feedback controller that accounts for uncertainties and changing variables in the model. Simulation results are used to illustrate advantages over the existing control schemes. Chapter 6 extends the idea of ADRC to the decentralized control framework. It presents the design technique for large-scale web winding system using the proposed control methodologies. Stability analysis by singular perturbation theory is carried out in Chapter 7 to further validate the success of ADRC applications. Chapter 8 summarizes the contributions of this dissertation, and discusses some open problems that might allow for more advanced controls in the future.

CHAPTER II

DYNAMICS OF WEB WINDING SYSTEMS

This chapter first reviews mathematical tools and assumptions for modeling of web winding systems. Then mathematical models are derived for a free web span, a roller, and a web interacting with a roller. The model for each sub-component of a web winding system will be developed essentially following the development in [34] but with some change of variables. These component models are then combined, resulting in the model of the general web winding system.

2.1 Mathematical Tools and Assumptions

Web dynamics are governed by Newton's laws of motion. In the case of web winding systems, we are concerned with the dynamics properties in different regions of various free spans. Therefore, Newton's laws are rewritten to describe the dynamics of a region of free web spans. This procedure is known as control volume analysis and is described in textbooks [5, 6, 34]. Various models for the web tension in web winding systems are based on the following laws [28, 34]:

1. Hooke's law, which models the elasticity of the web.

2. Mass conservation law, which states that the rate of mass accumulation in a control volume, is equal to the sum of the net rate of the mass inflow into the control volume and the rate of mass generation within the control volume. It describes the cross coupling between web velocity and web strain.

In order to simplify the modeling procedures, the following assumptions are made to develop the dynamics of web winding systems:

- There is no web slippage;
- The web is perfectly elastic, which means that stress is linearly proportional to strain tension in all spans;
- The web is homogeneous, and all the physical properties of the web such as modulus of elasticity, density of the web are constant;
- The web material is isotropic, so that machine direction stress prevails;
- The dynamics of load cell and idle rollers are neglected, which means that the rotational inertia of all idler rolls equal to zero;
- The wound-in and wound-out tension of the web are zero;
- The gear ratio between motor and roll is one to one;
- The bearing friction remains constant and not changing with transporting velocity and other physical conditions of the web material.

2.2 Dynamics of a Web Processing System

A web winding system is built from the equations of web tension behavior between two consecutive rolls and the equations describing the velocity of each roll. Shin [33] established the concept of "preliminary element" to model a web processing system, which is the combination of preliminary elements, such as a free web span, various kinds of rollers and rolls, a web interacting with roller, etc. Therefore, to model a web winding system, we will first derive the mathematical model for these preliminary elements.

Since most important elements of a web processing system are the web span and the roller, we will begin by developing mathematical models of these elements and then develop a model for the overall system.

2.2.1 Dynamics of a Free Web Span

To obtain the differential equation that describes the variation of tension in open web span, the principle of conservation of mass is applied to the control volume defined by the web span between two successive rollers.

A strip of web under longitudinal stretch will experience strains in three dimensions (see Figure 2): machine direction (MD), cross direction (CD), and Z direction (ZD) as follows:

$$\varepsilon_x = \frac{L_s - L_0}{L_0} = \frac{\Delta L_0}{L_0} \tag{2.1}$$

$$\varepsilon_w = \frac{w_s - w_0}{w_0} = \frac{\Delta w_0}{w_0} \tag{2.2}$$

$$\varepsilon_h = \frac{h_s - h_0}{h_0} = \frac{\Delta h_0}{h_0} \tag{2.3}$$

where L, w, and h represent the length, width and the hight of the web, respectively. Δ represents the incremental of the web in each direction and ε denotes the strain of the web. Subscripts x, w, and h represent the MD, CD and ZD direction, respectively. The subscript "s" represents the state of being stretched and the subscript "0" represents the original unstretched state. In the following paragraphs, we focus on MD direction from assumption that the MD stress prevails when stretched, and the subscript x for the MD direction will be omitted for the sake of simplicity .

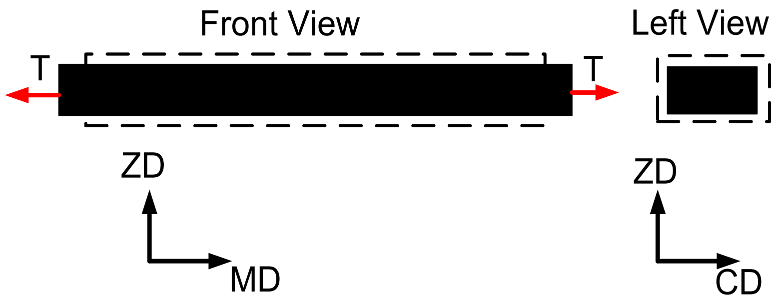

Figure 2: Illustration of a free web span

Assuming that the cross section stays constant, then according to the mass conservation law, the mass of the web remains constant between the state without stress and the state under stress. Thus, the following relationship can be obtained:

$$\rho_0 L\omega_0 h_0 = \rho_s L\omega_s h_s \tag{2.4}$$

$$\Rightarrow \rho_0 A_0 = \rho_s A_s(1+\varepsilon) \tag{2.5}$$

$$\Rightarrow \frac{m_s}{m_0} = \frac{\rho_s A_s}{\rho_0 A_0} = \frac{1}{1+\varepsilon} \tag{2.6}$$

where ρ and A denote the density and the cross section area of the web span respectively. m_s and m_0 denote the mass of the web after stretched and before stretched. Here ε denotes the strain in the MD direction as described in (2.1). Now consider a one-span web system as shown in Figure 3. Applying the mass conservation law on the web span from x_1 to x_2, it is known that the rate of the mass increase in the web span equals to the rate of mass entering the web span minus the rate of leaving the span. We can obtain

$$\frac{dm}{dt} = \frac{d}{dt}\left[\int_{x_1}^{x_2} \rho(x,t)A(x,t)dx\right] = \rho_2(t)A_2(t)v_2(t) - \rho_1(t)A_1(t)v_1(t) \tag{2.7}$$

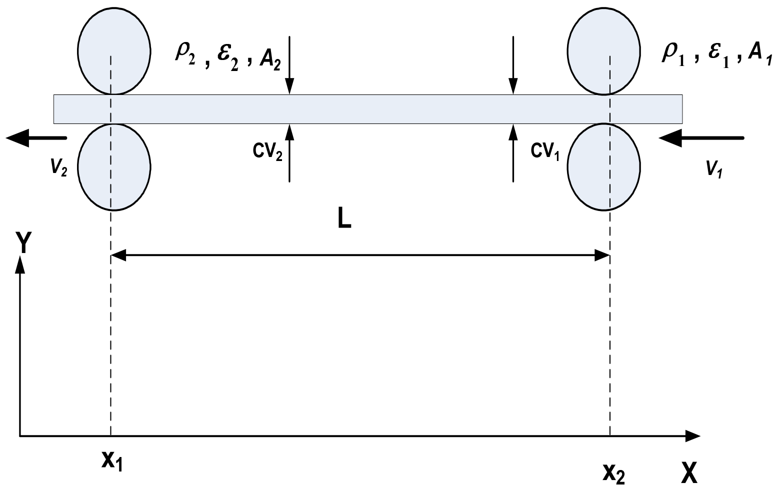

Figure 3: A single web span between two consecutive rolls

Under the assumption that strain in the web is uniformly distributed, the strain in the web span can be expressed as $\varepsilon_1(x,t) = \varepsilon_1(t)$, which implies that $\rho(x,t) = \rho_1(t)$ and $A(x,t) = A_1(t)$ are true. Integrating equation (2.7), we can obtain

$$m = \int_{x_1}^{x_2} \rho(x,t)A(x,t)dx = L\rho_1(t)A_1(t) \tag{2.8}$$

On applying (2.5), (2.8) to (2.7), we then obtain the following dynamics of the web span as:

$$L\frac{d}{dt}\left[\frac{1}{1+\varepsilon_1(t)}\right] = \frac{v_2(t)}{1+\varepsilon_2(t)} - \frac{v_1(t)}{1+\varepsilon_1(t)} \tag{2.9}$$

For small ε, it has the following approximation

$$\frac{1}{1+\varepsilon} \cong 1 - \varepsilon \tag{2.10}$$

Substitute (2.10) to (2.9), we have

$$\dot{\varepsilon}_1(t) = \frac{1}{L}\left[\varepsilon_2(t)v_2(t) - \varepsilon_1(t)v_1(t) + v_1(t) - v_2(t)\right] \tag{2.11}$$

From Hooke's law, it is known that tension and strain are approximately presented as

$$T = AE\varepsilon \tag{2.12}$$

where T is the tension, A is the cross-section area of the web, and E is Young's modulus of the web from the unstretched state. Substitute (2.12) into (2.11), we obtain the web tension dynamics as follows:

$$\dot{T}_1 = \frac{1}{L}\left[-v_1T_1 + v_2T_2 + AE(v_1 - v_2)\right] \tag{2.13}$$

The generalized web tension dynamics can be extended from one span (2.13) to the ith span as follows:

$$L\dot{T}_i = -v_iT_i + v_{i+1}T_{i+1} + A_iE_i(v_i - v_{i+1}) \tag{2.14}$$

where L is the length of the web span between two adjunct rollers. T_i and v_i denote the tension and velocity of the upstream rollers respectively. T_{i+1} and v_{i+1} denote the tension and velocity of the adjunct downstream roller respectively. E_i and A_i are Young's elasticity modulus and the cross-section area of the web respectively.

Complete details of this deviation and various other aspects, such as span tension dynamics can be found in [34]. Slightly different version of (2.14), obtained using different approximation schemes, were discussed in [17].

2.2.2 Roller Dynamics

A roller in a web winding system is driven by the web tension (T_i and T_{i+1}) and the corresponding external motor torque (u_i). The roller also experiences external frictional torque (F_i) as shown in Figure 4. We shall denote the downstream and upstream tension by T_i, T_{i+1} respectively for the ith roller dynamics development.

For a general roller, the equation of web motion can be derived by considering the torque balance at the two adjunct driven rolls as follows:

$$\frac{d}{dt}(J_i\omega_i) = u_i - \beta_{fi}\omega_i + R_i(T_{i+1} - T_i) \tag{2.15}$$

where J_i is the inertia, and ω_i is the angular velocity of the roller, u_i is the input motor torques, R_i is the radius of the roller, and $F_i = \beta_{fi}\omega_i$ is the friction force, where

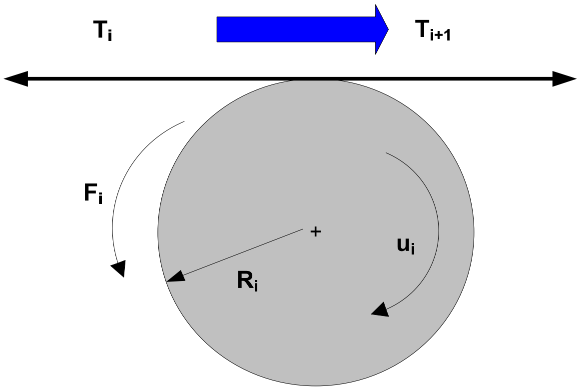

Figure 4: Roller dynamics

β_{fi} is the total friction coefficient. Note that the inertia terms on the left hand sides of equation (2.15) are time-varying for the unwind and rewind processing, since both the radius R_i and inertia J_i are changing during web processing. The second term of the right hand side of equation (2.15), which is the viscous friction coefficient β_{fi}, also changes with transporting velocity and other physical conditions.

2.3 Dynamics of a Multi-Span Web Winding System

Given a web winding system, the coupled dynamics are obtained by applying the models in equation (2.13) and (2.15) to each tension span and each roller. Care should be taken when writing the models for the rewinder and unwinder, since there is only one adjacent tension span and their radius and inertia are changing.

Let us consider the N roller web winding system, where each roller is associated with u_i, J_i, R_i, ω_i, and each tension span is associated with T_i, L_i, ω_i, and A_iE_i. The aforementioned assumptions and component models lead to the following equations that describe the dynamics of the general multi-span N-roller web winding system.

$$\frac{d}{dt}(J_1\omega_1) = u_1 - \beta_{f1}\omega_1 - T_1R_1(t) \tag{2.16}$$

$$J_i \frac{d}{dt}(\omega_i) = u_i - \beta_{fi}\omega_i + (T_{i-1} - T_i)R_i \tag{2.17}$$

$$\frac{d}{dt}(J_N \omega_N) = u_N - \beta_{fN}\omega_N + T_{N-1}R_N(t) \tag{2.18}$$

$$\frac{dT_i}{dt} = \frac{1}{L}\left[R_{i+1}\omega_{i+1}T_{i+1} - R_i\omega_i T_i + AE(R_i\omega_i - R_{i+1}\omega_{i+1})\right] \tag{2.19}$$

2.4 Summary

In Chapter 2, mathematical description of the dynamics of the web winding system has been presented and the mathematical models have been derived for a free-web span, a roller and a web interacting with the roller. Then the dynamics of a multi-span N roller web winding system has been summarized in the end.

CHAPTER III

BACKGROUND AND LITERATURE REVIEW

3.1 Introduction

A number of researchers have investigated the modeling and control of web winding systems. Swift [9] was one of the first references that investigated longitudinal dynamics. Campbell [4] presented the dynamic equations of a web under longitudinal tension in ordinary differential equation (ODE) form and developed linearized controllers based on current and voltage feedback. Grenfell [7] derived a mathematical model and applied it to a paper-making processing. Young and Reid [8] summarized the history of modeling web longitudinal tension dynamics. Based on the work above, King [10], Whitworth and Harrison [11], and Brandenburg [12] provided more specific nonlinear models. The nonlinear models derived in [10, 11, 12] have been used as the basis for tension controller design in some papers, for example, Shelton [13], Grimble [14], Boulter [15], Liu [16], Lynch [17] and Koc [18].

Web tension regulation is a rather challenging industrial control problem. A review of the web tension control problems can be found in [19]. Proportional-integral-derivative (PID) [20, 21], fuzzy logic [22, 23], neural network [24, 25], optimal control [26], and robust control approaches [27, 28] are used. Recently, robust Lyapunov-based feedback control [29, 30] and multivariable H_∞ controller with one or two degrees of freedom control strategies have been proposed for industrial web transport systems [31]. The role of active dancers in attenuation of periodic tension disturbances was studied in [32].

Regarding control structure, centralized control structure has many drawbacks and researchers have proposed distributed control [33, 34], decentralized control [81, 82, 83, 84, 85, 86, 87] and overlapping decentralized control [88, 89, 90, 91] to improve the performance over centralized control structure.

3.2 Web Tension Regulation

To meet the requirements of the control objects and specifications defined above, various advanced control strategies and methods have been proposed and applied to industry applications. A review of existing techniques on control system structures, tension regulations methods and tension estimations will be given in this subsection.

3.2.1 Structures

Centralized Control

Centralized control is the traditional control method which considers all the segments and interconnections to be a single dynamic system. Similar to all the large-scale system, the order of the controller in a multivariable control framework is high, which makes it difficult to implement in real time. In addition, because of the variation of radius and the presence of interaction, the control of tension is more difficult. Feedback and feed forward control are used to reject disturbance and to improve performance. Many control strategies, such as PID [20, 21], loop shaping [15], gain-scheduling [28], multivariable H_∞ control [18] are applied in centralized controller design in industrial practice.

Distributed Control

The main academic work on distributed control method is presented by Shin in his thesis and book on tension control [33, 34]. It assumes that all spans have the same length and all rollers have the same moment of inertia, the same radius and the same frictional coefficient. To improve the performance, Shin first derived an auxiliary dynamic model from the mathematical model for a unit process by defining a new state variable based on the relative velocity of the web span. Then, an auxiliary local controller is designed, which meets the required closed-loop performance specifications of subsystems. Finally, all closed-loop subsystem are combined into a composite system and checked to confirm that they meet the stability conditions for the overall system.

Decentralized Control

Centralized control is not normally feasible, because in practice there are many drive rolls to deal with. Decentralized control is essential for such large scale systems. When decentralized control is applied to web tension control systems, the interactions among control stations and the modeling are the major problems for the controller design. In the decentralized case, the interconnections between segments are usually neglected for control design purposes. The decentralized approach then greatly reduces the computational and hardware requirements. The goal of the method is to design a controller, which minimizes the influence of the remaining system and to guarantee the desired dynamics and stability of the total system.

The advantage of this method is that there are not any measurements of the quantities of coupling. It is necessary to know where the quantities of coupling are active in the subsystem. However, the designed control is robust against changes of the parameters in a limited range. Figure 5 is a 3-tension-zone web winding system, in which each tension zone is designed by a decentralized separate PI controller [18].

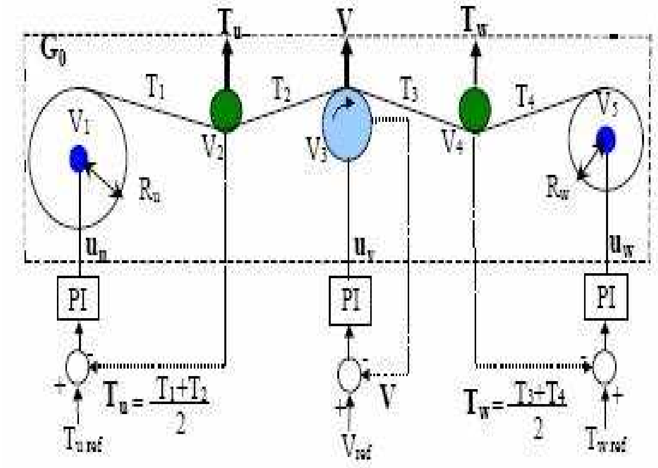

Figure 5: Structure of the decentralized control strategy

Overlapping Decentralized Control

Since a major problem on the decentralized controller design is the mutual interactions among different subsystems or control sections, a natural solution is to identify them. Overlapping in decentralized control adds extra degrees of freedom that allow improvements from disjoint decomposition [88, 89, 91]. This methodology of control assumes that overlapping information of controlled variables could be obtained from a couple of subsystems. It is based on overlapping decomposition of the system, which includes system expansion based on the inclusion principle, overlapping decomposition of the subsystem, controller design for each disjoint subsystem, and stability check for the entire system.

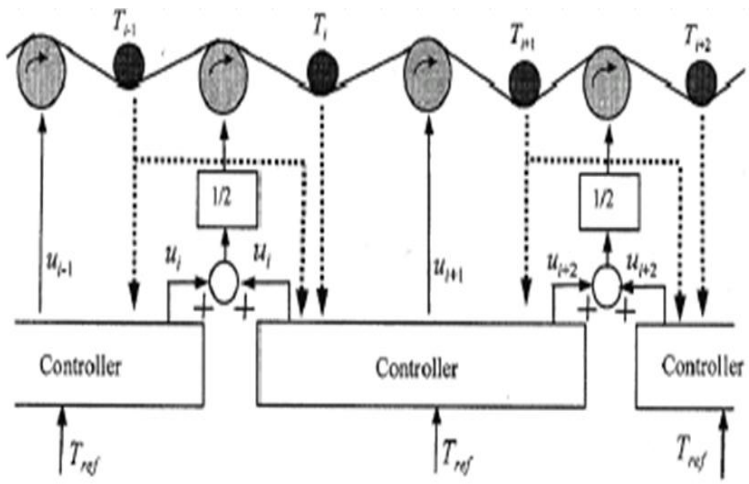

Figure 6: Structure of overlapping decentralized control strategy

Figure 6 [31] is a demonstration on overlapping decentralized control strategy, where two consecutive controllers share the some inputs and outputs. For instance, input signals of the driven roller located at the boundary of two subsystems come from two controllers.

3.2.2 Tension Control and Estimation

Open-loop draw control and closed-loop progressive set-point coordination control are the two control approaches that are commonly used in web processing industries for tension control. In progressive set-point coordination control, once an input is provided to an upstream driven roller, an input of the same magnitude is automatically provided to each of the driven rollers, which follows downstream. The approach is effective for the start-up or shutdown of a system. But it is not a desirable scheme for normal operation, since it forces tension in the downstream web span to be automatically changed when only the tension in the upstream span needs to be changed. Therefore, it is impossible to control the tension in each web span independently in a multi-span web transport system using progressive set-point coordination. In the draw control scheme, tension in a web span is controlled in an open-loop manner by controlling the velocities of the rollers at either end of the web span. Thus, tension is very sensitive to the velocity difference between the ends of the web span. On the other hand, feedback control of web tension can result in greatly improved accuracy, since the sensitivity of web tension to the velocity difference no longer exists. The accuracy of the feedback control depends on the accuracy of the tension sensor.

Generally, there are three tension regulation strategies widely used in the industry. The simplest approach is the indirect calculation of required motor torque from tension reference and radius. Many examples of this method are found in winder/unwinder tension control. Another approach is the feedback control scheme based on the direct detection of tension with load cells. The third approach uses the dancer roll as a measurement device and/or as a self-regulating device [49].

Tension Control Strategies

Tension control is so critical to the entire web transport system that many advanced control methods have been applied to solve this problem. Herein we review some of these control methods used today.

1) PID

PID control is the common method in industry because of its simplicity. Usually a cascade PID control loop is adopted, where tension control is in the outer loop and speed loop in the inner loop. In order to deal with changing variables, variable PID control [21] and other versions of PID, such as nonlinear PID [33] have been proposed to get better results. The main problem of PID control is that an interaction between tension and speed make it difficult to get a satisfying result and hard to tune. In addition, if the controller gain is tuned bigger to get better performance, the plant may become unstable.

2) Fuzzy Logic [22, 23]

An Fuzzy Logic Controller (FLC) is a non-linear controller. To find the setting of the Fuzzy controller it is not necessary to have a mathematical description of the process. But one must have a good physical knowledge of the process. The rules of an FLC are made with "$if \ldots, then \ldots$ " conditions. In conventional control, the process is modeled, but in FLC the expert is modeled. Some problems are solved better and in a shorter time with FLC as by a conventional non-linear control. Unfortunately, there are no defined criterion functions to find an optimal FLC. Usually one has to find the optimum with the trial and error method.

3) Neural Network

In the field of web tension control, there are a lot of nonlinearities and time-varying dynamic. One application of Neural Network (NN) is to learn the unknown time-dependent friction of the mechanical system for compensation [24]. Another application is the compensation of disturbances if a winder runs non-circular. The NN is able to learn such disturbances [25]. The weakness of NN is that it needs training data, which is time consuming and not efficient in industry.

4) Optimal Control

In [120], a Linear Quadratic Gaussian (LQG) method was proposed and applied to a multivariable web winding system. The interactions between tensions and linear velocities are considered and estimated by subspace identification method. An infinite horizon LQ regulator is developed, and in order to get an asymptotic precision, a rearranged LQ controller with reference input and an integrator is added. In addition, a Kalman filter was used to estimate the state vector. The weakness of LQG is that it is a model-based controller and its successful applications rely on the existence of an accurate model and sufficient knowledge of the parameters of the model, which are hard to satisfy in a web winding system.

5) Adaptive Control (Gain Scheduling)

Since radius and inertia of the roller are keep changing, some researchers proposed to use a gain-scheduling scheme to improve robustness to radius variations. In [28] the author pointed out that with a quasi-static assumption on radius variations, the transfer function between command signal and web tension appears to be inversely proportional to radius. Based on this observation, a new plant is obtained by multiplying the controller output signals by the radius. This new plant has the advantage of making the gain at low frequency less dependent on radius and inertia.

6) Nonlinear Active Disturbance Rejection Control (NADRC)

In [121], a nonlinear ADRC, proposed by Han [127, 128, 129] and simplified by Gao [139], is designed to accommodate for nonlinearity and uncertainties in the web tension control system. The results demonstrated that the control system was robust to a large range of parameter variations. Although good performance was observed, the initial NADRC [128, 129, 93] controller used many nonlinear gain functions and was difficult to tune. The practical implementation would also be difficult. The parameterized linear ADRC [140, 132, 130] resolved this implementation issue.

7) Other Control Methods

Besides the methods above, there are many other methods, such as model predictive control [141], time optimal control [26], self-tuning regulation [142], perfect control [143], and observer-based feedback control [144, 145, 146, 147, 148].

Tension Estimation

In cases where tension measurement is not available, observers that estimate the web forces can be applied. The earliest reference found on tension observers, was a full-order Kalman filter in [149]. Another reference [150] used an observer as part of a tension control system for a two-span web processing machine. The observers estimated the tension difference across each nip. Other works consider the estimation of rewind and effects of winder tension in order to perform closed-loop tension control [151, 152, 153].

The following subsections summarize the main observer techniques in the literature.

1) Observer Design Based on Frequency Response

Song *et al.* [145] used a formula to estimate web tension based on frequency response. The observer is designed based on the unwind/rewind roller dynamics as follows:

$$J_u \frac{d\omega_u(t)}{dt} = R_u T_u(t) - F_{uf} - K_u u_u(t) \tag{3.1}$$

where the subscript "u" denotes the unwind roller. The tension observer T_{obs} is then designed based on (3.1) neglecting the friction effect F_{uf}.

$$T_{obs}(t) = \frac{1}{R_u}[J_u \bar{\alpha}_u(t) + K_u u_u(t)] \tag{3.2}$$

where $\bar{\alpha}_u(t)$ denotes filtered angular acceleration of the unwind roller, which is computed by taking the derivative of the measured angular velocity of the unwind roll, and then passing through a second-order low-pass filter as follows:

$$\bar{\alpha}_u(s) = \frac{\omega_n^2}{s^2 + 2\xi\omega_n s + \omega_n^2} s\omega_u(s) \tag{3.3}$$

where $\bar{\alpha}_u(s)$ and $\omega_u(s)$ denotes the Laplace transformation of $\bar{\alpha}_u(t)$ and $u_u(t)$, and ω_n and ξ denote the natural frequency and damping ratio of the filter, respectively.

2) Observer Design Based on Computational Tension

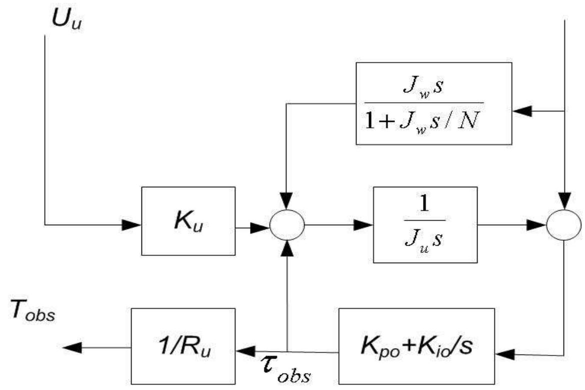

Figure 7: Diagram of tension observer

Lin [146] proposed an alternative approach to using the computational method for tension estimation based on Song's tension dynamics. The observer has a feedback configuration and a filtered inertia block as shown in Figure 7.

The output of the observer is shown as follows:

$$\tau_{obs}(t) = \frac{K_{po}s + K_{io}}{J_u s^2 + K_{po}s + K_{io}}[K_u \frac{J_u s}{1 + J_u s/N} - J_u s] \begin{bmatrix} u_u(s) \\ \omega_u(s) \end{bmatrix} \tag{3.4}$$

$$T_{obs}(t) = \frac{\tau_{obs}(t)}{R_u} \tag{3.5}$$

where $u_u(s)$ denotes the Laplace transform of $u_u(t)$. Proper values of N are between 3 and 10 as described in [146]. The larger the value of N is, the faster the observer responses can be. The stability of Lin's observer can be guaranteed by proper design of the PI gains.

3) Observer Design with Friction Compensation

The observer proposed in [146] is good as a torque observer; however, it is not good as a tension observer if acceleration or deceleration inertia of the roll arises. Lin *et al.* [147] continued to propose another observer. The outputs of the filtered inertia block were used as feedforward signals and added into the estimated torque. The sum of the filtered inertia and estimated torque provides good estimates of web tension in spite of acceleration or deceleration inertia of the roll. A block diagram of the observer with inertia compensation is shown in Figure 8 [147].

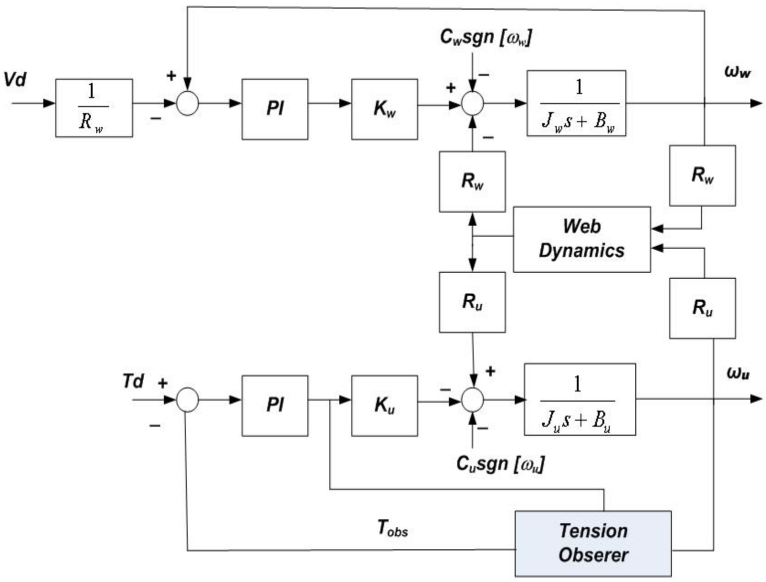

Figure 8: Modified diagram of a tension observer

The output of the observer is shown as follows:

$$
\begin{aligned}
T_{obs}(t) &= \frac{1}{R_u}\frac{K_{po}s+K_{io}}{J_u s^2+K_{po}s+K_{io}}\left[K_u\frac{J_u s}{1+J_u s/N}-J_u s-B_u\right]\begin{bmatrix} u_u(s) \\ \omega_u(s) \end{bmatrix} \\
&+ \frac{1}{R_u}\left(K_f\frac{J_u s}{1+J_u s/N}\omega_u(s)+\frac{C_u}{s}\operatorname{sgn}[\omega_u(t)]\right) \qquad (3.6)
\end{aligned}
$$

where B_u and C_u are the coefficient of bearing and Coulomb friction, J_u is the inertia of the roller, ω is the angular velocity of the wind/unwind, R is the radius of the wind/unwind, subscript w and u represent wind and unwind respectively, T_d and v_d represents tension and velocity reference respectively, and K is the gain of PID.

4) Nonlinear Observer Design

An observer that achieves a time-varying error linearizion was presented in [17]. The observer has a cascade structure. The estimate of a certain span's tension is determined by an ODE, which depends on the tension estimate of that span and the upstream span. The nonlinear observer is based on the tension dynamics:

$$\frac{dT_i}{dt} = \frac{1}{L}\left[r_{i+1}\omega_{i+1}T_{i+1} - r_i\omega_i T_i + AE(r_i\omega_i - r_{i+1}\omega_{i+1})\right] \tag{3.7}$$

First, the tension estimation is determined by

$$\dot{\hat{T}}_i = \frac{1}{L_i}\left[r_{i+1}\omega_{i+1}T_{i+1} - r_i\omega_i T_i + AE(r_i\omega_i - r_{i+1}\omega_{i+1})\right] + K_i\tilde{T}_i \tag{3.8}$$

where $\tilde{T}_i = T_i - \hat{T}_i$, K_i are the observer gains needed to be deigned. Consider T_i is still in the right hand of (3.8), and then the author defines a new variable to cancel T_i.

$$w_i = T_i - J_i(r_i)K_i\dot{\theta}_i/r_i \tag{3.9}$$

The new coordinate design is accurately based on the velocity dynamics

$$\frac{d}{dt}(J_i\omega_i) = U_i + (T_{i-1} - T_i)r_i - F_i(\omega_i) \tag{3.10}$$

After coordinate transformation, a nonlinear observer is obtained, whose right-hand side depend only on the measurements.

5) Sliding-mode Observer

As a comparison, Lynch [17] also provides a sliding-mode observer design. The full order sliding-mode observer uses discontinuous output injection depending on the unwinder and rewinder angular velocity error. The observer is given by

$$\frac{d}{dt}(J_i\omega_i) = U_i + (T_{i-1} - T_i)r_i - F_i(\omega_i) + K_i \operatorname{sgn}\tilde{\omega}_i \tag{3.11}$$

$$\dot{\hat{T}}_i = \frac{1}{L_i}\left[r_{i+1}\omega_{i+1}T_{i+1} - r_i\omega_i T_i + AE(r_i\omega_i - r_{i+1}\omega_{i+1})\right] + K_i \operatorname{sgn}\tilde{T}_i \tag{3.12}$$

where $\tilde{\omega}_i = \omega_i - \hat{\omega}_i$, and K_i is the positive observer gains.

6) Decentralized Observer

Centralized state space control often causes the total system to be complicated and thus often impractical for industrial applications. Decentralized control methods are often used, where the state space control and the observers are designed with subsystems of low order. Wolfermann proposed a decentralized observer in continuous moving webs in 1991 [153]. In order to solve the problems of disturbance and uncertainties in the system, a new adaptive decentralized control in state space form is proposed. The subsystem is also extended with a disturbance model, and the decentralized observer is calculated from the extended system.

3.2.3 Summary of the Solutions

During the past decades, many advanced control strategies and algorithms have been proposed and applied to web winding system control problems. However, few of these schemes are entirely satisfactory.

In terms of control strategy, centralized control is traditionally widely used for web tension regulation; but for large-scale system, it is too complex and hard to design and tune. Decentralized control has been applied to many large-scale systems, including web-winding system. The decentralized scheme is relatively simple but the performance may be deteriorated due to the neglected strong dynamic interactions between adjunct segments, which sometimes even make the entire system unstable. The overlapping decentralized control performs better by taking account of interactions dynamics. But it is more complicated to implement in industry.

Regarding tension control methods, strengthens and weakness of the control methods are summarized as follows: PID design was simple but the coupling between tension and speed consequently restricted performance. Robust controller designs could guarantee robust stability from disturbance and uncertainty. However, it was restricted to a small robustness range. Optimal multivariable control methods reduced the effect of interaction, but they require an accurate model and parameters. Intelligent control methods, such as fuzzy logic control and neural network, are time-consuming and difficult to design and implement in the real world. The advanced control methods, such as observed based feedback control and H_∞, are too complex to implement and not well understood by industry.

3.3 Decentralized Large-scale Web Winding Systems Control

3.3.1 Challenges

Web tension control system has a structure of multi-inputs and multi-outputs structure with strong coupling. In the early days, a centralized control structure was used to design controller. Since the system is a MIMO system, multivariable controllers were the reasonable choices. However, when the system becomes larger, it is not practical to implement the high order controllers. Decentralized control strategy is then commonly used, which is constructed as a form of decentralized subsystem structure. The controllers are designed at each subsystem, which removes the complexity of designing MIMO controllers. However, the interactions among the input signals should be estimated sufficiently to assure appropriate stability and performance of the decentralized control system.

In summary, the web winding system control problem is a challenging problem for the following reasons: the entire system is actually a large-scale system, which is still an open problem in study; the tension dynamics are highly nonlinear and sensitive to velocity variations; for each subsystem, the tension and velocity dynamics are coupled to each other; the coefficients of the tension and velocity dynamics are highly dependent on the operating conditions and web material characteristics. Furthermore,there are extensive external disturbances propagating throughout the whole system that keep affecting the behaviors of the system. And finally, the interactions between each tension zone make it difficult to design controllers.

3.3.2 Background

Inter-connected or networked small subsystems can been seen in many areas such as manufacturing systems, telecommunication systems and information systems. In such systems, it is possible to define subsystems, which interact with each other or are networked to form large-scale systems. Power networks, multiple aircraft formulation, wireless telecommunication systems, intelligent vehicle and highway systems are some of the examples of such physical systems [2]. The physical configuration and high dimensionality of such complex systems lead to centralized control being technically challenging and even economically infeasible. Now, with the rapid progress of microcomputers available at low cost, decentralized control schemes have gained greater attention and become a hot topic.

Large dimensionality, unavoidable uncertainty, and information structure constraints are the main characteristics of large-scale systems. It is these three features that motivate the development of decentralized control theory for such complex systems.

The decentralized control of interconnected systems is one of the research topics of large-scale control theory. A large-scale system consists of a number of interconnected subsystems. Complexities in large-scale systems make it difficult to design controller and analyze the performance for the entire system. In the decentralized framework, the system has several subsystems, where each controller locally controls each subsystem. Hence, the large-scale system is usually decomposed into smaller interconnected subsystems. Figure 9 shows a typical decentralized control structure, in which subsystems are interacting with each other and each local controller only controls the subsystem. Development of decentralized control theory based on the fundamental knowledge of centralized control theory is the main motivation behind much research done in the field. In the late 1960's, research on decentralized control and decomposition structure started. A survey of early results in the development of decentralized control of large-scale systems was summarized in [2], which also predicted future research direction of decentralized control theory. The basic framework of decentralized control was systematically organized in [3], where most decentralized control schemes and their applications for a variety of fields such as power networks and spacecraft systems were discussed.

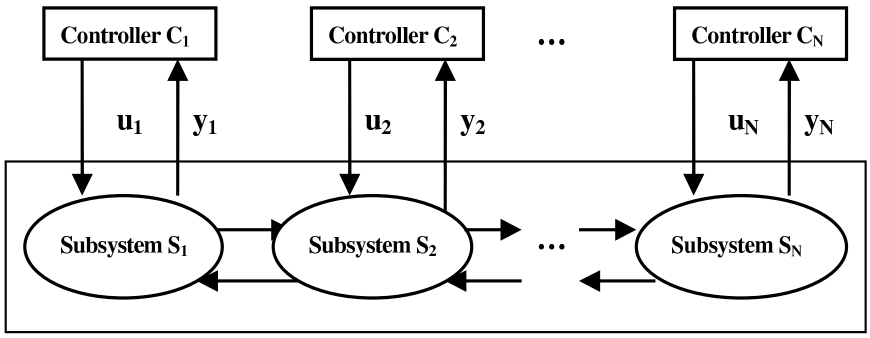

Figure 9: An illustration of a large-scale system

Decentralized control has been applied to large-scale systems for over three decades. Most recent applications of decentralized control include platoons of underwater vehicles, cooperative robotic systems etc. There are many reasons that make decentralized control a popular choice for large-scale systems. However the most prominent factor is its effective solution to problems of dimensionality, uncertainty and information structure constraints. When a system consists of many interconnected subsystems or has large dimension, it is computationally efficient to formulate control laws that use only local available information. Such an approach also helps reduce the implementation cost, since it can significantly reduce the information exchange among subsystems. Robustness is another attractive feature of decentralized control schemes, since they can make the closed-loop system tolerant of a range of uncertainties within the subsystems and the interconnections with other subsystems.

To make the overall large-scale system behave well, controller design strategy is an important issue in the operation of a large-scale system. For several decades, various strategies have been proposed to decentralized control for large-scale systems, but very few have been successfully implemented in industry applications. This section will briefly review the main ideas behind each of the control strategies attempted, followed by a discussion of the disadvantage of current state-of-the-art methods for decentralized control. The potential idea that could help to solve the problem will also be introduced in the end.

3.3.3 Design Methods

A comprehensive review of most of the results form decentralized control strategies available until 1982 can be found in a special issue of IEEE Transaction on Automatic Control (1983). Generalized research in decentralized control theory started with classical linear time-invariant (LTI) control. Necessary and sufficient conditions for existence of stabilizing decentralized controllers for LTI systems were proposed in [35] with an introduction of the concept of "fixed modes". Fixed modes are defined in association with a decentralized control system, in which linear, constant gain, state feedback controllers are used. Modes of the closed-loop large-scale systems, which cannot be influenced by a decentralized control scheme, are known as "fixed modes". It was shown in [35] that, like the centralized case, decentralized fixed modes are immovable. It was also shown in [36] that these fixed modes are immovable if constant state-feedback gains are used. However, with time-varying gains, the fixed modes related to the decentralized control system can be eliminated. Later on, many types of fixed mode were studied during extensive work on large-scale systems. In these work, two aspects of decentralized control were addressed: 1) which kind of fixed modes can be eliminated? 2) which controllers should be used? It is shown in [37] that all of the fixed modes except those associated with unstable zeros of complementary subsystem can be stabilized by periodically time-varying decentralized state feedback controllers.

It is important to note that the classical concept of fixed modes and relevant literature are developed for LTI large-scale systems. Motivated by the success of decentralized control scheme for LTI systems, efforts were made to develop decentralized control scheme for nonlinear large-scale systems. The first result, which extended classical centralized adaptive control theory to decentralized adaptive control, was developed in [38]. But the result in [38] was obtained for a class of large-scale systems, in which each subsystem only had relative degree of less than two. Later results on decentralized adaptive control were developed for more generalized class of large-scale systems, in which Lyapunov analysis played an important role. Conditions on relative degree of subsystem were relaxed in [39] to obtain a decentralized adaptive controller, in which matched interconnections and uncertainties are assumed to be bounded by the higher order polynomial in the norms of states. The matching condition is said to be satisfied if interconnections and uncertainties entered into the subsystem at the same point, where decentralized control input entered into the subsystem. Decentralized control of large-scale systems with matched condition was investigated extensively in the past [40, 41, 42]. Global decentralized adaptive control was obtained in [40], where a class of nonlinear systems was considered, which can be transformed to the output feedback canonical form. Decentralized model reference adaptive control (MRAC) was introduced in [41, 42], which developed decentralized adaptive schemes for a class of systems in which the matching condition is satisfied. Lower order control law was developed in [43] to show semi-global stability for large-scale systems with higher order polynomials of interconnections.

In practice, complete state measurements are usually not available at each individual subsystem for decentralized control. Therefore, decentralized feedback control based on output measurements became a research topic. There also has been a strong research effort in literature towards development of decentralized control schemes using decentralized observers, since one can design decentralized observers to estimate the state of individual subsystems that can be used for estimated state feedback control. Early work in this area can be found in [44, 45]. Two methods are used to design observer-based decentralized output feedback controllers for large-scale systems: 1) design local observer and controller for each subsystem independently, and then verify the stability of the overall closed-loop system. In this method, the interconnection in each subsystem is regarded as an unknown input [45, 46]; 2) design the observer and controller, and treat the output feedback stabilization problem as an optimization problem.

Recent work in [46, 47, 48, 49, 50, 51] has focused on the decentralized output feedback problem for a number of special classes of nonlinear systems. In [46], a decentralized observer-based control scheme with unknown inputs was described. A partially decentralized state observer was proposed in [47] and the implementation of the decentralized observers was also given. An adaptive tracking controller using output feedback for a class of nonlinear systems was proposed in [48]. It was shown in [49], considering systems with matched interconnections, that it is possible to asymptotically track the desired output with zero error in strictly decentralized adaptive control system. A control scheme for robust decentralized stabilization of multi-machine power systems, based on linear matrix inequalities, was proposed in [50]. A decentralized output feedback model reference adaptive controller for systems with delay can be found in [51]. A recent paper discussed the decentralized robust control of uncertain interconnected systems with an exponential convergence [42].

Decentralized controller can not access the entire state information. Therefore, interconnections between subsystems need to be analyzed, so that their influence on the system performance can be understood properly. As far as interconnected systems are concerned, there are two main approaches for the treatment of the interconnections in the literature. The first approach assumes that the interconnections satisfy the matching conditions bounded by first-order polynomials or higher-order polynomials of states. The second approach requires that the interconnections meet a triangular structure bounded by first-order polynomials or higher-order polynomials of states. The matching condition guarantees that Lyapunov redesign is possible, which begins with Lyapunov functions for nominal subsystems and then uses these Lyapunov functions to design decentralized feedback laws. Most of the work in the literature falls into this category. On the other hand, the triangular structure makes it possible to apply back-stepping technique to design the decentralized controllers.

In summary, the methods of solving the decentralized control problem can be categorized into five major areas: decentralized adaptive control; decentralized robust control; decentralized robust adaptive control; decentralized intelligent control; and decentralized decomposition solutions. The following sections outline the vast body of research and results in each area.

1) Decentralized Adaptive Control Scheme

The uncertainties and difficult to measure parameter values within a large-scale system attract adaptive techniques into this research. Much progress has been made in the field of decentralized adaptive control, such as [53, 54, 55, 56, 57, 58, 59, 60] and the references therein. Model reference adaptive control based designs for decentralized system haven been studied in [53]-[54] for the continuous time case and in [55] for discrete time case. These approaches, however, are limited to decentralized systems with linear subsystems and possibly nonlinear interactions. Decentralized adaptive controllers for robotic manipulators were presented in [56] and [57], while a scheme of nonlinear subsystems with a special class of interconnections was presented in [58]. It was shown in [58] that it is possible to provide stable tracking in decentralized systems that contain uncertainties, which are bounded by polynomials with known order.

When the internal states are not measurable or not easily obtained, output feedback control scheme has been applied in many cases. Particularly, a decentralized adaptive output control scheme was presented in [59] for a class of large-scale nonlinear systems that are transformed into the output feedback canonical form. The scheme guarantees global uniform bounds of the tracking error and all the states of the closed-loop system in the presence of parametric and dynamic uncertainties in the interconnections and bounded disturbances. However, the scheme cannot apply to the systems with unmodeled dynamics. The work in [60] presented a decentralized adaptive output feedback control scheme for large-scale systems with nonlinear interconnections. The scheme in [60] has several advantages: 1) it achieves asymptotic tracking; 2) the considered large-scale systems may possess an unknown, nonzero equilibrium. But the scheme cannot apply to the systems with unmodeled dynamics and disturbances.

Makoudi *et al.* [61] proposed a new decentralized model reference adaptive control for interconnected systems. The main idea was to predict the interconnection outputs acting on each subsystem. This method was based on expressing the interconnections as a linear combination of a set of orthogonal known functions of basis. It was also shown that this scheme was robust with respect to unmodeled dynamics.

2) Decentralized Intelligent Control Approaches

Since model based control methods need an accurate model of the plant and are sensitive to parameter variations and to the existence of disturbances, model free control methods have been developed for decentralized control problem. Because they do not require the exact mathematical model for the system and only some input-output data are employed to obtain an effective model, intelligent control algorithms have been applied to solve this complicated system. Basically, there are three approaches that intelligent methods have been applied to decentralized control problem, which includes fuzzy logic based, neural network based, and the combination of fuzzy-neural network based decentralized control.

To estimate the unknown dynamics, neural networks have been exploited to approximate unknown functions and dynamics uncertainness. Due to the functional approximation capabilities of radial basis neural networks, the dynamics for each subsystem are not required to be linear in a set of unknown coefficients as is typically required in decentralized adaptive schemes. In addition, each subsystem is able to adaptively compensate for disturbances and interconnections with unknown bounds. Hwang *et al.* [62] presented a fuzzy decentralized variable structure tracking control scheme with an application to a two-joint-robot control. In this paper, each nonlinear interconnected subsystem was approximated by a weighed combination of fuzzy linear pulse transfer function systems. Spooner *et al.* [63] reported a decentralized adaptive control of nonlinear systems using radial basis neural networks, which approximates the unknown functions on-line. The proposed approach is able to adaptively compensate for disturbances and interconnected with unknown bounds. Hovakimyan [64] proposed a coordinated decentralized output feedback control of interconnected system based on neural networks. A linear parameterized neural network is used to model the interconnection effects on-line. Da [65] showed a new type of fuzzy neural networks sliding mode controller for interconnected uncertain nonlinear systems. The combination of fuzzy neural network has both the learning and reasoning abilities, and therefore can handle the disturbance and uncertainties. The approach does not require the bounds of uncertainty and disturbances in each subsystem.

3) Globally Robust H_∞ Based Decentralized Control

Motivated by considerable success of centralized H_∞ control in many applications, the decentralized linear H_∞ control techniques was first applied for linear interconnected systems with linear interconnections in reference [66]. Later on, the nonlinear H_∞ almost disturbance decoupling problem was solved in the sense that the designed internally stable system can maintain arbitrary L_2 gain from the disturbance input to output [67, 68]. Guo *et al.* [69] further developed decentralized nonlinear H_∞ control with an effort to close the gap between decentralized and centralized H_∞ control. Guo's work combined the decentralized adaptive control and centralized nonlinear H_∞ control for structured systems and applied the proposed methods to large scale power systems control. The control law was obtained through recursive back-stepping procedures where any given L_2 gain must satisfy given conditions.

Another approach of robust decentralized control is global stabilization control. The back-stepping design idea was applied to construct decentralized robust controllers by Chen [70] and Xie [71] for the first time and initially used in decentralized adaptive control by Jain and Khorrami [72]. Xie [73] designed decentralized robust control for a more general class of interconnected nonlinear systems with decentralized strict feedback form and single input minimum-phase subsystems. In Xie's two papers, the interconnections were assumed to be bounded by higher order polynomials of the states in the first integrator of every subsystem, whose coefficients have a lower triangular structure.

Liu [74] *et al.* investigated the problem of decentralized robust stabilization for a class of large scale nonlinear systems with parameter uncertainties and nonlinear interconnections. Each system of the interconnected system was assumed to be controlled by multiple inputs and to be in a nested structure. The uncertain parameters and/or disturbances were allowed to be time-varying and entered the system nonlinearly. The nonlinear interconnections were bounded by higher-order polynomials in the decentralized strict feedback form. It was proved that the global decentralized robust asymptotic stabilization problem can be solved for the uncertain interconnected nonlinear systems by applying a recursive design procedure.

4) Decentralized Robust Adaptive Control

The adaptive control is only robust to sufficiently fast unmodeled dynamics and sufficiently small bounded disturbance. Recently, robust adaptive control of nonlinear systems has emerged as an active research area and is extended to decentralized control framework.

The purpose of adding a robust control component is to deal with those cases with significant disturbance and uncertain nonlinearities. The upper bound on the disturbance must be known in the design of the controller. Liu *et al.* [75] proposed a decentralized robust adaptive controller of nonlinear systems with unmodeled dynamics. First, a modified dynamic signal was introduced to each subsystem to dominate the unmodeled dynamics in the interactions between each subsystem and an adaptive scheme was used to counter the effects of the interactions. Then, a systematic design procedure was employed to obtain the decentralized robust adaptive output feedback controllers. The approach guaranteed that all the signals in the closed-loop system were bounded in the presence of unmodeled dynamics. Using combined back-stepping and small gain approaches, [76] presented an adaptive output feedback control scheme for nonlinear un-modeled dynamics. As an extension of the centralized case, a decentralized robust adaptive output feedback regulation scheme was presented for a class of large scale nonlinear systems.

Zhang *et al.* [77] presented a robust decentralized adaptive stabilization of interconnected systems. The backstepping technique was used to design totally decentralized adaptive controllers for large-scale systems with both strong static interactions and weak dynamic interactions. The L_∞ and L_2 bounds of tracking error were set to chosen the design parameters.

5) Decentralized Control Using Overlapping Decomposition

Decomposition is a prerequisite for decentralized control, breaking down a large system into a number of subsystems of lower dimension. There are several decomposition methods for large scale systems that are convenient for parallel computations, such as nested epsilon decompositions, and overlapping decompositions [3].

Decomposition for systems with the overlapping structure has been used to solve problems in many fields, such as automated highway systems, electric power systems, and large space structures. Within the mathematical framework of the inclusion principle, the underlying methodology is essentially based on expanding the state space (and, eventually, input and output spaces), so that the overlapping subsystems appear as disjoint, applying standard methods for decentralized control design, and contracting the obtained controller for implementation. An overlapping decomposition of the original system corresponds to a disjoint decomposition of the expanded system. A decentralized solution for the (disjoint) pieces of the expanded system is then contracted to obtain a solution for the original system. Satisfaction of the inclusion conditions is essential for transferring properties of the expanded system to the original one.

An overlapping decomposition of a large-scale system allows the subsystems to share some common parts and thus provides greater flexibility in the choice of the subsystems. The concept of overlapping decompositions has been successfully applied to various large scale problems including decentralized optimal control, parallel distributed systems and hybrid system control, etc. In some cases, overlapping decompositions have been shown to be successful, while disjoint decompositions have failed.

3.3.4 Large-scale Web Winding Systems

Web winding process covers wide ranges of applications and is composed of many rolls connected to guide rolls, dancer rolls and motors. Then the entire processing lines are regarded as large-scale systems mechanically connected together with the web materials, which is expected to operate at the desired speed and tension levels.

Over the years, centralized multivariable control, distributed control, decentralized control, overlapping decentralized control have been proposed to solve large-scale web processing lines control problem. Traditional centralized control has some limitations and is not practical because it has too many driven rolls in practice. By the possible perfect elimination of the undesirable effects caused by the interconnecting terms, centralized multivariable control approach can guarantee good closed-loop performances. However, when the system is in large-scale and becomes complicated, it is hard to implement. Recently, decentralized control, overlapping decentralized control has shown better results.

1) Decentralized Control

For practical considerations, the decentralized scheme has received more attention in recent years. The reliability, the ease of implementation, the operator acceptance and the less computational requirement, are among the most relevant properties that make the decentralized controllers more widely used in the control of web winding processes. Furthermore, the system is more easily managed in the decentralized context, and does not require the whole system to be put out of order.

When decentralized control is applied to web winding systems, the interactions among control stations and the modeling issues are the major problems for the controller design. In the decentralized case, the interconnections between segments are usually neglected for control design purposes. The decentralized approach then greatly reduces the computational and hardware requirements [81, 83, 84, 85, 86, 87, 88]. The advantage of this method is that no measurement of the quantities of coupling is required. It is only necessary to know where the quantities of coupling are active in the subsystem. The designed control is robust against changes of the parameters in a wide range. Sakamoto [83, 84, 85] discussed the controller design for decentralized web tension control system with the aid of some forms of interaction measures. Pagilla *et al.* [86] investigated the robust control of large-scale interconnected system for general interconnections and applied it to a decentralized web tension control system. Knittle *et al.* [87] applied decentralized robust H_∞ control to a three-tension-zone web winding system.

2) Overlapping Decentralized Control

Since a major problem on the decentralized controller design is mutual interactions among different subsystems or control sections, a natural solution is to identify them. Web winding system can be treated as an interconnected system of overlapping subsystems (the subsystems share common components). This leads researchers to consider control structures based on overlapping. Overlapping in decentralized control adds extra degrees of freedom that allow improvements from disjoint decomposition. This methodology of control assumes overlapping information of controlled variables obtained from a couple of subsystems [88, 89]. It is based on overlapping decomposition of the system, which includes system expansion based on inclusion principle [79], overlapping decomposition of the subsystem, controller design for each disjoint subsystem and stability check for the entire system. Sakamoto [90, 91] applied the overlapping decomposition concept to a web winding system and showed the results by decentralized PI control. Claveau [92] *et al.* extended the previous work by Knittel [31] to an overlapping decentralized control method and applied H_∞ control to each subsystem.

3.4 Summary

In this chapter, web tension control problem has been review in a systematic way. First, the control strategy regarding existing technique on control system structure, tension regulation methods and tension estimation have been reviewed. Then the problem has been expanded to large-scale decentralized control problems. Finally, background and literature review of decentralized control are then provided in detail.

CHAPTER IV

ACTIVE DISTURBANCE REJECTION CONTROL

Most control systems will unavoidably encounter disturbances, both internal (pertaining to unknown, nonlinear, time-varying plant dynamics) and external, and the system performance largely depends on how effectively the control system can deal with them. Thus, one of the original and fundamental problems in control theory is the problem of disturbance rejection. This led us to investigate disturbance rejection techniques.

This chapter will first investigate what is disturbance and how to rejection disturbances in terms of controller design. Then different disturbance rejection control strategies will be reviewed in detail. Based on the reviews, this chapter will focus on the disturbance observer based approaches. A novel active disturbance rejection strategy will be reviewed as a potential method to be applied in this dissertation. Finally, the central idea behind this strategy will be discussed for the applications in the following chapters.

4.1 Disturbance Rejection

Definition of Disturbance

Before going into the disturbance rejection topic, we want to clarify the definition of disturbance. A typical open-loop control system with disturbances and

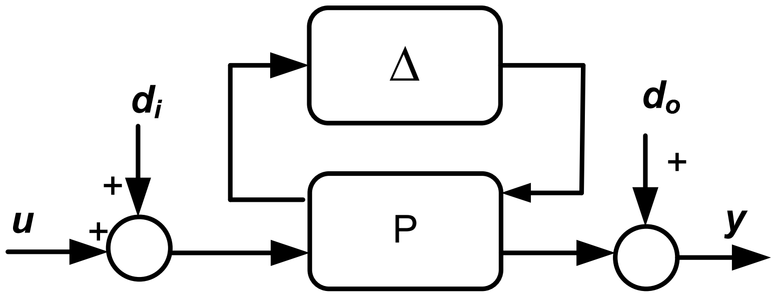

Figure 10: A generalized plant with disturbances and uncertainties

uncertainties introduced is shown in Figure 10, which consists of a plant P, an input disturbance d_i, an output disturbance d_o, and the generalized uncertainties Δ of the plant.

The external disturbance is independent of system states, which includes both the input disturbance d_i and the output disturbance d_o. The input disturbance is usually introduced into the control signal u and the output disturbance d_o is added to the output of the plant and contribute to the system output y.

In our new definition, we extended conventional notion of disturbance to a more general concept of a disturbance, which includes both the external disturbance d_i and d_o, and the unknown dynamics Δ. The unknown dynamics refer to the discrepancies between the real plant and its nominal model P_0, which represents the known information of the plant.

In summary, there are three disturbances definitions: Input disturbance (d_i), output disturbance (d_o), and generalized disturbance ($f(\cdot) = d_i + d_o + \Delta$). These disturbances will be studied in the following disturbance rejection framework.

How to Reject Disturbances?

Control theory related to disturbance rejection has focused in two main categories in terms of different patterns of disturbance rejection. One is the passive and the other one is active disturbance rejection method.

Passive Disturbance Rejection

Modern control methods, such as adaptive control and robust control, close the loop in Figure 10, which includes the disturbance to the feedback as shown in Figure 11, and design controller C to passively reject the disturbances to the effect of the plant. From this aspect, modern control methods fall into the passive disturbance rejection category.

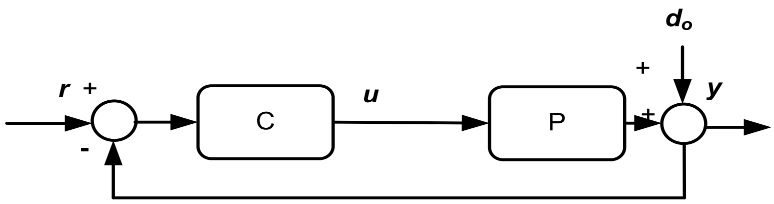

Figure 11: Passive disturbance rejection control diagram

Figuratively speaking, two technology upgrades are offered in the modern control framework: adaptive control [155] and robust control theory [156]. The former refers to a class of controllers whose gains are adjusted using a particular adaptation law to cope with the unknowns and changes in the plant dynamics; while the latter is based on the optimal control solution, assuming that the plant dynamics is mostly known and LTI, with the given bound on the uncertainties in frequency domain. The combination of the two offers the third alternative: robust adaptive control [157]. While these proposed solutions show awareness of the problem and progress toward solving it, they are far from resolving it because, among other reasons, they still rely on accurate and detailed mathematical model of the plant and they often produce solutions, such as the H_∞ design, that are rather conservative. Therefore, as improvements of, rather than departure from, the model-based design paradigm, adaptive control and robust control, as solutions to the disturbance rejection problem, didn't travel very far from their source: model-based classical control theory. Such approaches are deemed passive as they accept disturbances as they are and merely deal with them as one of the design issues, as opposed to the problem that the control system must contend with.

Active Disturbance Rejection

In regard to external disturbances, it is well known that good disturbance rejection is achieved with a high loop gain together with a high bandwidth, assuming that the plant is LTI and accurately described in a mathematical model. Things get a little complicated and interesting when such assumptions do not hold, as in most practical applications, where it is the internal disturbance that is most significant. In many regards, much of the literature on control can be seen as various responses to this dilemma. That is, how do we take a well-formulated and time-tested, classical control theory and apply it to Nonlinear and time-varying (NTV) and uncertain plants in the real world?

In contrast, from the 70s in the last century to the present, there have been many researchers, although scattered and overlooked for the most part, who suggested various approaches to disturbance rejection that, compared to the modern control framework, are truly active. They are distinctly different from the standard methods in that the disturbance, mostly external, is estimated using an observer and canceled out, allowing control design to be reduced to one that is disturbance free. Thus the disturbance rejection problem is transformed to the disturbance observer design, a survey of which can be found in [94]. To be sure, most of these disturbance observers, including the Disturbance Observer (DoB) [101, 97, 95], the Perturbation Observer

(PoB) [98, 99, 103], the Unknown Input Observer (UIO) [105, 95], can be traced to Internal Model Control (IMC) [102], where the LTI model of the plant is explicitly used in the observer design.

An illustration example of the active disturbance rejection paradigm is shown in Figure 12, where P_0 refers to the design model of the true plant P. In contrast to the passive disturbance rejection method, the active disturbance rejection method feeds back the estimation of disturbances $\hat{d}_o$ instead of the real disturbances d_o to the input reference r.

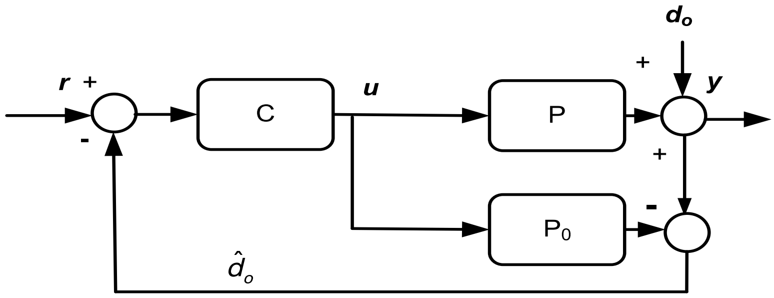

Figure 12: Active disturbance rejection diagram

4.2 Active Disturbance Rejection Techniques

Disturbance observer based approaches have gained much attention and are especially welcome by engineers for their easy implementation and practical successes. Since then, there were a number of works and its applications [96] - [100]. Although there exist diverse versions of the disturbance compensation method based on the identical idea with the disturbance observer, they share the same common characteristics, which have been formulated for linear systems in frequency domain with output feedback. The above schemes can be classified into two sets again. The first one is the inverse-plant-model based compensators including internal model control (IMC) [102], disturbance observer (DoB) [96] - [100], perturbation observer (PoB)

[98, 99, 103]. IMC was the first method to estimate and compensate external disturbances in Linear Time Variant (LTI) system. The original DoB was proposed by T. Umeno *et al.* [101] in 1991 in a 2-DOF of format following the idea of IMC. PoB is similar to DoB in concept but implemented in discrete time domain. The second one is the state space based methods, which can estimate both the internal states and external disturbances. Model estimation, unified input output (UIO), and extended state observer are among the three typical methods. ME was proposed in 1994 by A. Tornambe *et al.* [104] and assumed that up to $(n+1)^{st}$ order derivatives of the plant output should be measurable, which is not realistic in most industrial applications. UIO [105] is another variation of DoB, where the external disturbance is formulated as an augmented state and estimated using a state observer. ESO was proposed by Han [128, 129] in the active disturbance rejection control (ADRC) strategy, where the generalized disturbances are estimated by ESO as an extra state.

Herein, the above active disturbance rejection methods will be reviewed and studied in detail in terms of three different disturbances as follows.

4.2.1 Output Disturbance Rejection: Internal Model Control

IMC was published in 1970s and became widely known for the introduction by Garcia and Morari, and their unifying review in 1982 [107]. IMC relies on internal model principle Internal Model Principle (IMP), which states that it is necessary to place the disturbance dynamics in the feedback control loop for achieving asymptotic tracking.

IMC feedback the estimated disturbances $\hat{d}_o$ to the reference signal r, which is then added to the reference signal as the final input signal to the controller C. From the aspect of controller design, it is an open-loop mechanism, since the estimated disturbances are not compensated directly in the controller design.

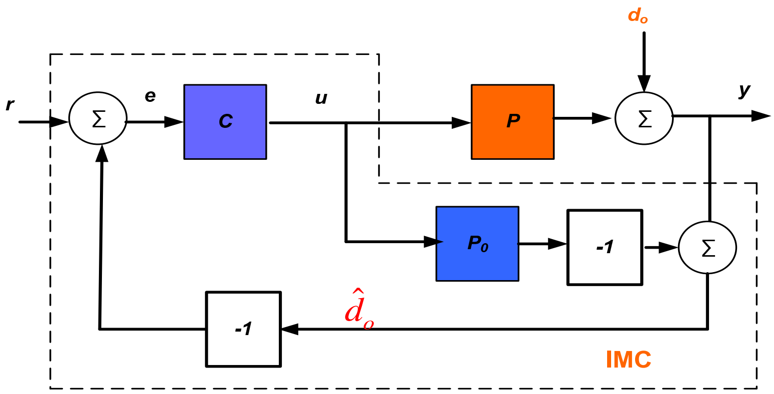

Figure 13: Diagram of the IMC

A general structure of IMC is shown in Figure 13, where d_o is the output disturbance, the manipulated u is introduced to both the plant P and its nominal plant P_o. The output y is compared with the nominal model, resulting an estimation of $\hat{d}$, which is

$$\hat{d}_o = (P - P_o)u + d_o \tag{4.1}$$

Assuming there is no noise and $P = P_o$, then $\hat{d}_o$ is equal to the unknown disturbance.

Remarks:

IMC was one of the earliest control method dedicated to estimate and compensate external disturbances in LTI system. The following disturbance observers are based on the idea of IMC. IMC was developed based on the assumption that plant always has an invertible transfer function. Therefore, a crucial step in applying IMC is system inversion.

4.2.2 Input Disturbance Rejection

Although originated from the idea of IMC, disturbance observers feedback the estimated disturbances into the controller u instead into the reference input r. From this respect, we call the disturbance observer based methods the closed-loop active disturbance rejection control.

Herein we review some of the famous disturbance observer based methods in terms of the time sequence to illustrate the idea of active disturbance rejection mechanism.

Unified Input Output (UIO)

In 1971, C. D. Johnson in [95] proposed a direct external disturbances cancellation method called disturbance accommodation control (DAC), which was later refereed as UIO by E. Schrijver [96]. Since then, there were other work on UIO, such as a discrete UIO in [105] and a modified UIO in [97].

UIO assumed that the input disturbance d can be generated by a fictitious autonomous dynamic system of order m as follows:

$$\begin{cases} d = C_d \xi \\ \dot{\xi} = A_d \xi \end{cases} \tag{4.2}$$

where A_d is a matrix of $m \times m$, and C_d is a matrix of $1 \times m$. The state space form of the nominal plant model is presented as follows:

$$\begin{cases} \dot{x} = Ax + Bu \\ y = Cx \end{cases} \tag{4.3}$$

where A is a matrix of $n \times n$, B is a matrix of $n \times 1$, and C is a matrix of $1 \times n$. The fictitious disturbance generator in (4.2) is then added to the original plant (4.3), resulting in the augmented plant as follows:

$$\begin{cases} \dot{v} = A_u v + B_u (u + d) \\ w = C_u v \end{cases} \tag{4.4}$$

where

$$A_u = \begin{bmatrix} A & BC_d \\ 0 & A_d \end{bmatrix}_{(n+m)\times(n+m)}, B_u = \begin{bmatrix} B \\ 0 \end{bmatrix}_{(n+m)\times 1}, C_u = [\ C \quad 0\ ]_{1\times(n+m)}$$

Based on (4.4), an observer is constructed as follows:

$$\dot{z} = A_u z + B_u u + L_u C_u (v - z) \tag{4.5}$$

where L_u is the observer gain vector.

The well designed observer in (4.5), is supposed to estimate not only the states of the plant, but also the states of the fictitious disturbance.

Remarks

Assuming the dynamics of the external disturbances are known, UIO is different from IMC in disturbance estimation. The advantage of UIO is, as a state observer, UIO estimates not only disturbances but also states. However, UIO assumed that both the models of the plant and the external disturbances are known. Accordingly, the disadvantage of UIO is that it required the models of the plant and the disturbances to build the observer and design controller.

Disturbance Observer (DoB)

The first DoB was proposed by T. Umeno *et al.* in [101] in 1991, where DoB was designed as the inner loop of a 2-DOF controller to reject external disturbances. It follows the same idea of IMC: separate the disturbances from the plant and cancel it. The only difference between DoB and IMC is that DoB deals with the input disturbance d_i rejection while IMC deals with the output disturbance d_o. Similar to the idea of UIO, DoB was implemented to estimate internal disturbance in the transfer function format.

DoB was implemented in frequency domain using a Q filter, which cuts off the disturbance in low frequency region. To some extent, the design of DoB, is the design of the low-pass Q filter.

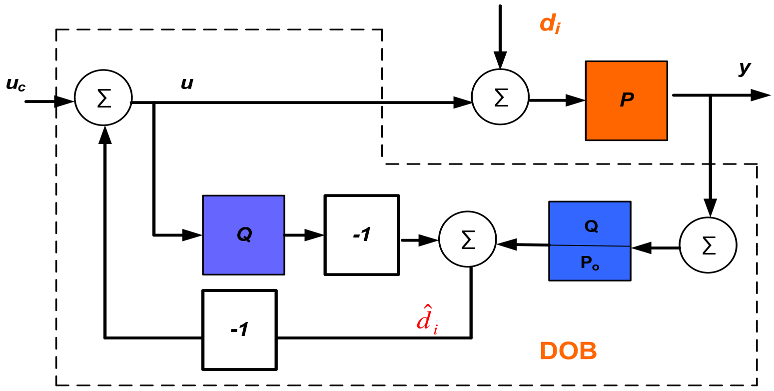

Figure 14: Diagram of the DoB

As shown in Figure 14, since the real plant P and its nominal model P_o are not equal in the real world, the difference between the control inputs to them can be estimated. Based on this observation, the estimation of external disturbance d_i, is obtained from the difference between control signal u and the output signal combined with the inverse of the nominal plant filtered by a Q filter. The DoB algorithm is expressed in the following equation:

$$\hat{d}_i = Q\left(\hat{P}_o^{-1} y - u\right) \tag{4.6}$$

Because the direct feedback would result in an algebraic loop, a filter is necessary in the DoB design. In addition, the Q filter can also filter the measurement noise in the feedback signal. Therefore, the design of the Q filer is an essential part of DoB.

Remarks

DoB simplifies the external disturbance rejection design to a low-pass filter design, which makes it easy to understand by industry. As a transfer function based design method, DoB also has the same disadvantages as IMC: it requires that the nominal plant model and its inverse are available.

Model Estimator (ME)

ME was proposed in 1994 by A. Tornambe *et al.* [104] for robust decentralized control of both SISO and MIMO systems.

For a n^{th} order system

$$\begin{cases} \dot{x}_1 = x_2 \\ \dots \\ \dot{x}_{n-1} = x_n \\ \dot{x}_n = a(x) + b(x)u \end{cases}, \tag{4.7}$$

ME assumed that all the states are measurable, and the functions $a(x)$ and $b(x)$ are known. The equation describing the dynamics of $\dot{x_n}$ can be rewritten as follows:

$$\dot{x}_n = f(x,u) + u \tag{4.8}$$

where $f(x,u) = a(x) + (b(x) - 1)u$.

The control law is designed as follows:

$$\begin{aligned} u &= -\beta_0 x_1 - \beta_1 x_2 - \dots - \beta_{n-1} x_n - \hat{f}(x,u) \\ &= \sum_{i=0}^{n-1} \beta_i x_{i+1} - \hat{f}(x,u) \end{aligned} \tag{4.9}$$

where

$$\begin{cases} \hat{f}(x,u) = g(x,u) + \sum_{i=0}^{n-1} k_i x_{i+1} \\ \dot{g}(x,u) = -k_{n-1} g - k_{n-1} \sum_{i=0}^{n-1} k_i x_{i+1} - \sum_{i=0}^{n-2} k_i x_{i+2} - k_{n-1} u \end{cases} \tag{4.10}$$

where $\beta_i, i = 0, \dots, n-1$, are positive constants, and $k_i, i = 0, \dots, n-1$ are arbitrary constants.

After some manipulations, the control law is obtained as follows:

$$u = -\frac{1}{b(x)}\left(\sum_{i=0}^{n-1}\beta_i x_{i+1} + a(x) - \tilde{f}(x,u)\right) \tag{4.11}$$

where $\tilde{f}(x,u) = f(x,u) - \hat{f}(x,u)$. The parameters $\beta_i, i = 0, \ldots, n-1$, are chosen so that the spectrum of the polynomial $\beta(s) = \beta_0 + \beta_1 s + \cdots, +\beta_{n-1}s^{n-1} + s^n$ is in the left half plane.

Remarks

ME can estimate unknown dynamics of the system by the mechanism shown above. Although rigorous stability proof is provided for ME, it is under the assumption that the plant model is completely known. Another disadvantage of ME is that, it assumed that the up to $(n-1)^{st}$ order derivatives of the plant output are measurable, which is not usually realistic in real world.

Summary

IMC, DoB, UIO and ME have been reviewed in terms of disturbance rejection mechanism. The common properties of these disturbance observers based methods are summarized as follows:

1) Adaptive Control Property: These methods can generate as much control effort as is required to compensate the current disturbances. This is a distinguished characteristics from other fixed gain robust control approaches where a sufficiently large deterministic gain is inevitable to cover the worst case of the disturbance. Hence they achieved the adaptive control property.

2) Integral Control Property: These methods can generate dynamic compensation terms based on the comparison between the external inputs and nominal plant, which characterize the typical integral control property.

3) Model-based Property: All these methods assume that the plant model is linear and known, and external disturbance is independent of the plant, which are the characteristics of the model-based methods.

Therefore, to apply these model-based methods, a linear model has to be extracted or simplified from the real plant. Even a linearized model is obtained, the inverse or pseudo-inverse of the plant model has to be derived for implementation of DoB and PoB.

Some differences among these disturbance observers are also summarized as follows:

1) IMC, DoB, PoB are based on linear transfer function, while ME and UIO are formulated in the state space form;

2) IMC, DoB, and PoB require the availability of the inverse of the plant model, and are designed to estimate the disturbance only. While UIO can estimate both the internal states and external disturbances, and ME can estimate unknown dynamics of the system.

3) Amongst these disturbance observers, only ME has provided the stability proof, while other methods only have frequency domain stability analysis.

4.2.3 Generalized Disturbance Rejection

The above model based disturbance observers have achieved a lot of successful applications. However, these disturbance rejection methods are designed for LTI systems and need a precise nominal model. We all know that most physical plants are nonlinear time-varying system, which cannot be described by the LTI nominal models that are used in these model-based disturbance rejection methods. Furthermore, most of the disturbances are arbitrary and cannot be readily identified. Therefore, some other approaches attempt to jump out of the box of model-based methodology, and can estimate and cancel the disturbances in real time. Among the few techniques to address this model independent control strategy, time-delay control (TDC), and active disturbance rejection control (ADRC), have attracted much attention as an effective robust, nonlinear control algorithm.

Furthermore, please note that the above active disturbance rejection methods are designed to estimated ONLY external disturbances. The following TDC and ADRC can estimate the generalized disturbances, which include both the external disturbances and the unknown dynamics.

Time Delay Control (TDC)

TDC was first introduced by Youcef-Toumi *et al.* [108, 109] in 1991 and was designed for control of systems with unknown dynamics and disturbances. This approach approximates the nonlinear dynamics and uncertainties with the time-delayed values of control inputs and derivatives of state variables at the previous time step and calculates the current control action that can quickly cancel unknown dynamics and unexpected disturbance.

Considering the following nonlinear differential equation:

$$\dot{x} = g(x) + b(x)u + d \tag{4.12}$$

where x denotes the state vector of the system, u denotes the input vector, $g(x)$ denotes the nonlinear function in companion form, which may be unknown, yet bounded, $b(x)$ denotes the control vector, and d denotes disturbances.

Introducing in (4.12) a constant matrix, $\hat{b}(x)$, representing the nominal value of $b(x)$, we can rearrange (4.12) into the following

$$\begin{aligned} \dot{x} &= g(x) + b(x)u + d \qquad (4.13) \\ &= \left[g(x) + (b(x) - \hat{b}(x))u + d\right] + \hat{b}(x)u \\ &= f(x, u, t) + \hat{b}(x)u \end{aligned}$$

where $f(x,u,t)$ denotes the total uncertainty including the uncertainty in the plant and disturbances. The control objective is to makes the plant in (4.12) follow accurately a desired error dynamics in the presence of unknown dynamics and unexpected disturbance. To get the desired error dynamics as follows

$$\dot{e} = A_m e \tag{4.14}$$

where $e = x_d - x$, denotes an error vector with x_d denoting the reference command vector, and A_m denoting the desired error dynamics matrix. The control law is designed as follows:

$$u(t) = \hat{b}^+ \left[\dot{x}_d - f(x,u,t) - A_m e\right] \tag{4.15}$$

where $\hat{b}^+$ denotes a pseudo-inverse of $\hat{b}$. $f(x,u,t)$ can be approximated by $\hat{f}(x,u,t)$ as follows:

$$\hat{f}(x,u,t) \approx f(x,u,(t-L)) = \dot{x}(t-L) - \hat{b}u(t-L) \tag{4.16}$$

where L denotes a sufficiently small time delay.

Combining (4.15) and (4.16), the final control law can be obtained as follows:

$$u(t) = \hat{b}^+ \left[\dot{x}_d - \hat{f}(x,u,t) - A_m e\right] = u(t-L) + \hat{b}^+ \left[\dot{x}_d - \dot{x}(t-L) - A_m e\right] \tag{4.17}$$

Remarks

TDC has shown advantages to deal with NTV system. However, to apply TDC to a plant, it is necessary to be able to measure all of the state variables and their derivatives. Unfortunately, this is not always the case in practice. In many plants, even state variables are not always available, not to mention their derivatives. Hence, the measurability requirement presents a serious limitation on the implementations of TDC to real plants.

Another variation of TDC is perturbation observer (PoB). As a special case of TDC, with the condition of $L = 1$ in discrete time domain, PoB assumes the actual disturbances change quite smoothly between each control interval. Assume the discrete nominal plant model is described as follows:

$$\begin{cases} x(k+1) = Ax(k) + B(u(k) + d(k)) \\ y = Cx(k) \end{cases} \tag{4.18}$$

At k time point, $x(k)$, $x(k-1)$, and $u(k-1)$ are known and can be used to calculate the previous external disturbance, $d(k-1)$, through the inverse operation as shown in the following equation:

$$\hat{d}(k-1) = B^{+}(x(k) - Ax(k-1)) - u(k-1) \tag{4.19}$$

Assuming that the external disturbance changes little from $(k-1)$ to k time interval, which means $d(k) \approx d(k-1)$, $\hat{d}(k)$ is obtained with a digital Q filter applied as follows:

$$\hat{d}(k) = Q(B^{+}(x(k) - Ax(k-1)) - u(k-1)) \tag{4.20}$$

Active Disturbance Rejection Control (ADRC)

In contrast to TDC, ADRC does not require the availability of the state variables and their derivatives. ADRC was first proposed by J. Han in 1995 [127, 128] and further simplified and parameterized by Gao [139, 140], respectively. ADRC shares the same idea of TDC because both of them do not require an exact mathematical model and be able to robust to a wide range of uncertainties and disturbances. However, ADRC has gone further by attaching an extended state observer (ESO), which only require the plant input-output data, and not necessarily require measuring all of the state variables and their derivatives as required by TDC.

ADRC stipulates that if any external disturbances and unknown dynamics can be estimated in real time, then they can be compensated and canceled without an explicit modeling of the disturbances and unknown dynamics. The extended state observer is then designed to achieve the online estimation function, with an augmented state estimating the combination of the unknown dynamics and disturbances to the internal states.

Up to now, ADRC has been successfully implemented in a wide range of applications including motion control [132, 133, 134], jet engine control [135], MEMS Gyroscope control [136] and process control [137], etc.

4.3 Proposed Active Disturbance Rejection Control - ADRC

The ADRC with ESO control strategy, therefore, can estimate the effect of any unknown dynamics (internal or external) and compensate in real time via ESO. From the aspect of disturbance estimation and compensation, there is nothing novel from ADRC compared with TDC. However, the estimation by ESO is novel and different from other methods. From this aspect, the design of the ESO is thus the key element of ADRC. ESO was first proposed by Han [127] using nonlinear functions to make the observer more efficient. It was selected heuristically based on experimental results. Although the nonlinear functions make the observer work better, it increases the complexity and makes the parameter tuning process a nightmare. Gao [139] parameterized the tuning process and simplified to the linear case. In this dissertation, the discussion about ADRC is limited to the linear ADRC.

Consider a general nonlinear n^{th}-order minimum phase systems represented by:

$$y^{(n)} = f(y, \dot{y}, \cdots, y^{(n-1)}, w, u) + bu \tag{4.21}$$

where y is the system output, u is the control signal, b is a constant and w represents external disturbances. $f(y, \dot{y}, \cdots, y^{(n-1)}, w, u)$ is the function describing the system dynamics, which includes unknown dynamics and external disturbances.

In the ADRC framework, the external disturbance (w) and unknown dynamics are combined to form a generalized term $f(y, \dot{y}, \cdots, y^{(n-1)}, w, u)$. For the sake of simplicity, here we simply call it $f(\cdot)$. The entire $f(\cdot)$ is assumed unknown and denoted as the *total disturbance*. It is the combination of the internal dynamics of the system and external disturbance. If the total disturbance can be estimated and cancelled, the system is then reduced to a simple n^{th}-order integral plant with a scaling factor b, making the control problem much easier.

Instead of following the traditional design path of modeling and obtaining the explicit mathematical expression of $f(\cdot)$, ADRC seeks to actively estimate and then cancel $f(\cdot)$ in real time, thereby reducing the problem to the control of an integral plant as follows:

$$u = (-\hat{f}(\cdot) + u_0)/b \tag{4.22}$$

which reduces the plant in (4.21) to

$$y^{(n)} = f(\cdot) - \hat{f}(\cdot) + u_0 \approx u_0 \tag{4.23}$$

At this point, the original unknown NTV plant of (4.21) is transformed to a simple plant that is quite easy to control. This is the key idea and main benefit of ADRC. It only works, of course, if $f(\cdot)$ can be estimated effectively, which is the problem to be discussed next.

ESO

An extended state observer (ESO) is designed to achieve the online estimation of $f(\cdot)$ with an augmented state estimating the combination of the unknown dynamics and disturbances $f(\cdot)$ to the internal states. Define $x = [x_1, x_2, \ldots, x_n, x_{n+1}]^T =$

$[y, \dot{y}, \cdots, y^{(n-1)}, f]^T$, the plant in (4.21) can be rewritten in the following form:

$$\begin{cases} \dot{x}_1 = x_2 \\ \vdots \\ \dot{x}_{n-1} = x_n \\ \dot{x}_n = x_{n+1} + bu \\ \dot{x}_{n+1} = \eta \end{cases} \tag{4.24}$$

where η is the derivative of $f(\cdot)$ and is unknown. The reason for increasing the order of the plant is to make $f(\cdot)$ a state set, such that a state observer can be used to estimate it. Han [128] proposed a nonlinear observer of the following form:

$$\begin{cases} \dot{z}_1 = z_2 + g_1(y - z_1) \\ \vdots \\ \dot{z}_{n-1} = z_n + g_{n-1}(y - z_1) \\ \dot{z}_n = z_{n+1} + g_n(y - z_1) + bu \\ \dot{z}_{n+1} = g_{n+1}(y - z_1) \end{cases} \tag{4.25}$$

where z_i is the estimate of y^{i-1}, and z_{n+1} is the estimation of the extended state η. $g_i(\cdot)$, $i = 1, \cdots, (n+1)$, are appropriate nonlinear functions, which are used to make the observer more efficient. Intuitively, it is a nonlinear gain function, where small errors correspond to higher gains.

However, the ESO is hard to tune for so many parameters, Gao [140] then parameterized it to a linear case as follows:

$$\begin{cases} \dot{z}_1 = z_2 + l_1(y - z_1) \\ \vdots \\ \dot{z}_{n-1} = z_n + l_{n-1}(y - z_1) \\ \dot{z}_n = z_{n+1} + l_n(y - z_1) + bu \\ \dot{z}_{n+1} = l_{n+1}(y - z_1) \end{cases} \tag{4.26}$$

where l_i are the linear gain parameters to be determined later. The proposed linear observer is therefore denoted as the linear extended state observer (LESO). The observer gain vector $l = [l_1, \ldots, l_{n+1}]^T$, can be obtained using any known method, such as the pole-placement technique. Gao [130] proposed to place all the poles at the same location to reduce the number of tuning parameters. The observer gains are solved as functions of a single tuning parameter, ω_o.

Control Law

With the well-tuned ESO, such that z_1, z_2,... and z_{n+1} closely track y, $\dot{y}$, ... and $f(\cdot)$, respectively. The control law

$$u = (u_0 - z_{n+1})/b \tag{4.27}$$

then reduces the plant to $y^{(n)} = (f(\cdot) - z_{n+1}) + u_0 \approx u_0$, and the control law can be designed as

$$u = \frac{1}{b}\left[k_0(y_{r1} - z_1) + k_1(y_{r2} - z_2) + \cdots + k_{n-1}(y_{rn} - z_n) - z_{n+1}\right] \tag{4.28}$$

where $y_r = [y_{r1}, y_{r2}, \ldots, y_{rn}]^T$ is the reference signal, k_i is the control gains and can be parameterized as the function of the bandwidth of the closed-loop system, ω_c, which can be tuned later.

Remarks

1. ADRC can be viewed as the combination of TDC and DoB. However, ESO extended an extra state to estimate $f(\cdot)$ and does not require the plant model, which is different from other model based disturbance observers, such as IMC, DoB, UIO, PoB, and ME.

2. The design parameters are ω_c and ω_o. The only actual tuning parameter is ω_o, since ω_o is generally chosen as several times larger than ω_c. The only plant

information needed is the approximate value of b. Since this parameter has clear physical meanings, it is assumed that we have reasonable knowledge of it.

Note that the unknown external disturbance and the internal uncertain dynamics are combined and treated as a generalized disturbance. The novelty of this approach is the augmentation of the observer, which allows the unknown term $f(\cdot)$ to be actively estimated and canceled, thereby achieving active disturbance rejection.

The architecture of ADRC is shown in Figure 15, which composed of two main parts, the controller and the observer ESO,where $w(t)$ is the external disturbance, y_d is the desired reference signal, and b is the coefficient of the control input $u(t)$. The critical component here is obviously the ESO.

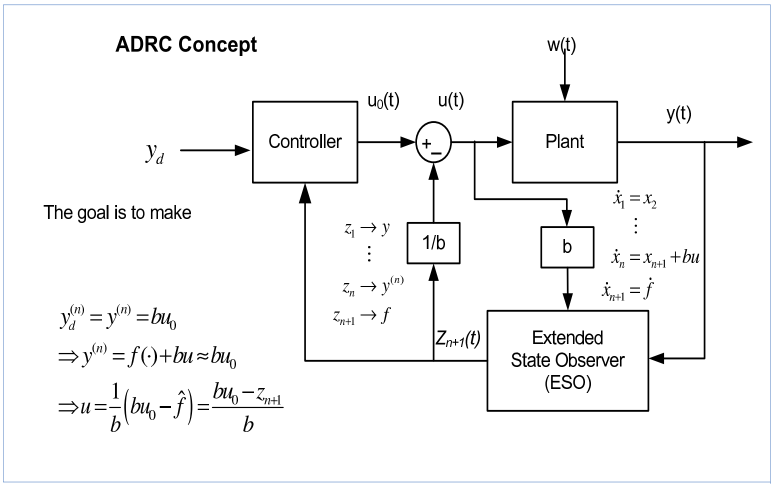

Figure 15: An illustration of ADRC configuration

CHAPTER V

TENSION AND VELOCITY REGULATION IN ACCUMULATORS

5.1 Introduction

In this chapter, the accumulator in a large-scale web winding system is studied. Although much work has been done in tension control of a web [4, 7, 8, 10, 12, 13], very little is known in modeling and control of accumulators in web processing lines. An overview of the lateral and longitudinal behavior and control of moving webs was presented in [8]. A review of the problems in tension control of webs can be found in [19]. Discussions on tension control versus strain control and torque control versus velocity control were given in [13].

Both open-loop and close-loop methods are commonly used in web processing industries for tension control purposes. In the open-loop control case, the tension in a web span is controlled indirectly by regulating the velocities of the rollers at either end of the web span. An inherent drawback of this method is its dependency on the knowledge of an accurate mathematical relationship between the velocities and tension, which is highly nonlinear and highly sensitive to velocity variations. Still, simplicity of the controller outweighs this drawback in many applications. Closing the tension loop with tension feedback is an obvious solution to improve accuracy and reduces sensitivity to modeling errors. It requires tension measurement, for example, through a load cell, but can be justified by the resulting improvements in tension regulation.

Some researchers have proposed to design tension observers in place of tension measurements, which could reduce the hardware complexity and cost. One trade-off is the increased complexity in the control algorithm and its tuning. In addition, the discrepancies between the estimated and the actual tension will likely cause the performance of the tension loop to suffer. The design of the observer also requires a fairly accurate mathematical model of the tension dynamics, which may not be available. It is not surprising to see that most of today's tension feedback loops employ tension measurement.

Accumulators in web processing lines constitute an important element in all of the web processing lines. Functional importance of these in web processing lines is quite substantial as they are primarily responsible for continuous operation of web processing lines. A preliminary study on modeling and control of accumulators is given in [144]. A dynamic model for accumulator spans that consider the time-varying nature of the span length was developed in [119].

In this chapter, control of the accumulator carriage in conjunction with control of the driven rollers both upstream and downstream of the accumulator is considered. The average dynamic model developed in [144] is further simplified based on practical observations and is used for controller design. A robust disturbance rejection control strategy is proposed for a class of tension and velocity regulation problems found in accumulators. The proposed control system actively estimates and rejects the effects of both dynamic changes in the system and external disturbances. Both open-loop and closed-loop tension regulation schemes are investigated. A tension observer is designed in order to facilitate close-loop tension control in the absence of a tension transducer. The performance of existing schemes and the proposed ones are compared in the end.

5.2 Dynamic Behavior of the Accumulator

A typical web processing line includes an entry section, a process section and an exit section. Operations such as wash and quench on the web are performed in the process section. The entry and exit section are responsible for web unwinding and rewinding operations with the help of accumulators located in each sections.

Accumulators are primarily used to allow for rewind or unwind core changes while the process continues at a constant velocity. Dynamics of the accumulator directly affect the behavior of web tension in the entire process line. Tension disturbance propagates along both the upstream and downstream of the accumulator due to the accumulator carriage.

Since there is no difference between the entry accumulator and exit accumulator, except that one is for unwinding and the other is for rewinding operations. The focus of this section is the exit accumulators. A sketch of the exit accumulator is shown in Figure 16, which includes a carriage and N web spans.

As a special case of web transporting system, the accumulator's span length varies with the motion of the carriage. From Newton's law and the dynamics of the general web span, a modified tension model is obtained by considering the average tension dynamics in [27]. The dynamics of the carriage tension and the entry/exit

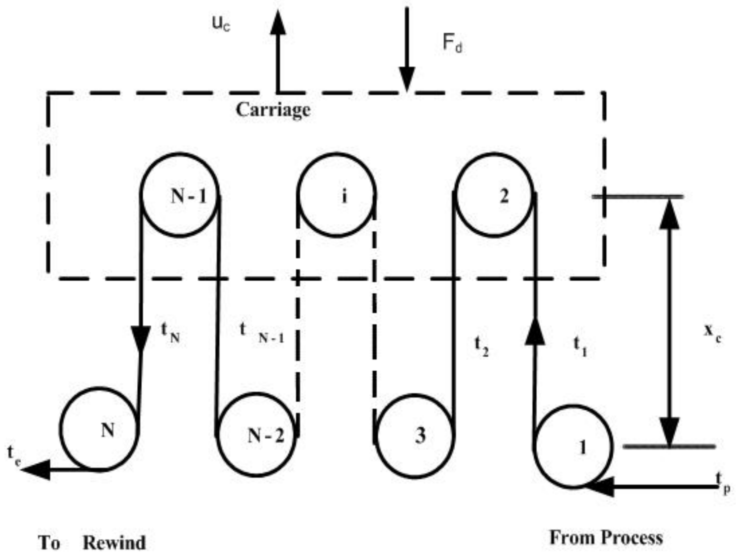

Figure 16: A sketch of an exit accumulator

rollers in the accumulator are summarized in [29] as follows:

$$\dot{t}_c(t) = \frac{AE}{x_c(t)}\left(v_c(t) + \frac{1}{N}\left(v_e(t) - v_p(t)\right)\right) \tag{5.1}$$

$$\dot{x}_c(t) = v_c(t) \tag{5.2}$$

$$\dot{v}_c(t) = \frac{1}{M_c}\left(-Nt_c(t) - V_f v_c(t) - F_d(t) + u_c(t)\right) - g \tag{5.3}$$

$$\dot{v}_e(t) = \frac{1}{J}(-\beta_f v_e(t) + R^2(t_r - t_c(t)) + RK_e u_e(t) - R^2\delta_e(t)) \tag{5.4}$$

$$\dot{v}_p(t) = \frac{1}{J}(-\beta_f v_p(t) + R^2(t_c(t) - t_r) + RK_p u_p(t) + R^2\delta_p(t)) \tag{5.5}$$

where $v_c(t)$,$v_e(t)$ and $v_p(t)$ are the carriage velocity, exit-side and process-side web velocity, respectively. $x_c(t)$ is the carriage position, t_r is the desired web tension in the process line and $t_c(t)$ is the average web tension. N is the number of web spans. $u_c(t)$, $u_e(t)$ and $u_p(t)$ are the carriage, exit-side and process-side driven roller control inputs, respectively. The disturbance force, $F_d(t)$, represents the friction in the carriage guides, rod seals and other external forces on the carriage. K_e and K_p are positive gains. $\delta_e(t)$ and $\delta_p(t)$ are disturbances on the exit side and process line. The other constant coefficients in (5.1) to (5.5) are described in Table I.

Table I: Plant Coefficients

	Values	Discriptions
M_c	$7310\ kg$	Mass of the carriage
A	$35.07 \times 10^{-4}\ m^2$	Cross sectional area of web
E	$6.90 \times 10^7\ N/m^2$	Modulus of elasticity
R	$0.1524\ m$	Radius of roller
N	34	Number of web spans
J	$2.1542\ kg \cdot m^2$	Moment of inertia
V_f	$35.037 \times 10^5\ N \cdot s/m$	Viscous friction coefficient
β_f	$2.25 \times 10^{-3}\ N \cdot m \cdot s$	Bearing friction coefficient

5.3 Design Considerations

5.3.1 Design Objective

The objective of the control system design is to determine a control law such that the carriage velocity $v_c(t)$, exit velocity $v_e(t)$, process velocity $v_p(t)$ as well as the tension $t_c(t)$, all closely follow their desired trajectories. It is assumed that $v_c(t)$, $v_e(t)$ and $v_p(t)$, are measured and available as feedback variables. The controller also needs to satisfy the following design specifications:

- Response of the tension and the roller speed should be as quick as possible;
- Tension control performance should be kept to guarantee the required product quality;
- The effect of interaction and disturbance should be suppressed as much and as quickly as possible;
- The entire closed-loop system should be robust to parameter uncertainties and disturbances.

5.3.2 Existing Control Methods

Industry Controller (IC)

PID is still the predominant method in industry, and web applications are no exception. It is simple to use and easy to set up, but its performance is obviously very limited. Over the years, practicing engineers address the performance limitation by adding feed-forward terms inside the PID algorithm. One such industry controller (IC) is described in the literature [29] for the position and velocity control of the accumulator carriage, the exit-side driven roller and process-side driven roller. The control law is described as follows:

$$u_{cI}(t) = M_c(\dot{v}_c^d(t) + g + \frac{v_f}{M_c}v_c^d(t) + \frac{N}{M_c}t_c^d) \tag{5.6}$$

$$u_{eI}(t) = \frac{J}{RK_e}(\frac{B_f}{J}v_e^d(t) + \dot{v}_e^d(t) - k_{pe}e_{ve}(t) - k_{ie}\int e_{ve}(\tau)d\tau) \tag{5.7}$$

$$u_{pI}(t) = \frac{J}{RK_p}(\frac{B_f}{J}v_p^d(t) + \dot{v}_p^d(t) - k_{pp}e_{vp}(t) - k_{ip}\int e_{vp}(\tau)d\tau) \tag{5.8}$$

where e_{ve} and e_{vp} are the tracking errors defined as: $e_{vp}(t) = v_p(t) - v_p^d(t)$, $e_{ve}(t) = v_e(t) - v_e^d(t)$. $u_{cI}(t)$, $u_{eI}(t)$ and $u_{pI}(t)$ are the carriage, exit-side and process-side driven roller control inputs. v_c^d, v_e^d and v_p^d are the desired velocity of carriage, exit-side, and process-side rollers, respectively, and $\dot{v}_c^d, \dot{v}_e^d, \dot{v}_p^d$ are their derivatives. k_{pe} and k_{pp} are proportional gains and k_{ie}, k_{ip} are integral gains of the PID controller.

Lyapunov Based Control (LBC)

To make the control design more systematic, researchers have been working on advanced design methods based on the mathematical model of the accumulator. For example, a Lyapunov based control (LBC) method is proposed in [29], which results in the following control law:

$$u_c(t) = M_c(\dot{v}_c^d(t) + g + \frac{v_f}{M_c}v_c^d(t) + \frac{N}{M_c}t_c^d - \frac{AE}{x_c(t)}\hat{e}_{tc}(t) - e_{xc}(t) + \frac{N}{M_c}\hat{e}_{tc}(t) - \gamma_3 e_{ve}(t)) \tag{5.9}$$

$$u_e(t) = \frac{J}{RK_e}(\frac{B_f}{J}v_e^d(t) + \dot{v}_e^d(t) - \gamma_e e_{ve}(t) - (\frac{AE}{Nx_c(t)} - \frac{R^2}{J})\hat{e}_{tc}(t) - \frac{R^2}{J}\delta_e \operatorname{sgn}(e_{ve})) \tag{5.10}$$

$$u_p(t) = \frac{J}{RK_e}(\frac{B_f}{J}v_p^d(t) + \dot{v}_p^d(t) - \gamma_p e_{vp}(t) - (\frac{AE}{Nx_c(t)} - \frac{R^2}{J})\hat{e}_{tc}(t) - \frac{R^2}{J}\delta_p \operatorname{sgn}(e_{vp})) \tag{5.11}$$

Tension is estimated based on the error dynamics of the velocity loops, such that

$$\begin{cases} \dot{\hat{t}}_c(t) = (\dfrac{2AE}{x_c(t)} - \dfrac{N}{M_c})e_{vc}(t) + (\dfrac{2AE}{Nx_c(t)} - \dfrac{R^2}{J})(e_{ve}(t) - e_{vp}(t)) \\ \hat{t}_c(0) = \hat{t}_{c0} \end{cases} \tag{5.12}$$

where γ_3, γ_e and γ_p are the controller gains to be selected.

The related tracking errors are defined as follows: $e_{tc}(t) = t_c(t) - t_c^d(t)$, $\hat{e}_{tc}(t) = \hat{t}_c(t) - t_c^d$, $\tilde{e}_{tc}(t) = t_c(t) - \hat{t}_c(t)$, $e_{vc}(t) = v_c(t) - v_c^d(t)$, $e_{xc}(t) = x_c(t) - x_c^d(t)$.

5.3.3 Why New Solutions Are Needed

Tension and velocity control in the accumulator is a challenging problem for the following reasons:

- There is a strong coupling between the carriage dynamics, strip tension dynamics and the roller dynamics;
- The tension dynamics are highly nonlinear and sensitive to velocity variations;
- The coefficients of (5.1) to (5.5) are highly dependent on the operating conditions and web material characteristics, and vary with conditions;
- There are extensive external disturbances, which propagate through the system and even make the system unstable in some cases.

Since the velocities are controlled in open-loop by feed-forward and classical PI control method, the industry controller needs to be re-tuned when the operating conditions are changed or when the external disturbance appears. In addition, the industrial controller has a poor performance in the presence of disturbance. LBC improves the industrial controller by adding auxiliary error feedback terms to get better performance and disturbance rejection. However, it is designed specifically to deal with disturbances of certain kinds. When the module uncertainties and other unexpected disturbances appear in the real world, the performance may not be adequate.

5.4 Proposed Control Strategy

In developing new solutions for this difficult industry problem, performance and simplicity are stressed. That is, the new controller must have a much better performance than the existing ones, and it should also be simple to design, implement, and tune. A key observation in this research is that there are two control problems to consider: velocity and tension. The three velocity loops are very similar in nature and finding a better solution would be a good first step. The tension problem is crucial because of its nonlinear dynamics and the coupled relationship with velocity loops. The velocity control problem below will be addressed first, followed by the solutions to the tension control problem.

5.4.1 A New Solution for Velocity Control

Velocity loop control in the accumulator is the key to the tension loop control since they are coupled with each other. ADRC is known for its efficient disturbance rejection control. It is also a good candidate for decoupling control by treating all the unknown coupled dynamics as one generalized term $f(\cdot)$ and cancel it in real time with the help of ESO. In this case, ADRC will be applied to the velocity loop control by treating the coupling tension dynamics as disturbances and thereby decoupling the tension dynamics from velocity loops.

In order to apply ADRC to velocity loop control, we need to formulate the velocity loops and rewrite the velocity equations (5.3)-(5.5) as follows:

$$\dot{v}_c(t) = f_c(t) + b_c u_c(t) \tag{5.13}$$

$$\dot{v}_e(t) = f_e(t) + b_e u_e(t) \tag{5.14}$$

$$\dot{v}_p(t) = f_p(t) + b_p u_p(t) \tag{5.15}$$

where

$$\begin{aligned} f_c(t) &= \frac{1}{M_c}(-Nt_c(t) - F_d(t) - M_c g) && (5.16) \\ f_e(t) &= \frac{1}{J}(-B_f v_e(t) + R^2(t_r - t_c(t)) - R^2\delta_e(t)) && (5.17) \\ f_p(t) &= \frac{1}{J}(-B_f v_p(t) + R^2(t_c(t) - t_r) + R^2\delta_p(t)) && (5.18) \end{aligned}$$

The plants in (5.13)-(5.15) are all of the form

$$\dot{v}(t) = f(t) + bu(t) \tag{5.19}$$

where $v(t)$ is the velocity to be controlled, $u(t)$ is the control signal, and the value of b is known, approximately. $f(t)$ represents the combined effects of internal dynamics and external disturbance. From (5.19), it can be seen that it is exactly the format of the first-order ADRC control problem as described in section 4.3. Following the general ADRC design procedure, we will first design a second-order ESO and then design an ADRC controller.

Second-order ESO Design:

Rewrite the plant (5.19) in a state space form as follows:

$$\begin{cases} \dot{x}_1 = x_2 + bu \\ \dot{x}_2 = h \\ y = x_1 \end{cases} \tag{5.20}$$

Let $x_1 = v$, with $x_2 = f(\cdot)$ added as an augmented state, and $\eta = \dot{f}(\cdot)$ as unknown disturbance. The state space model of (5.20) is obtained as follows:

$$\begin{cases} \dot{x} = Ax + Bu + E\eta \\ y = Cx \end{cases} \tag{5.21}$$

where

$$A = \begin{bmatrix} 0 & 1 \\ 0 & 0 \end{bmatrix}, B = \begin{bmatrix} b \\ 0 \end{bmatrix}, C = \begin{bmatrix} 1 & 0 \end{bmatrix}, E = \begin{bmatrix} 0 \\ 1 \end{bmatrix}$$

Based on (5.21), $f(\cdot)$ can be estimated by LESO, which is constructed as follows:

$$\begin{cases} \dot{z}_1 = z_2 + L_1(y - z_1) + bu \\ \dot{z}_2 = L_2(y - z_1) \end{cases} \tag{5.22}$$

where L_1 and L_2 are the design parameters. By setting $\lambda(s) = |sI - (A - LC)| = s^2 + L_1 s + L_2$ equal to the desired error dynamics, $(s + \omega)^2$, the observer gains are solved as functions of a single tuning parameter, ω_o. It is demonstrated in [139] that $L_1 = 2\omega_o$, $L_2 = \omega^2$ can be parameterized and assign eigenvalues of the observer to $-\omega_o$.

With a functioning LESO, which results in $z_1 \rightarrow v$ and $z_2 \rightarrow f(\cdot)$, the control law will be designed as follows:

$$u = (-z_2 + u_0)/b \tag{5.23}$$

This reduces the plant to an approximate integral plant

$$\dot{v}(t) = (f(t) - z_2(t)) + u_0(t) \approx u_0(t) \tag{5.24}$$

which can be easily controlled by

$$u_0(t) = k_p(r(t) - z_1(t)) \tag{5.25}$$

By setting the controller equal to the desired transfer function, $\omega_c/(s + \omega_c)$, the controller gains are solved as functions of one tuning parameter, ω_c. Set $k_p = \omega_c$, where ω_c is the desired closed-loop bandwidth.

Remarks

1. To show how z_2 converges to f, it is clear from (5.19) that $f = \dot{v} - bu$. After solving (5.22) and (5.24) for z_2 by superposition, the result is simply a filter version of f as follows:

$$z_2(s) = (sv(s) - bu(s))\frac{\omega_0^2}{(s+\omega_0)^2} \tag{5.26}$$

where the term $\frac{\omega_0^2}{(s+\omega_0)^2}$ is a second-order filter.

2. The LESO is further simplified by substituting (5.21) from (5.20) to remove an algebraic loop and decouple z_2, allowing ADRC to be presented in PID form as follows:

$$u = k_p(r - z_1) - \frac{b}{L_2}\int (y - z_1)dt \tag{5.27}$$

3. The disturbance observer-based PD controller achieves zero steady state error without using an integrator in the controller.

4. The PD controller can be replaced with other advanced controller if necessary.

5. The tuning parameters are ω_c and the only model parameter needed is the approximate value of b in (5.19).

The diagram for the above controller combines with the LESO (5.21 - 5.23) is shown in Figure 17. It is applied separately for all three velocities loops.

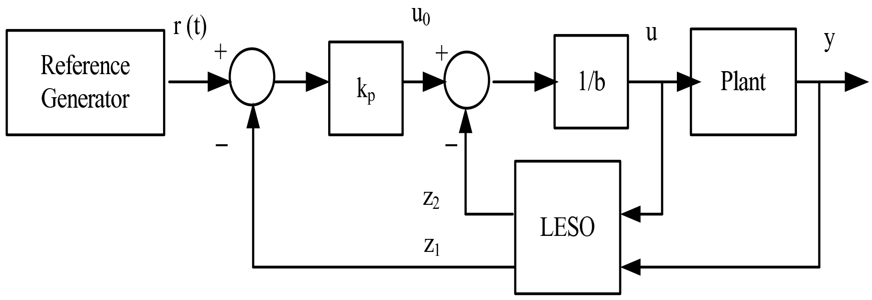

Figure 17: ADRC based velocity control

5.4.2 Tension Control Methods

Both open-loop and close-loop solutions to tension regulation will be discussed in this section. The open-loop tension control is simple and economic, while the closed-loop tension control is more precise but requires an additional sensing device.

Open-Loop Tension Regulation

High quality velocity regulation allows the tension to be controlled open-loop, if the model of the tension dynamics (5.1) is accurate. From (5.1), the tension can be computed as

$$t_c(t) = t_c(0) + \int_0^t \frac{AE}{x_c(t)}(v_c(t) + \frac{1}{N}(v_e(t) - v_p(t)))dt \tag{5.28}$$

where $t_c(0)$ is the initial value of tension.

For the open-loop control, let the desired velocities: v_c^d, v_e^d, and v_p^d, be carefully chosen so that (5.28) yields

$$t_c(t) = t_c^d, t \geq t_1 \tag{5.29}$$

For a given initial condition $t_c(0)$ and a given time constraint t_1, if all three velocity loops are well-behaved, the actual tension should be close to the desired value. This method will be tested in simulation in a later section. Note that, for this purpose, the desired velocities must satisfy the following condition

$$v_c^d(t) = -\frac{v_e^d(t) - v_p^d(t)}{N}, t \geq t_1 \tag{5.30}$$

The above approach is a low cost, open-loop solution. As the operating condition changes, the tension dynamics (5.1) could vary, causing variations in tension. For the tension is not measured, such variations go unnoticed until visible effects on the product quality appear. To maintain accurate tension control, industry users usually are willing to install a tension sensor, which regulates the tension in a feedback loop, as discussed below.

Observer-based Closed-loop Tension Regulation

A tension transducer, such as a load cell, can be used for closed-loop tension control. Nevertheless, it requires installing physical instruments, additional machine space, and new adjustments. Therefore, implementing tension control without tension sensors would be beneficial from an economic point. For this purpose, a tension observer is designed in this section.

Recall in (5.1)-(5.5), tension is coupled with velocity loops, and we use an ADRC controller to decouple the tension from the velocity loops. Actually, tension is thrown into $f(\cdot)$ part, which is estimated and canceled out in ESO.

Let us look at the function $f(\cdot)$ in three velocity loops, and it turns out that if the other terms of $f(\cdot)$ are known, tension can be estimated through equation (5.16)-(5.18) and presented as follows:

$$\begin{aligned} \hat{t}_{cc}(t) &= -\frac{M_c}{N}(f_c(t) + \frac{1}{M_c}(-F_d(t) - M_c g)) && (5.31) \\ \hat{t}_{ce}(t) &= \frac{1}{R^2}(-Jf_e(t) - B_f v_e(t) + R^2 t_r) && (5.32) \\ \hat{t}_{cp}(t) &= \frac{1}{R^2}(Jf_p(t) + B_f v_p(t) + R^2 t_r) && (5.33) \end{aligned}$$

With an efficient LESO, $z_1 \rightarrow v$ and $z_2 \rightarrow f(\cdot)$. That is, from ESO, $f_c(t)$, $f_e(t)$ and $f_p(t)$ can be obtained. Since the other parts in $f(t)$ are all known in this problem, tension estimation from three velocity loops can be calculated based on (5.31)-(5.33). Finally, the tension observer is obtained from the average of three tension estimations.

$$\hat{t}_c(t) = \frac{1}{3}(\hat{t}_{cc}(t) + \hat{t}_{ce}(t) + \hat{t}_{cp}(t)) \tag{5.34}$$

The complete block diagram for the velocity and tension control loops are illustrated in Figure 18.

The simulation results are shown in the next section, where the proposed method is compared to the two previous methods.

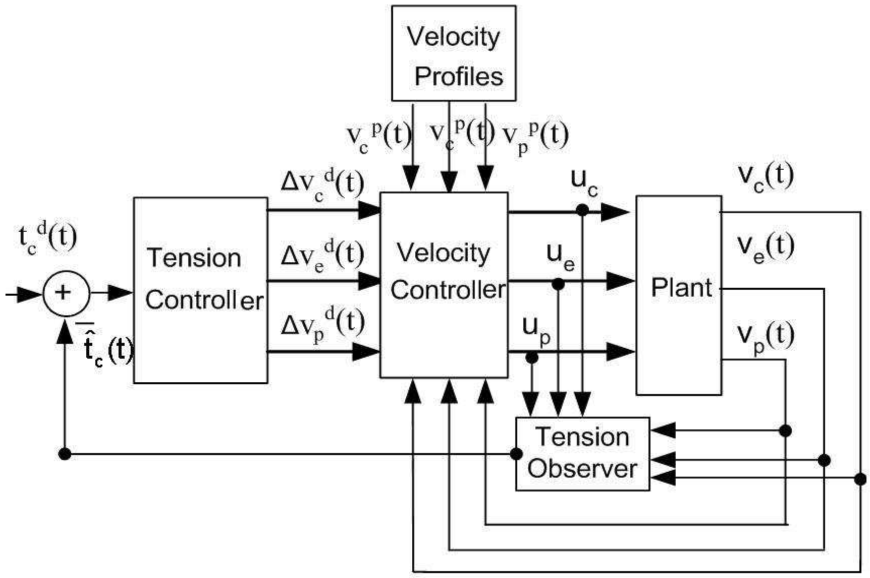

Figure 18: Configuration of ADRC based tension/velocity control system

5.4.3 Simulation and Comparison

In this section, four types of control systems are compared via simulations, including:

1) IC in equations (5.6) to (5.8);

2) LBC in equations (5.9) to (5.11);

3) Open-loop tension control;

4) Closed-loop tension control.

The comparison of these controllers is carried out in the presence of disturbances. In addition, to demonstrate the feasibility of the proposed methods, they are implemented in discrete-time form with a sampling period of 10 ms.

A. Simulation Setup

The control schemes are investigated by conducting simulations of an industrial continuous web processing line. The desired tension in the web span is 5180 N. The desired process speed is 650 fpm. A typical scenario of the exit speed and the carriage speed during a rewind roll change is depicted in Figure 19.

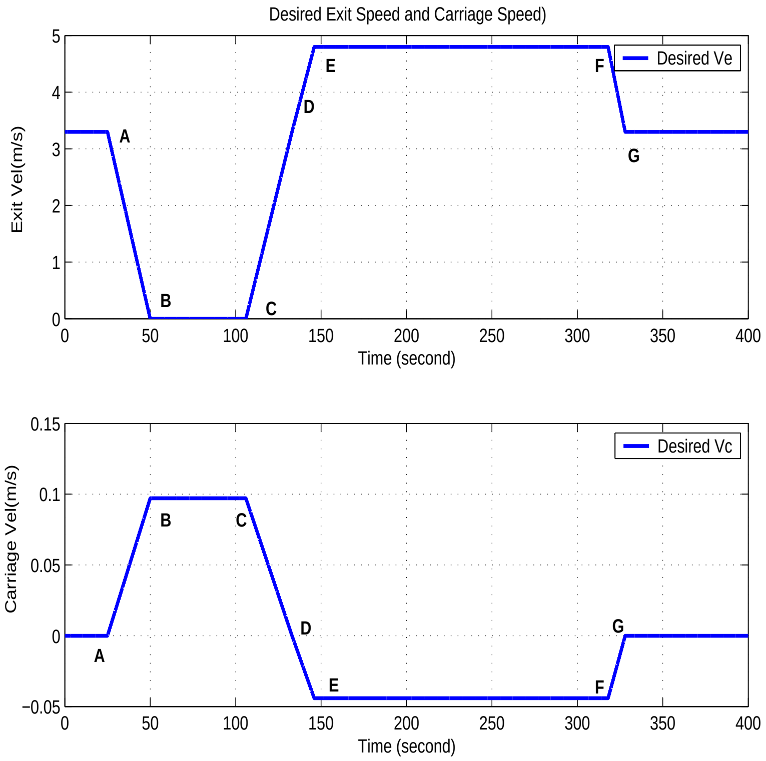

Figure 19: Desired exit speed and the carriage speed

To make the simulation results realistic, three sinusoidal disturbances are injected. $F_d(t)$ in (5.3) is a sinusoidal disturbance with the frequency of 0.5 Hz and amplitude of 44 N, and is applied only in three short specific time intervals: 20 : 30 seconds, 106 : 126 seconds, and 318 : 328 seconds as shown in Figure 20. $\delta_e(t)$ and $\delta_p(t)$, in equation (5.4) and (5.5), are also sinusoidal functions with the frequency of 0.2 Hz and the amplitude of 44 N. They are applied throughout the simulation, as shown in Figure 21.

B. Parameterization Setup and Tuning Procedures

Following the parameterization and design procedure described above, ω_c and ω_o are the two parameters need to be tuned. As discussed in [139], relationship between ω_c and ω_o is $\omega_o \approx (3 \sim 5)\omega_c$. So we only have one parameter to tune, which is ω_c. The other important parameter needed is the approximate value of b in (5.19).

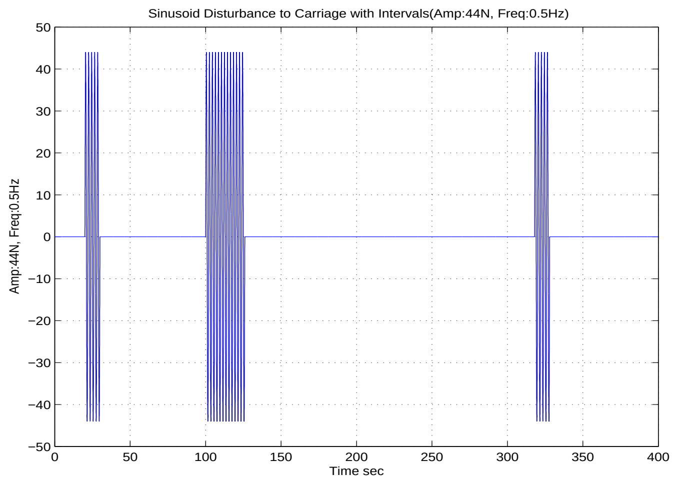

Figure 20: F_d: Interval sinusoidal disturbance for carriage velocity loop

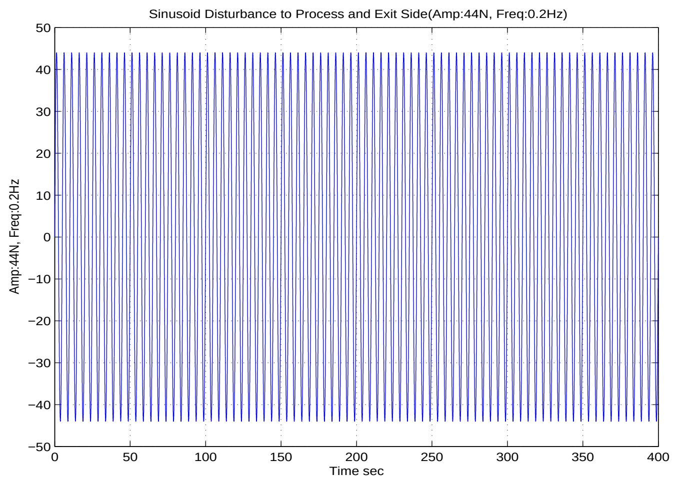

Figure 21: δ_e and δ_p: Sinusoidal disturbances for the exit and process loops

For this problem, the best estimate of b in (5.13), (5.14) and (5.15) is as follows: b_c = 1.368e-4, $b_e = 0.7057$, $b_p = 0.7057$, and $b_t = AE/5 = 3.76106$.

A cohesive ADRC design and optimization procedure is given as follows:

Step 1: Design parameterized ESO and controller where ω_o and ω_c are design parameters;

Step 2: Choose an approximate value of b in different plant, such as b_c, b_e, b_p and b_t;

Step 3: Set $\omega_o = 5\omega_c$ and simulate/test the ADRC in the simulation;

Step 4: Incrementally increase ω_c until the noise levels and/or oscillations in the control signal and output exceed the specified tolerance;

Step 5: If necessary, slightly increase or decrease the ratio of ω_c and ω_o.

The parameters of the four controllers are shown in Table II, where k_{pe}, k_{pp}, k_{ie} and k_{ip} are the gains in (5.6)-(5.8) for the IC. γ_3, γ_e, and γ_p are the gains in (5.9)-(5.11) for the LBC. b_c, b_e, and b_p are specific values of b in (5.19) for the carriage, exit, and process velocity loops, respectively. Similarly, ω_{oc}, ω_{oe} and ω_{op} are the observer gains in equation (5.22), and ω_{cc}, ω_{ce}, ω_{cp} are the controller gains (k_p) in equation (5.25). ω_{ct} is the corresponding ADRC parameters for the tension dynamics in (5.1).

Table II: Gain used in the simulation

	Velocity Loops	Velocity Loops
IC	k_{ie}=0.1,k_{ip}=0.1,k_{pe}=100,k_{pp}=100	
LBC	γ_3=100, γ_e=100,γ_p=100	
ADRC1	ω_{cc}=15, ω_{ce}=40,ω_{cp}=40	
ADRC2	ω_{cc}=15, ω_{ce}=40,ω_{cp}=40	ω_{ct}=12

C. Simulation Results and Comparison

The velocity and tension tracking errors resulting from ADRC1 are shown in Figure 22. Obviously, the velocity and tension tracking errors are quite small, despite the fact that the controller design is not based on the complete mathematical model of the plant and there are significant disturbances in the process.

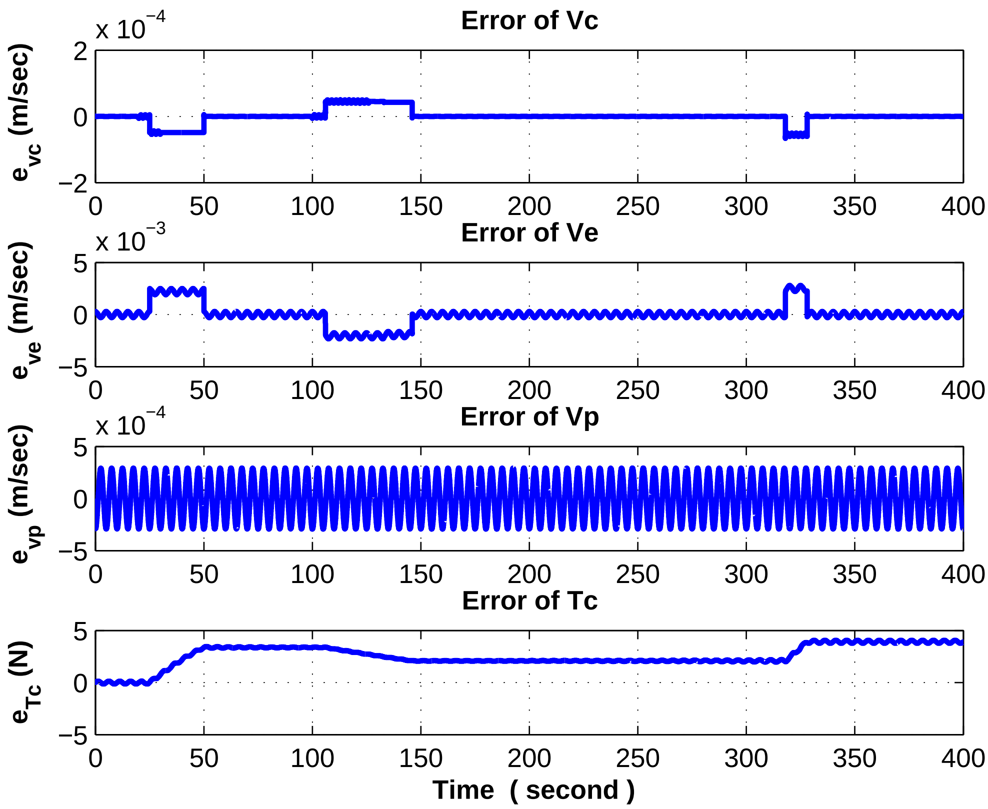

Figure 22: Error signals in ADRC1

The comparisons of IC, LBC and ADRC1 are shown in Figures 23 and Figure 24, in terms of the tracking errors and control signals for the carriage velocity loop. Note that the carriage velocity errors indicate that ADRC1 is much better than the other two methods and the control signal indicates that the ADRC controller actively responds to the disturbances. Similar characteristics are also found in the exit and process velocity loops.

Due to the poor results of IC, only LBC, ADRC1, ADRC2 are compared in the tension control results in Figure 25. Note that, with a direct tension measurement, ADRC2 results in negligible tension errors. Furthermore, even in an open-loop control, ADRC1 has a smaller error than LBC. This can be attributed to the high

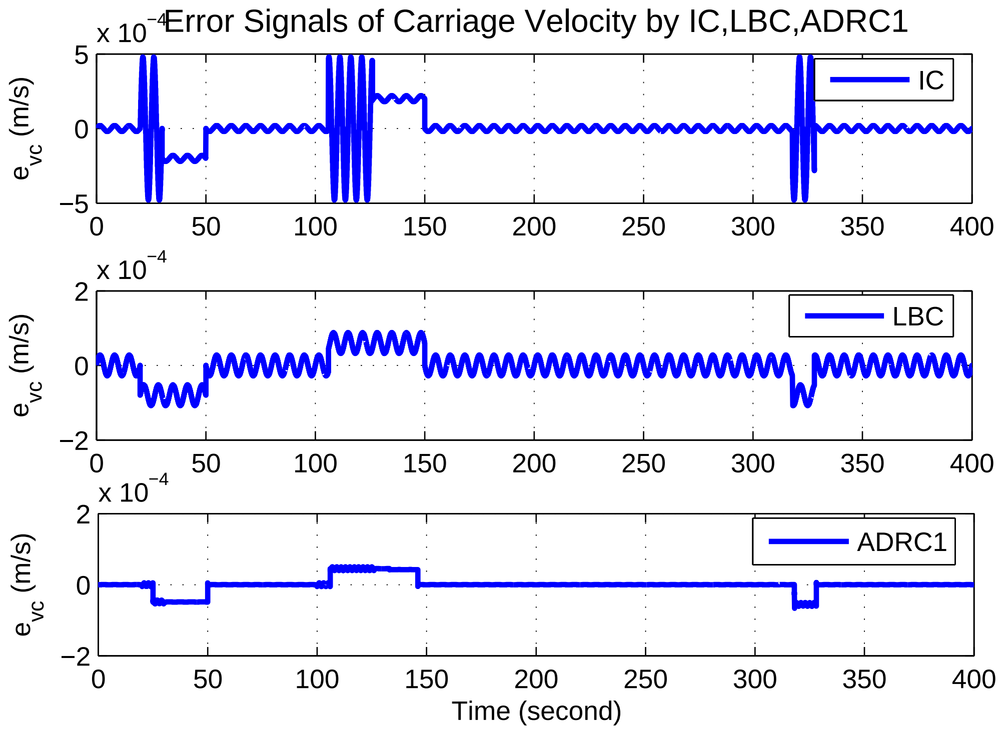

Figure 23: Carriage velocity error by different controllers

quality velocity controllers in LADRC1.

The velocity and tension errors of all four control systems are summarized in Table III.

Table III: Simulation Comparison

	Maximum Error				RMS			
	v_c(m/s)	v_e(m/s)	v_p(m/s)	t_c(N)	$v_c(m/s)$	$v_e(m/s)$	$v_p(m/s)$	$t_c(N)$
IC	5.0e-4	8.5e-3	8.5e-3	8.8e+4	1.0e-4	1.0e-3	1.0e-3	71.0
LBC	1.2e-4	2.7e-3	1.4e-3	12.8	3.0e-5	5.0e-4	6.0e-4	11.1
ADRC1	8.0e-5	1.5e-3	2.0e-4	4.1	1.0e-5	1.0e-5	2.0e-4	2.8
ADRC2	7.0e-5	1.3e-3	2.0e-4	1.5	1.0e-5	1.0e-5	2.0e-4	1e-2

Overall, these results reveal that the proposed ADRC controllers have a distinct advantage in the presence of sinusoidal disturbances and a much better performance in tension control.

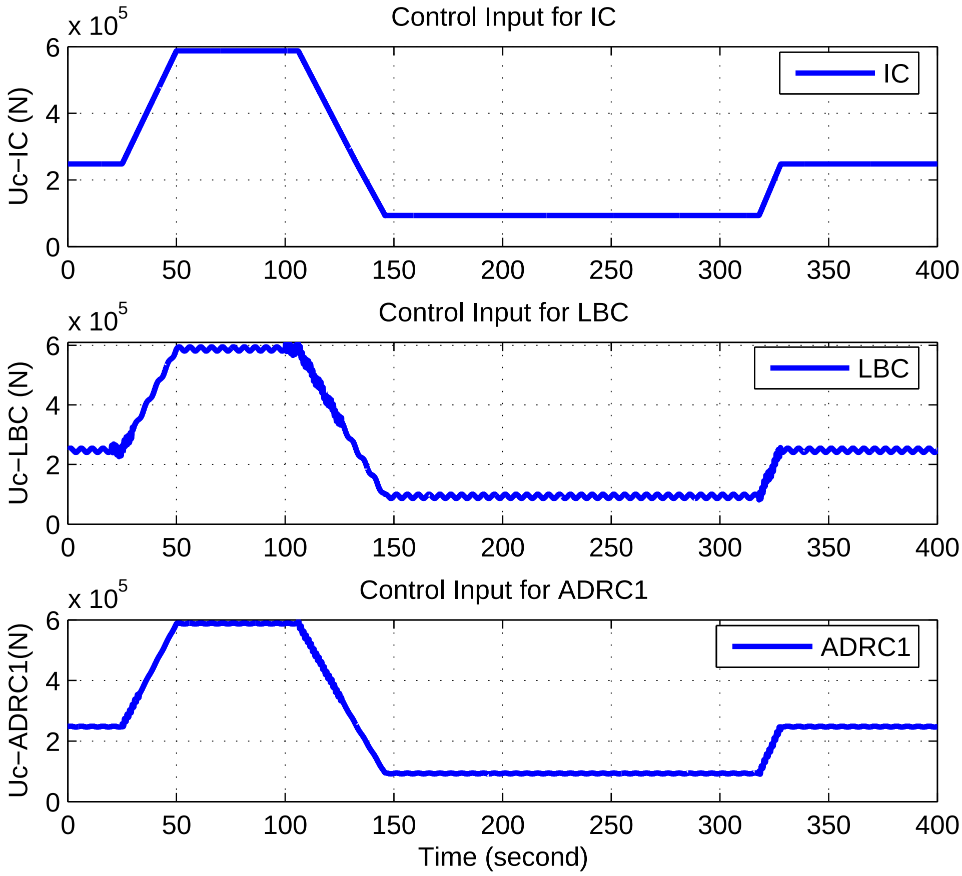

Figure 24: Control signal for carriage roller by IC, LBC and ADRC1

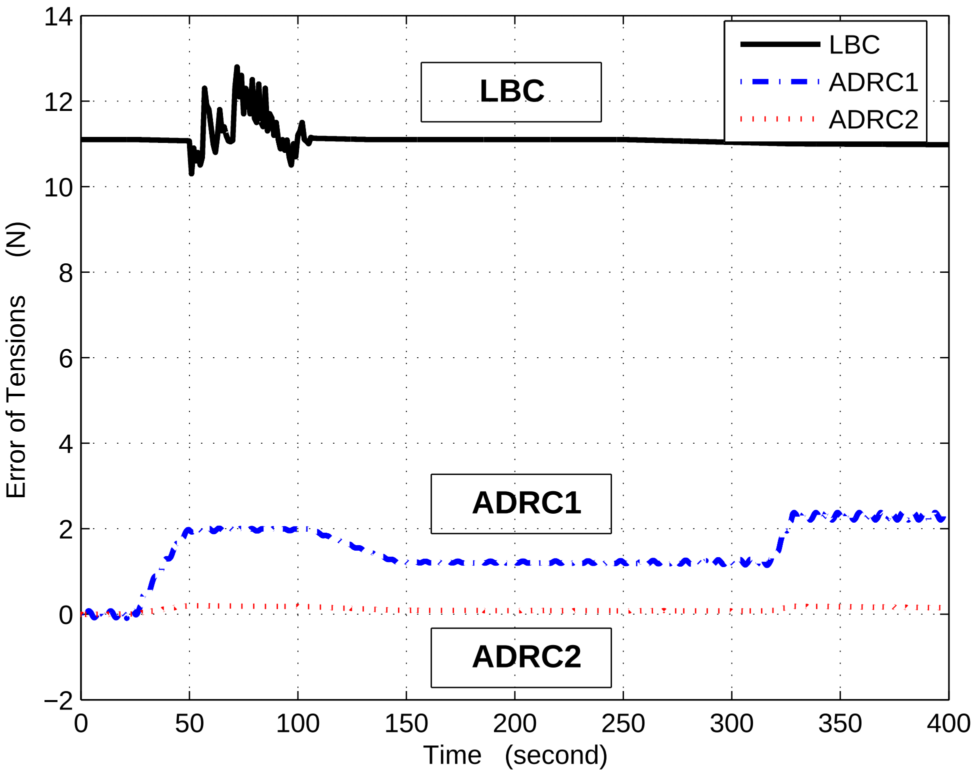

Figure 25: Tension errors comparison among LBC,ADRC1 and ADRC2

5.5 Summary

A new control strategy is proposed for web processing applications, based on the active disturbance rejection concept. It is applied to both velocity and tension regulation problems. Although only one section of the process, including the carriage, the exit, and the process stages, is included in this study, the proposed method applies to both the upstream and downstream sections to include the entire web line. Simulation results, based on a full nonlinear model of the plant, have demonstrated that the proposed control algorithm results in not only better velocity control but also significantly less web tension variation. The proposed method is promising because: 1) no detailed mathematical model is required; 2) zero steady state error is achieved without using the integrator term in the controller; 3) the controller is able to cope with a large range of the plant's dynamic change; and finally 4) excellent disturbance rejection is achieved.

CHAPTER VI

DECENTRALIZED CONTROL OF WEB WINDING SYSTEMS

As a real industrial example of large-scale systems, large-scale web winding systems with many different processes will be studied in the decentralized control framework in this chapter.

The presence of tension terms in the roller velocity dynamics, and conversely roller velocity terms in the tension dynamics lead the web winding system to be an interacting large-scale system. Given measurements of all states variables, the system can be controlled by multivariable control methods. Numerous attempts have been presented with promising results [33, 123, 148]. These results are in the form of static full state feedback, although the process of obtaining gains differs. Though powerful, multivariable control does have its limitations. Being centralized, the control scheme must be completely redesigned if the system is changed in some way. For example, adding one process to the system may force the system to be redesigned since the system dimension has been grown by one. Furthermore, failure in a section of one web tension zone can lead to catastrophic failure in the overall control system. Decentralized structure can alleviate these problems associated with centralized control structure. Although widely applicable to the industry, traditional decentralized control structure also introduces other issues.

The aim of this chapter is to provide a novel approach to the traditional decentralized control problem. A large-scale web processing line, where the mutual interaction between each control station is the major problem, is used as a case study in demonstrating the validity and practicality of the new method.

6.1 The Key Idea

In the decentralized control case, the interconnections between segments are usually neglected for control design purposes. However, the interconnections are affecting the subsystems. Furthermore, an extra degree of freedom that models the dynamics is added in the overlapping decentralized framework, which adds to the complexity of implementation. To solve these issues, we propose a trade-off between decentralized and overlapping decentralized control strategy. That is, we consider the interconnections as disturbances and uncertainties in each subsystem. Since ADRC can actively estimate and compensate the disturbances, a coordinated ADRC appears to be reasonable in handling such interconnected large-scale systems.

6.2 Large-scale Web Processing Lines

It is common in the web handling industry to divide a processing line into many tension zones by defining the span between two successive driven rollers as a tension zone. A typical web winding system with $(N+1)$-tension-zone is shown in Figure 26.

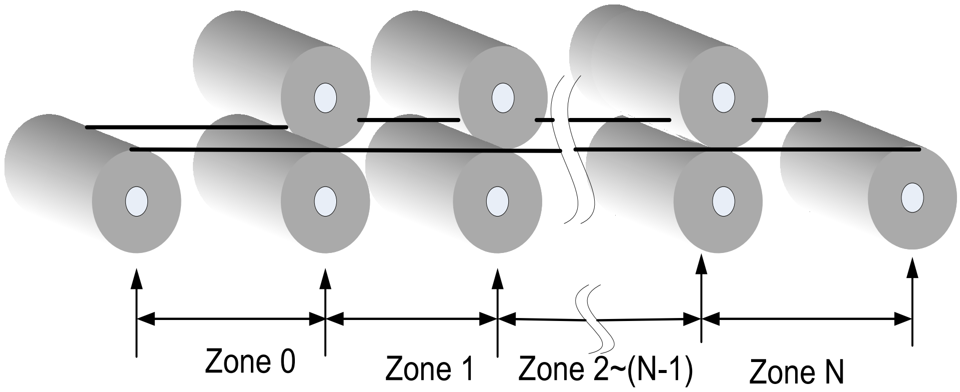

Figure 26: An illustration of a $(N+1)$-tension-zone system

The corresponding decentralized control structure is shown in Figure 27, where each tension zone is designed by a decentralized controller. Except for tension zone 1 (master speed section), which consists of only one velocity loop, all other tension zones consist of two control loops: one velocity loop and one tension loop. The corresponding controllers are tension controller C_T and velocity controller C_V.

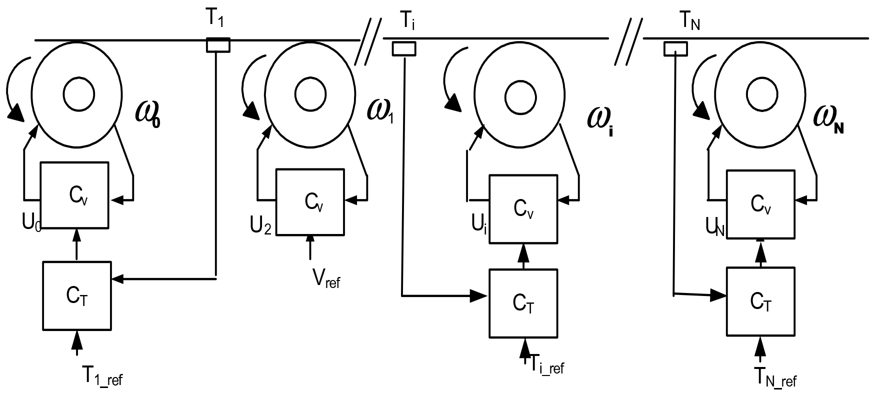

Figure 27: Diagram of a decentralized web tension control system

Consider a large-scale web processing line, which consists of the unwind/rewind rolls and $(N-1)$ intermediate driven rollers. The master speed roller is given to a driven roller upstream of the unwind roll in almost all web processing lines. The purpose of the master speed roller is to regulate web line speed and is not used to regulate tension in the spans adjacent to it. The unwind/rewind rolls release/accumulate material to/from the processing section of the web line. Thus their radii and inertia are time-varying. The dynamics of each section of the web processing line are presented in the following section.

Here we define the unwind section as tension zone 0, and the rewind section as tension zone N. All the other sections between unwind and rewind zones are the process zones. Then we will build the models for each tension zone according to the governed tension and velocity dynamics given in (2.13) and (2.15).

Unwind section

Dynamic behavior of the web tension T_1 , in the span immediately downstream from the unwind roller is given by

$$\dot{T}_1 = \frac{1}{L_1}\left[v_1 T_1 - v_0 T_0 + AE(v_1 - v_0)\right] \tag{6.1}$$

where L_1 is the length of the web span between unwind roller and master speed roller. T_0 represents the wound-in tension of the web in the unwind roll. v_1 and v_0 are the transporting velocity of the unwind roller and the adjunct master roller. The velocity dynamics of the unwind roller is as follows:

$$\frac{d}{dt}(J_0\omega_0) = -u_0 - \beta_{f0}\omega_0 + T_1 R_0 \tag{6.2}$$

where J_0 and R_0 represent the inertia and the radius of the unwind roller, respectively. β_{f0} is the coefficient of friction in the unwind roll shaft. Since in the process of unwind, the radius and the rotational moment of inertia are changing, (6.2) can be rewritten as

$$\dot{J}_0\omega_0 + J_0\dot{\omega}_0 = -u_0 - \beta_{f0}\omega_0 + T_1 R_0 \tag{6.3}$$

where ω_0 is the angular velocity of the unwind roller.

Below we will try to derive the expression of derivative of J_0 and ω_0. At any instant of time t, the rotational moment of inertia of the unwinding rollers change as the roll diameters change, and can be expressed as follows:

$$J_0 = J_{c0} + J_{cu} \tag{6.4}$$

where J_{c0} is the inertia of the driving shaft and the core amounted on it, which is a constant. J_{cu} is the inertia of the cylindrically wound web material on the core. J_{cu} is not constant because the web is continuously released into the process. The inertia of J_{cu} can be expressed as follows:

$$J_{cu} = \frac{\pi}{2} t_\rho t_w (R_0^4 - R_{u0}^4) \tag{6.5}$$

where t_ρ is the density of the web material, t_w is the web width. R_{u0} is the radius of the empty core mounted on the unwind roll-shaft, and R_0 is the time changing radius of the material roll. The rate of change in J_0 caused by the rate of change of radius, can be given by deviating (6.4) as follows:

$$\dot{J}_0 = \dot{J}_{cu} = 2\pi t_p t_w R_0^3 \dot{R}_0 \tag{6.6}$$

The angular velocity of the unwind roller has a relationship with transport velocity of the web by

$$v_0 = R_0 \omega_0 \tag{6.7}$$

Differentiating both sides of (6.7), we can get the expression of $\dot{\omega}_0$ as

$$\dot{\omega}_0 = \frac{\dot{v}_0}{R_0} - \frac{\dot{R}_0 v_0}{R_0^2} \tag{6.8}$$

The diameters of the unwinding rolls change as the winding process goes on. This change can be mathematically represented as follows:

$$\dot{R}_0 \approx -\frac{e_w}{2\pi}\omega_0 = -\frac{e_w}{2\pi}\frac{v_0}{R_0} \tag{6.9}$$

where e_w is the web thickness. Note that (6.9) is an approximation because the thickness affects the rate of change of the radius of the roll after each revolution of the roll. The continuous approximation is valid since the thickness is very small. By substituting (6.3) through (6.9) into (6.2), the roller dynamic can be obtained as follows:

$$J_0\dot{v}_0 = -R_0u_0 - \beta_{f0}v_0 + T_1R_0^2 - \frac{e_w}{2\pi}\left(\frac{J_0}{R_0^2} - 2\pi t_\rho t_w R_0^2\right)v_0^2 \tag{6.10}$$

Combining the tension dynamics in (6.1) and roller dynamics in (6.10) gives the dynamics of the unwind section as follows:

$$\begin{cases} J_0\dot{v}_0 = -R_0u_0 - \beta_{f0}v_0 + T_1R_0^2 - \dfrac{e_w}{2\pi}\left(\dfrac{J_0}{R_0^2} - 2\pi t_\rho t_w R_0^2\right)v_0^2 \\ \dot{T}_1 = \dfrac{1}{L_1}\left[v_1T_1 - v_0T_0 + AE(v_1 - v_0)\right] \end{cases} \tag{6.11}$$

Master speed section and process section

Since the radius and inertia of the master speed roller are not changing with time, J_1 and R_1 are constant. The dynamics of the master speed roller is given by

$$J_1\dot{v}_1 = R_1u_1 - \beta_{f1}v_1 + R_1^2(T_2 - T_1) \tag{6.12}$$

The dynamics of web tension and velocity of the rollers in the process section are given by

$$\begin{cases} J_i\dot{v}_i = R_iu_i - \beta_{fi}v_i + R_i^2(T_{i+1} - T_i) \\ \dot{T}_i = \dfrac{1}{L}\left[v_{i+1}T_{i+1} - v_iT_i + AE(v_i - v_{i+1})\right] \end{cases} \tag{6.13}$$

Rewind section

The dynamics of roller velocity entering the rewind roll can be determined along similar procedures as presented for the unwind roll. The only difference between them is the changing direction of the radius and inertia. The signal for the derivative of radius and inertia are positive instead of negative in the unwind processing.

The dynamics of the rewind section is shown as follows:

$$\begin{cases} J_N\dot{v}_N = R_Nu_N - \beta_{fN} - R_N^2T_N + \dfrac{e_w}{2\pi}\left(\dfrac{J_N}{R_N^2} - 2\pi t_w t_\rho R_N^2\right)v_N^2 \\ \dot{T}_N = \dfrac{1}{L_N}\left[v_NT_N - v_{N-1}T_{N-1} + AE(v_N - v_{N-1})\right] \end{cases} \tag{6.14}$$

where L_N is the length of the web span between rewind roller and the previous transporting roller. T_N and T_{N-1} represent the wound-out tension of the web in the rewind roll and the adjunct roller. v_N and v_{N-1} are the transporting velocity of the rewind roller and the adjunct roller. J_N and R_N represent the inertia and the radius of the rewind roller, respectively. β_{fN} is the coefficient of friction in the rewind roll shaft.

The dynamic models given in equations (6.1) to (6.14) are nonlinear and time varying. The plant for each subsystem is summarized as follows:

$$S_0 \;:\; \begin{cases} \dot{T}_1 = \dfrac{1}{L_1}\left[v_1 T_1 - v_0 T_0 + AE(v_1 - v_0)\right] \\ \dot{v}_0 = -\dfrac{\beta_{f0}}{J_0}v_0 - \dfrac{R_0}{J_0}u_0 + \dfrac{1}{J_0}\left[T_1 R_0^2 - \dfrac{e_w}{2\pi}\left(\dfrac{J_0}{R_0^2} - 2\pi t_\rho t_w R_0^2\right)v_0^2\right] \end{cases} \tag{6.15}$$

$$S_1 \;:\; \dot{v}_1 = -\frac{\beta_{f1}}{J_1}v_1 + \frac{1}{J_1}R_1 u_1 + \frac{R_1^2}{J_1}(T_2 - T_1) \tag{6.16}$$

$$S_i \;:\; \begin{cases} \dot{T}_i = \dfrac{1}{L_i}\left[v_{i+1}T_{i+1} - v_i T_i + AE(v_i - v_{i+1})\right] \\ \dot{v}_i = -\dfrac{\beta f_i}{J_i}v_i + \dfrac{R_i}{J_i}u_i + \dfrac{R_i^2}{J_i}(T_{i+1} - T_i) \end{cases} \tag{6.17}$$

$$S_N \;:\; \begin{cases} \dot{T}_N = \dfrac{1}{L_N}\left[v_N T_N - v_{N-1}T_{N-1} + AE(v_N - v_{N-1})\right] \\ \dot{v}_N = -\dfrac{\beta_{fN}}{J_N}v_N + \dfrac{R_N}{J_N}u_N + \dfrac{1}{J_N}\left[-R_N^2 T_N + \dfrac{e_w}{2\pi}\left(\dfrac{J_N}{R_N^2} - 2\pi t_w t_\rho R_N^2\right)v_N^2\right] \end{cases} \tag{6.18}$$

where S_0, S_1, S_i, S_N stand for the subsystem of unwind section, the master speed roller section, the process sections between unwind and rewind section, and rewind section, respectively.

6.3 Existing and Proposed Solutions

Prior to the design of a proper control system, the control objectives for the decentralized control of web winding systems must be clearly defined. The goal for this particular large-scale system is to design a controller for each subsystem, which minimizes the influence of the remaining subsystems. This section will review the general assumptions made to large-scale control problem formulation, then existing control solutions will be analyzed in terms of their weakness. Finally, an ADRC based decentralized control strategy will be proposed to overcome those weaknesses caused by traditional decentralized control methods.

6.3.1 Assumptions

Consider an interconnected large-scale nonlinear system S comprised of $(N+1)$ interconnected subsystems $S_i (i = 0, \ldots, N)$. Each subsystem S_i is presented as follows:

$$S_i : \dot{y}_i = \sigma_i(y_i) + b_i u_i + \Delta_i(y) \tag{6.19}$$

where $i = 0, \ldots, N$;

$y_i \in R^{n_i}$ is the output of the subsystem S_i;

$y = [y_0^T, y_1^T, \cdots, y_N^T]^T$ is the overall output of S;

$u_i \in R^{m_i}$ is the control input of the subsystem S_i;

$\sigma_i \in R^{n_i}$ is the internal dynamics of the subsystem S_i;

Δ_i is the interactions of the ith subsystems S_i with other subsystems;

The following assumptions are made on the system (6.19) as follows

Assumption 1: The system is a minimum phase system without any "zero dynamics."

Assumption 2: The constant vectors $b_i \in R^{n_i}$ are known.

Assumption 3: The vectors $\sigma_i(y_i)$ are unknown and bounded.

Assumption 4: The interconnections $\Delta_i(y)$ are unknown and bounded.

Assumption 5: Denote $f_i(y_i, y) = \sigma_i(y_i) + \Delta_i(y)$, and $\dot{f}_i(y_i, y) = \eta_i(y_i, y)$, It is assumed that the derivative of $\eta_i(y_i, y)$ is bounded, i.e., $\|\dot{\eta}_i(y_i, y)\| \leq \theta_i$, where θ_i is a positive constant.

The objective of the decentralized control design is to determine a control law for each individual subsystem such that the outputs $y_i(t)$ follow the desired trajectory y_{ir} for all $i = 0, \ldots, N$.

6.3.2 Summary of the Existing Control Methods

From the literature review in Section 3.3, it can be seen that there are two challenges in the decentralized control of large-scale systems, which are interconnections assumptions and controller design.

Assumptions on Interconnection Dynamics

First, let's review existing assumptions on interconnections. Literature study has shown that the interactions in the subsystem are usually bounded by polynomial-type nonlinearities. The interconnections are assumed to be linear and nonlinear form in the literature [52, 60, 72]. One of a typical linear form [52] is expressed as follows:

$$\Delta_i(x) = \sum_{j=0, j \neq i}^{N} \mathrm{K}_{ij} x_j \tag{6.20}$$

where $\mathrm{K}_{ij} \in R^{n_i \times n_j}$ are linear interconnection matrixes, which are assumed to be bounded.

There are also many nonlinear forms of interconnections. Usually, the interconnections are composed of two parts: higher order polynomials of its own states and high-order polynomials of the states from other subsystems, one of which is as follows:

$$\Delta_i^T(x)\Delta_i(x) \leqslant \sum_{j=2}^{p_i} \sum_{k=0}^{N} \delta_{ij} \left\| x_k \right\|^j \tag{6.21}$$

where p_i is the order of the polynomials, δ_{ij} are unknown positive constants for i, j. Sometimes, the interconnections are also bounded by the sum of the tracking errors as follows:

$$\left| \Delta_i \left(x_1, \ldots, x_N \right) \right| \leqslant \sum_{j=1}^{N} \gamma_{ij} \left\| e_j \right\| \tag{6.22}$$

where $\|e_j\|$ is the norm of the tracking error of the $j-$th subsystem, defined as $e_j = x_j^r - x_j$, and γ_{ij} are some unknown constants.

Note that the restrictions on the interconnections shown in (6.20) are very general which include many types of interconnections considered in the existing literature as special case. For example, the interconnections bounded by first-order polynomials [55, 56], high-order polynomials [71, 73] *et al.*

Control Methods

Second, let's examine the control methods. Basically, we can find that all these assumptions are made to model the unknown parts of the nominal plant and make the plant model more precisely. Based on the well understood model and the interactions dynamics, different modern control methods are applied to deal with the unmodeled interactions. Adaptive control is used to deal with slow but well-defined changes in dynamics; robust control is based on small gain theory and only robust to small bounded disturbance and unmodeled dynamics; intelligent control methods, such as fuzzy logic control and neural network control, are time-consuming in design and also difficult to implement in the real world; the industry PID controller is simple in form but difficult to tune. If anything changes in the system, very often this results in poor performance or even instability.

6.3.3 Proposed Method

Based on the analysis of existing methods on decentralized control of large-scale systems, a novel approach to these issues is proposed in this section. The decentralized control problem is first reformulated in the active disturbance rejection framework. Then a linear observer and controller for each individual subsystem will be designed, without requiring the precise knowledge of the dynamics of interconnections from other subsystems.

Design Objectives

Based on the analysis of the state-of-the-art of decentralized control methods, our design objectives are:

1. Construct a decentralized controller that is easy to implement, robust to uncertainties, and stability guaranteed;

2. Relax the required knowledge of the dynamics of interconnections from other subsystems;

3. Relax restrictions on the required knowledge of interconnections and uncertainties;

4. Maintain the stability of the constructed decentralized closed-loop system.

Design Strategy: Treat Subsystem Interactions as Disturbances

In this section, we will propose a new control strategy that can meet our design philosophy. As mentioned previously, one of the most important problems in decentralized control is to relax restrictions on the interconnections and uncertainties. To solve this problem, the ADRC paradigm will be applied to this special case. The idea is that instead of treating external disturbances and unknown dynamics as one term for disturbance rejection purpose, ADRC is further extended to treat the unknown interconnections dynamics as one generalized term $f(\cdot)$, estimating them and canceling their effect in real time in order to render the system as a decoupled centralized control problem.

Based on the analysis above, all the combined effect of disturbances, changing dynamics, uncertainness, and interactions between each subsystem are treated in one term $f_i(y_i, y)$ in the framework of active disturbance rejection control. The expression of $f_i(y_i, y)$ is defined as follows:

$$f_i(y_i, y) = \sigma_i(y_i) + \Delta_i(y) \tag{6.23}$$

Substituting (6.23) into (6.19) gives the standard ADRC form as follows:

$$S_i : \dot{y}_i = f_i(y_i, y) + b_i u_i, i = 0, \ldots, N. \tag{6.24}$$

To this end, a linear ADRC is applied to each subsystem and constitutes a decentralized ADRC based control system as shown in Figure 28, where each subsystem is controlled by a linear ADRC.

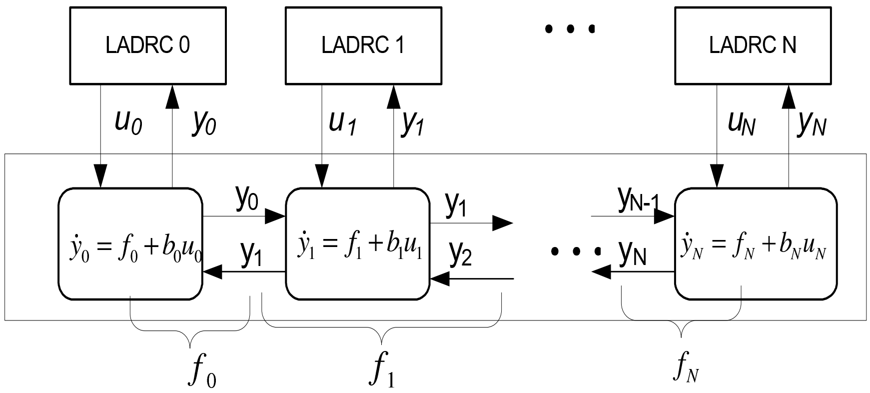

Figure 28: ADRC based decentralized control strategy

By treating the unknown interconnections as generalized $f(\cdot)$ term, ADRC actively estimates and cancels the changing dynamics of the interactions from other subsystems. Therefore, ADRC decouples each subsystem from other subsystems and makes the decentralized control problem a stand-alone centralized control problem. Thus, the proposed method will not require the interconnections to be bounded by polynomial-type combinations of the states within themselves and the other subsystems states. What we need to assume is that all the combined effect of disturbances, changing dynamics, uncertainness, and interactions between each subsystems are bounded over the domain of interest. In addition, the derivative of the combined term $f(\cdot)$ is also bounded. This is reasonable in most practical systems.

Decentralized ADRC Control System Design

For the ith subsystem in a large-scale system, the control system design can be divided into three steps.

A. Solving the Subsystem Control Problem

First step is the reformulation of the original problem in (6.24). For the sake of simplicity, we denote $f_i(y_i, y)$ as $f_i(\cdot)$. In order to estimate $f_i(\cdot)$, an additional state is added to the original system (6.24). Let $x_{i1} = y_i$, $x_{i2} = f_i(\cdot)$, then subsystems (6.24) become second order systems of the form:

$$\begin{cases} \dot{x}_{i1} = x_{i2} + b_i u_i \\ \dot{x}_{i2} = \eta_i(\cdot) \\ y_i = x_{i1} \end{cases} \tag{6.25}$$

where $f_i(\cdot)$ is added as an augmented state, and $\eta_i(\cdot) = \dot{f}_i(\cdot)$ is unknown but bounded.

The state space form of (6.25) can be rewritten as

$$\begin{cases} \dot{x}_i = A_i x_i + B_i u_i + E_i \eta_i \\ y_i = C_i x_i \end{cases} \tag{6.26}$$

where

$$A_i = \begin{bmatrix} 0 & 1 \\ 0 & 0 \end{bmatrix}, B_i = \begin{bmatrix} b_1 \\ 0 \end{bmatrix}, E_i = \begin{bmatrix} 0 \\ 1 \end{bmatrix}, C_i = \begin{bmatrix} 1 & 0 \end{bmatrix}$$

B. Linear Observer Design

The $f_i(\cdot)$ term can be estimated by ESO and designed as follows:

$$\begin{cases} \dot{z}_i = A_i z_i + B_i u_i + l_i(y_i - \hat{y}_i) \\ \hat{y}_i = C_i z_i \end{cases} \tag{6.27}$$

where l_i is the observer gain vector to be selected. By setting $\lambda_i(s) = |sI - (A_i - l_i C_i)| = s^2 + l_1 s + l_2$ equal to the desired error dynamics $(s + \omega_o)^2$, the observer gains are functions of one single tuning parameter, ω_o.

C. Controller Design

The next step is the controller design. Here a crucial step is that we want to get the plant to be a pure integral format, so that it can be easier to design controller. As described in Chapter III, the control law is designed as

$$u_i = \frac{1}{b_i}[-z_{i2} + u_{i0}] \tag{6.28}$$

This reduced the plant to approximate an integral plant

$$\dot{y}_i = (f_i(\cdot) - z_{i2}) + u_{i0} \approx u_{i0} \tag{6.29}$$

Let y_{ir} be the desired output, u_{i0} can be selected as

$$u_{i0} = k_{i1}(y_{ir} - z_{i1}) \tag{6.30}$$

where k_{i1} are the controller gains to be selected. For the purpose of easy tuning, let

$$k_{i1} = \omega_c \tag{6.31}$$

where ω_c is the bandwidth of the closed-loop system.

Remarks:

1. It can be seen that the proposed control strategy can meet the requirement of our design philosophy: easy to implement, less model information.

2. Unlike exact linearization approach, which needs a nonlinear transformation and an explicit expression of the interconnections, what we do is estimate it and then cancel it in real-time. This enables us to deal with difficult issues caused by the uncertainties, nonlinearities and unknown nonlinear functions of the interconnections.

3. The only requirement left to meet is the proof of stability of the closed-loop system. The singular perturbation based stability analysis of the proposed controller will be given in the next chapter.

In summary, the advantage of the proposed method is that the precise knowledge of the interconnection dynamics does not need to be known. Furthermore, the constraints on the interconnections are not necessarily being polynomials. What is really needed to be known is that the interconnections are bounded, which is usually true in practice.

6.4 Application to a Web Winding System

This section explains the design of decentralized controller proposed in the previous section for large-scale web winding systems. In order to fit the proposed control strategy into the specific web winding system, let us first look back at the decentralized web winding system control problem. In Section 6.3, we have developed the mathematical model for each subsystem. In this section, we will reformulate the dynamics for each subsystem in the ADRC control framework.

6.4.1 Reformulation of Web Winding Dynamics

Defining the new variable for the unwind section as $y_1^T = [T_1, v_0]$, for the master speed roller as $y_2 = v_1$, for the ith subsystem as $y_i^T = [T_i, v_i]$,$i = 2, 3, \ldots, (N-1)$, and for the rewind section as $y_N^T = [T_N, v_{N-1}]$, we can get the expression of each subsystem as follows:

$$S_0 : \dot{y}_0 = \sigma_0(y_0) + b_0 u_0 + \Delta_0(y) \tag{6.32}$$

where

$$b_0 = \begin{bmatrix} 0 \\ -R_0/J_0 \end{bmatrix}, \Delta_0(y) = \begin{bmatrix} (AE + T_1)v_1/L_1 \\ 0 \end{bmatrix}$$

$$\sigma_o(y_0) = \begin{bmatrix} -[T_0 + AE]v_0/L_1 \\ -\frac{b_{f0}}{J_0}v_0 + \frac{1}{J_0}\left[T_1 R_0^2 - \frac{e_w}{2\pi}\left(\frac{J_0}{R_0^2} - 2\pi t_\rho t_w R_0^2\right) v_0^2\right] \end{bmatrix}$$

$$S_1 : \dot{y}_1 = \sigma_1(y_1) + b_1 u_1 + \Delta_1(y) \tag{6.33}$$

where

$$b_1 = \frac{R_1}{J_1}, \Delta_1(y) = \frac{R_1^2}{J_1} T_1, \sigma_1(y_1) = -\frac{\beta_{f1}}{J_1} v_1 + \frac{R_1^2}{J_1} T_2$$

$$S_i : \dot{y}_i = \sigma_i(y_i) + b_i u_i + \Delta_i(y) \tag{6.34}$$

where

$$b_i = \begin{bmatrix} 0 \\ -R_i/J_i \end{bmatrix}, \Delta_i(y) = \begin{bmatrix} (AE + T_{i+1}) v_{i+1}/L_i \\ 0 \end{bmatrix}$$

$$\sigma_i(y_i) = \begin{bmatrix} -[T_i + AE] v_i / L_i \\ -\frac{\beta_{fi}}{J_i} v_i + \frac{R_i^2}{J_i}(T_{i+1} - T_i) \end{bmatrix}$$

$$S_N : \dot{y}_N = \sigma_1(y_N) + b_N u_N + \Delta_N(y) \tag{6.35}$$

where

$$b_N = \begin{bmatrix} 0 \\ -R_N/J_N \end{bmatrix}, \Delta_N(y) = \begin{bmatrix} (AE + T_N) v_N / L_N \\ 0 \end{bmatrix}$$

$$\sigma_N(y_N) = \begin{bmatrix} -[T_N + AE] v_{N-1} / L_N \\ -\frac{b_{fN}}{J_N} v_N + \frac{1}{J_N} \left[T_N R_N^2 - \frac{e_w}{2\pi} \left(\frac{J_N}{R_N^2} - 2\pi t_\rho t_w R_N^2 \right) v_N^2 \right] \end{bmatrix}$$

In summary, the equations from (6.32) to (6.35) defined above can be rewritten as following forms:

$$S_i : \dot{y}_i = \sigma_i(y_i) + b_i u_i + \Delta_i(y) \tag{6.36}$$

So far we have formulated the dynamic models of decentralized web winding system to be arranged in the standard decentralized systems problem as defined in equation (6.19). Next section, we will investigate the control of this decentralized web winding system by ADRC.

6.4.2 Implementation of ADRC

A control block diagram for the industrial web winding system of one single tension zone is shown in Figure 29. It can be seen that a cascaded structure of tension and velocity loop is applied. In other words, the output of the tension loop is fed into the velocity loop and added to the velocity reference to get a real velocity reference signal for the velocity loop.

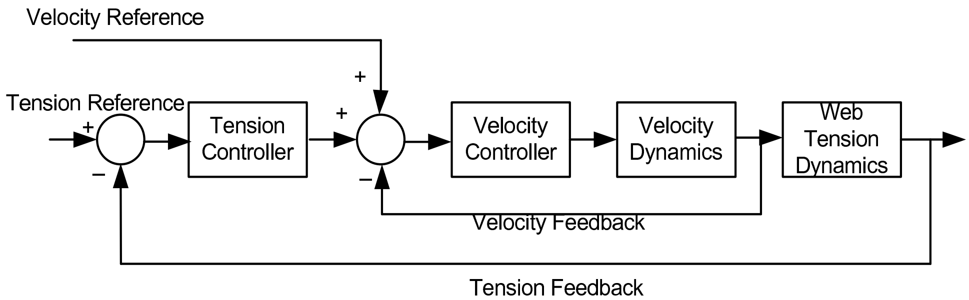

Figure 29: Cascaded structure of industrial control

Based on the observer designed in equation (6.27) and controller derived in equation (6.28) to (6.31), the proposed control laws are applied to both tension and velocity loops in each subsystem.

In a large-scale web winding system, there is always a master speed roller; the reference velocities of the transport rollers in the process line are set equal to the master speed roller. The diagram of a four-tension zone web winding system is shown in Figure 30, where the first tension zone is unwind section, the second master speed roller, the third a process roller section, the last the rewind section.

Because of interconnections between tension zones, the variations of velocities and tensions propagated to all subsequent sections. As shown in Figure 30, the velocity variations propagated downstream, while the tension variations propagated upstream. The directions of the propagations are demonstrated in different arrow directions. It is those factors that cause the traditional decentralized controller design and tuning procedure to be a challenging problem, since the plant dynamics keep changing.

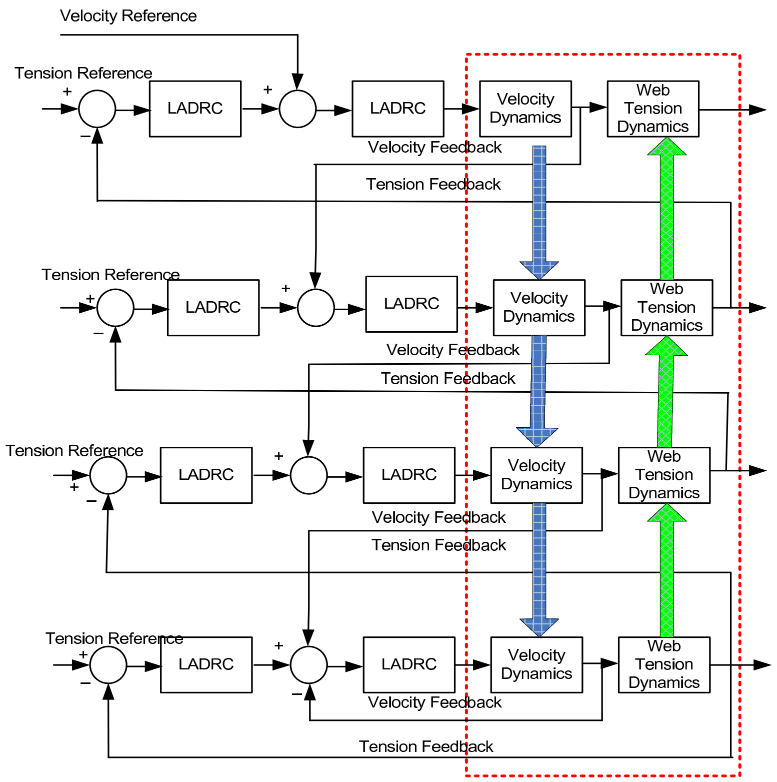

Figure 30: The illustration of the decentralized tension control system

However, it is NOT a problem for ADRC due to its decoupling nature. The changing dynamics are decoupled by ADRC, thereby making the decentralized control a centralized control problem. Furthermore, because each subsystem except for the master roller section has the same structure, we only need to design one control system for one of the subsystem, and duplicate the controller for other subsystems. This feature will reduce the tuning time and implementation cost in practice.

6.4.3 Assumptions Checks

The disturbance and its derivative are assumed to be locally bounded as described in Assumptions 1-5 in Section 6.3.1. The existence of these bounds will be checked in this section.

The combined functions for each subsystem is summarized as follows:

$$f_0(\cdot) = \sigma_0 + \Delta_0 = \begin{bmatrix} \frac{1}{L}[v_1 T_1 - v_0 T_0 + AE(v_0 - v_1)] \\ -\frac{b_{f0}}{J_0} v_0 + \frac{1}{J_0}\left[T_1 R_0^2 - \frac{e_w}{2\pi}\left(\frac{J_0}{R_0^2} - 2\pi t_\rho t_w R_0^2\right) v_0^2\right] \end{bmatrix} \tag{6.37}$$

$$f_1(\cdot) = \sigma_1 + \Delta_1 = -\frac{b_{f1}}{J_1} v_1 + \frac{R_1^2}{J_1}(T_2 - T_1) \tag{6.38}$$

$$f_i(\cdot) = \sigma_i + \Delta_i = \begin{bmatrix} \frac{1}{L}[v_{i+1} T_{i+1} - v_i T_i + AE(v_i - v_{i+1})] \\ -\frac{\beta_{fi}}{J_i} v_i + \frac{R_i^2}{J_i}(T_{i+1} - T_i) \end{bmatrix} \tag{6.39}$$

$$f_N(\cdot) = \sigma_N + \Delta_N = \begin{bmatrix} \frac{1}{L}[v_{i+1} T_{i+1} - v_i T_i + AE(v_i - v_{i+1})] \\ -\frac{b_{fN}}{J_N} v_N + \frac{1}{J_N}\left[-R_N^2 T_N + \frac{e_w}{2\pi}\left(\frac{J_N}{R_N^2} - 2\pi t_w t_\rho R_N^2\right) v_N^2\right] \end{bmatrix}$$

where $f_0(\cdot)$, $f_1(\cdot)$, $f_i(\cdot)$, and $f_N(\cdot)$ denote the generalized term of $f(\cdot)$ for unwind section, master speed section, process section and rewind section, respectively.

We will first show that combined function $f_i(\cdot)$ and its derivative $\dot{f}_i(\cdot)$ are bounded in the ith subsystem, then consider three special cases, which include the unwind section, the master speed section and the rewind section with a little bit difference from the general case.

$$\begin{aligned} |f_{i1}(\cdot)| &\leq \frac{1}{L_{i\min}}\left[|v_{i+1} T_{i+1}| + |v_i T_i| + |AE_{\max} v_i| + |AE_{\max} v_{i+1}|\right] && (6.40) \\ &\leq \frac{1}{L_{i\min}}\left[\frac{1}{2}(v_{i+1}^2 + T_{i+1}^2) + \frac{1}{2}(v_i^2 + T_i^2) + AE_{\max}|v_i| + AE_{\max}|v_{i+1}|\right] \\ &\leq \frac{1}{L_{i\min}}\left[\frac{1}{2}(y_{i+1}^2 + y_i^2) + AE_{\max}|y_{i1}| + AE_{\max}\left|y_{(i+1)1}\right|\right] && (6.41) \\ |f_{i2}(\cdot)| &\leq \left|\frac{\beta_{fi}}{J_i} v_i\right| + \left|\frac{R_i^2}{J_i} T_{i+1}\right| + \left|\frac{R_i^2}{J_i} T_i\right| && (6.42) \\ |f_i(\cdot)| &= |f_{i1}(\cdot)| + |f_{i2}(\cdot)| \end{aligned}$$

For the master speed section, $f_1(\cdot)$ is bounded by $|f_{i2}(\cdot)|_{i=1}$. For the unwind subsystem and rewind subsystem, there are an added-on term due to radius and inertia changing in these two sections. The added-on term is shown in the following equations:

$$\Pi_k(\cdot) = -\frac{b_{fk}}{J_k}v_k + \frac{1}{J_k}\left[-R_k^2 T_k \pm \frac{e_w}{2\pi}\left(\frac{J_k}{R_k^2} - 2\pi t_w t_\rho R_k^2\right)v_k^2\right] \tag{6.43}$$

$$\leq \left|\frac{b_{fk}}{J_k}v_N\right| + \frac{1}{J_k}\left[\left|R_k^2 T_k\right| + \left|\frac{e_w}{2\pi}\frac{J_k}{R_k^2}v_k^2\right| + \left|e_w t_w t_\rho R_k^2 v_k^2\right|\right] \tag{6.44}$$

$$\dot{\Pi}_k(\cdot) \leq \frac{b_{fk}}{J_k}\left|\dot{v}_N\right| + \frac{1}{J_k}\left[R_k^2\left|\dot{T}_k\right| + \frac{e_w}{\pi}\frac{J_k v_k}{R_k^2}\left|\dot{v}\right| + \left|2e_w t_w t_\rho R_k^2 v_k \dot{v}_k\right|\right] \tag{6.45}$$

where $k = 0$ or N. It is shown that the added-on term is bounded. Since the added-on term is bounded, it is easy to check that the whole subsystem is bounded for the unwind and the rewind subsystem.

$$\left|f_0(\cdot)\right| \leq \frac{1}{L_{0\min}}\left[\frac{1}{2}(y_1^2 + y_0^2) + AE_{\max}\left(\left|y_{0,1}\right| + \left|y_{1,1}\right|\right)\right] + \left|f_{i2}(\cdot)\right|_{i=0} + \Pi_0(\cdot)$$

$$\left|f_N(\cdot)\right| \leq \frac{1}{L_{N\min}}\left[\frac{1}{2}(y_N^2 + y_{N-1}^2) + AE_{\max}\left(\left|y_{N-1,1}\right| + \left|y_{N,1}\right|\right)\right] + \left|f_{i2}(\cdot)\right|_{i=N} + \Pi_N(\cdot)$$

From the above equations, it can be concluded that the bound of the disturbances and their derivatives exist and meet those Assumptions 1-5 in Section 6.3.1.

6.5 Simulation and Results

The web processing application under consideration directly falls into the large-scale system control problem. We will test the proposed control methods in a four-tension-zone web processing line in this section.

The block diagram of the four-tension-zone web winding model is shown in Figure 31. Note that the diagram is a little different from the decentralized structure shown in Figure 30. Here we set the master roller speed as tension zone 1 without tension zone 0 of a unwind section. The reason is that the control of unwind and rewind section is almost the same; the only difference between them is the changing direction of radius and inertia. We also assume that the web tensions can be measured by the load cells, the radius of the winding roll can be measured by a potentiometer, and the angular velocities of the rolls can be measured by tachometers.

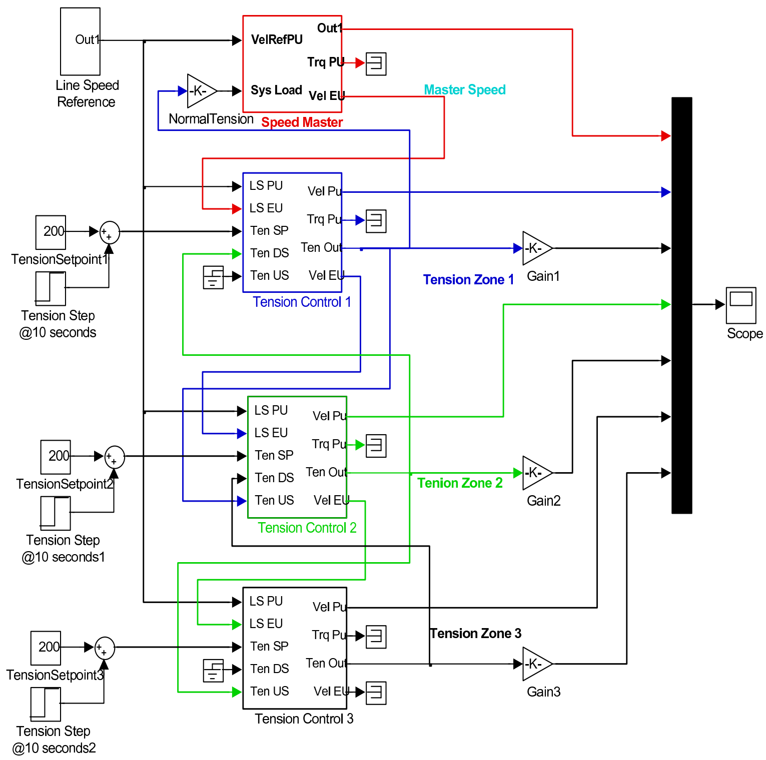

Figure 31: Simulation diagram

6.5.1 Simulation Setup

The simulation system is composed of four subsystems, and each of them is subjected to interferences from other subsystems. A subsystem of the upstream tension control loop, for example, has an interference from the speed master and the downstream tension loops. As can be seen from Figure 31, it constitutes a decentralized control system.

The velocity set point is 1500 m/s and the reference tension is 200 lbs. In the simulation, they are scaled to 0.5 m/s and 0.4 lbs respectively. In addition, a step tension disturbance of 50 lbs is added to the upstream and downstream tension set point during the 10^{th} second. A step velocity disturbance of 300 m/s is added to the velocity set point at the 5^{th} second.

6.5.2 Simulation Results

The simulation results are demonstrated by applying both PID controller and the proposed ADRC controller to the decentralized web winding system.

To test the robustness to disturbances and uncertainties, we have tested both cases: Case 1: variation of tension at the 10^{th} second, and Case 2: variation of both tension (10 th second) and velocity (5^{th} second). Figure 32 - 33 shows the results for Case 1, and Figure 34 and 35 show the results of Case 2.

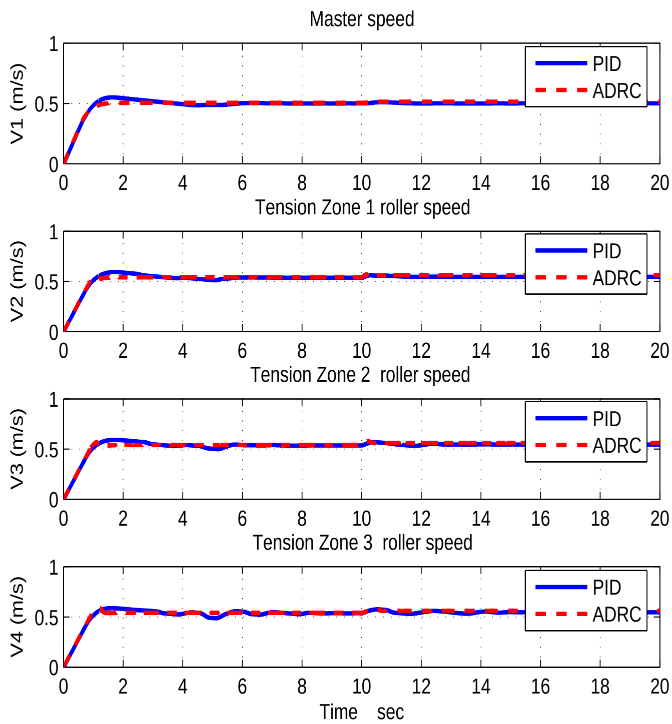

Figure 32: Velocity responses to tension variation at 10^{th} second

From the simulation results, it can be seen that ADRC has a much better tracking performance in both speed and tension loops. It also can be observed that

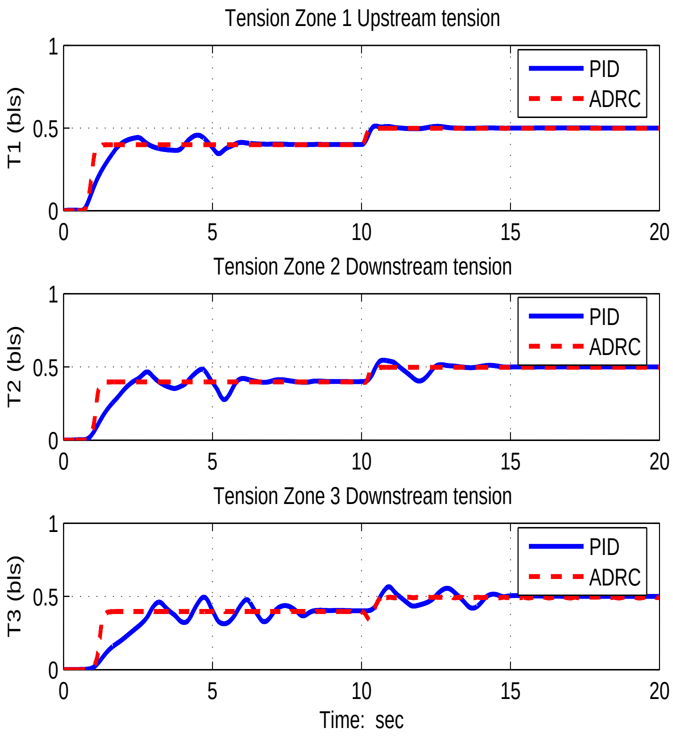

Figure 33: Tension responses to tension variation at 10^{th} second

ADRC has a much shorter recovery time when a variation in tension and velocity setpoint occurs.

It is worthwhile pointing out that the observer and controller for each subsystem has the same parameters. I only tune for one subsystem and copy the tuned parameters to the other subsystems. That is the beauty of the proposed approach: easy to tune.

6.6 Summary

A decentralized robust controller has been developed based on linear active disturbance rejection control paradigm. The extended state observer is designed to estimate the unknown interactions among each subsystem. The proposed controller is then implemented on a four-tension-zone web winding processing line. Simulation

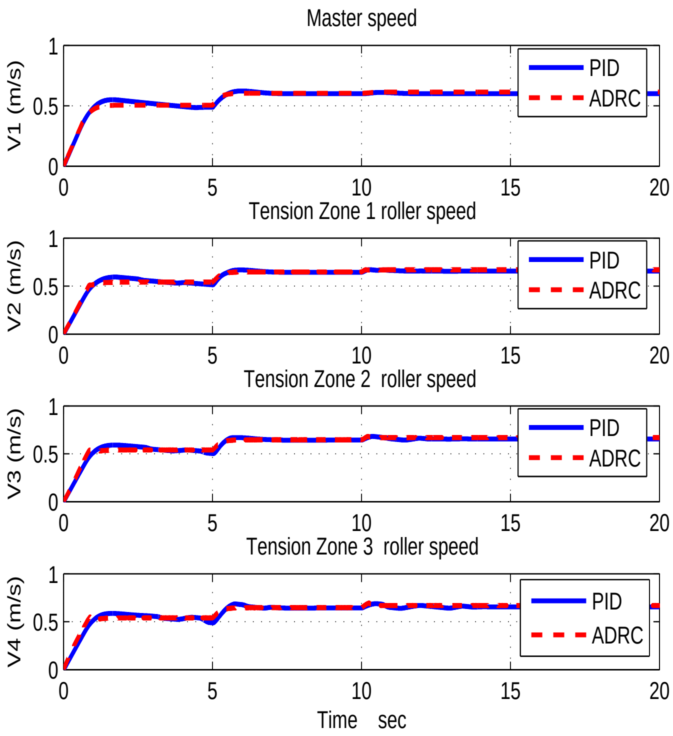

Figure 34: Velocity responses to both tension and velocity variations

results show that the proposed control method has better tension and velocity regulation results than industrial PID controller. The stability of the closed-loop system will be proven in the next chapter. Although only four sections of the process are included in this study, the proposed method is very promising to apply to both the upstream and downstream sections to include the entire web line.

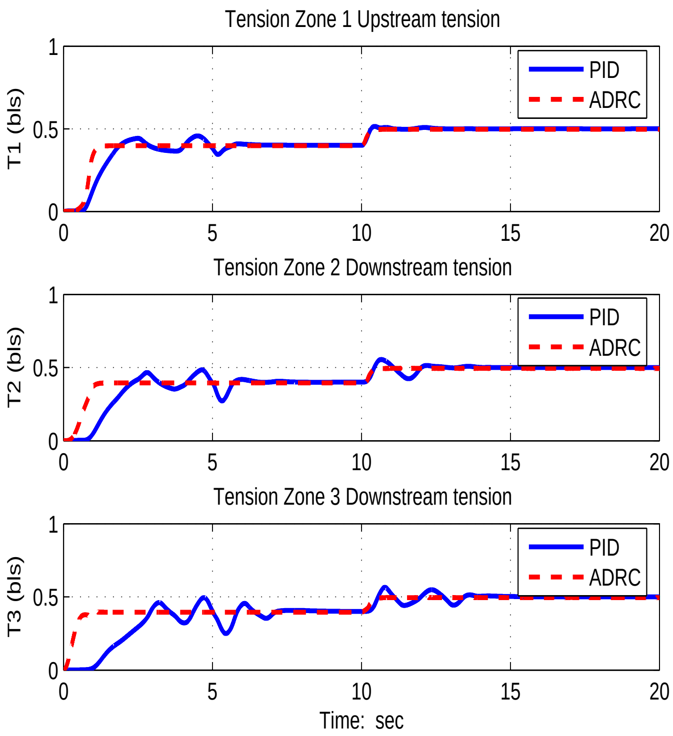

Figure 35: Tension responses to both tension and velocity variations

CHAPTER VII

STABILITY ANALYSIS OF ADRC

Since ADRC has demonstrated the validity and the advantage in different applications [130], many of its properties have been studied by researchers in the past few years. Bounded input and bounded output (BIBO) stability had been proved in [140]. Frequency domain analysis of linear ADRC had been conducted in [106]. The convergence and the bounds of the estimation and tracking errors of ESO were presented in [110]. Stability analysis of nonlinear ADRC was studied by Huang [111].

In this chapter, the stability analysis of the closed-loop system is carried out using singular perturbation theory. The idea is that we divide the closed-loop system into two separated sub-systems: a fast subsystem (dynamics of observer) and a slow subsystem (dynamics of controller). Taking advantage of the results in [119], we provide a necessary condition of the exponential stability for the linear disturbance rejection control.

7.1 Singular Perturbation Theory

The singular perturbation theory in control was designed to analyze models which depend on a small scalar parameter and can be written as follows:

$$\begin{cases} \dot{x} = f(x, z, \varepsilon, t) \\ \varepsilon \dot{z} = g(x, z, \varepsilon, t) \end{cases} \tag{7.1}$$

Given a small positive parameter ε, the system with two-time-scale property can be split into two coupled subsystems, which described a relatively fast and slow part of the original system. Therefore, we can use a systematic way to conduct stability analysis for the separated subsystems, which can be obtained by letting the parameter ε tends to zero and re-scaling the fast subsystem.

Singular Perturbation Theory - Standard Form

Before studying the stability properties of the proposed system, we introduce some relevant results in singular perturbation theory. Many of the following results can be found in [118].

Definitions A nonlinear system is said to be *singularly perturbed* if it has the following form:

$$\begin{cases} \dot{x} = f(x, z, \varepsilon, t), x(t_0) = x^o, x \in R^n \\ \varepsilon \dot{z} = g(x, z, \varepsilon, t), z(t_0) = z^o, z \in R^m \end{cases} \tag{7.2}$$

where ε represents a small parameter. We assume that functions f and g are sufficiently smooth with respected to x, z, ε, t.

System (7.2) is said to be a *standard form* if and only if the following assumptions are satisfied.

Assumption 1: System (7.2) has a unique solution and it has a unique equilibrium point at the origin $(0, 0)$.

Consider system (7.2): let $\varepsilon = 0$, then we have

$$\begin{aligned} \dot{x} &= f(x, z, 0, t), \\ g(x, z, 0, t) &= 0 \end{aligned} \tag{7.3}$$

Assumption 2: System (7.3) has a unique root $z = \phi(x)$.

Then we obtain a slow or reduced subsystem

$$\dot{x} = f(x, \phi(x), t) \tag{7.4}$$

and a fast or boundary layer subsystem

$$\frac{d\hat{z}}{d\tau} = g(x, \hat{z}(\tau) + \phi(\bar{x}, t), 0, t) \tag{7.5}$$

where $\tau = t/\varepsilon$.

Now we have our first theorem below.

Theorem 1. *Suppose that Assumption 1 and Assumption 2 hold for (7.2), then as $\varepsilon \to 0^+$, the asymptotic solution of (7.4) and (7.5) approximate the solution of (7.2) for all $t \geq t_0 \geq 0$ with*

$$\begin{cases} x(\varepsilon, t) - \bar{x}(t) = O(\varepsilon) \\ z(t, \varepsilon) - \phi(\bar{x}, t) - \hat{z}(\tau) = O(\varepsilon) \end{cases} \tag{7.6}$$

(7.6) is uniformly valid for $t \in (t_0, \infty)$, where $\bar{x}(t)$ and $\hat{z}(\tau)$ are the solutions of the reduced (slow) and boundary layer (fast) systems (7.4) and (7.5), respectively.

Singular Perturbation Theory - Asymptotic Solutions

The Steady-State-Model. Let the parameter ε tend to zero, which means that the second equation of (7.1) is considered in steady state $z|_{\varepsilon \to 0} = \bar{z}(x, t)$, we obtain the steady-state system by the following steps:

Step 1: Let $\varepsilon = 0$ and solve the reduced (slow) equation $g(\bar{x}, \bar{z}, 0) = 0$ to obtain solution:

$$\bar{z} = \phi(\bar{x}) \tag{7.7}$$

where the bar is used to indicate that the variable belongs to the original system with $\varepsilon = 0$.

Step 2: Substitute (7.7) into the first equation of (7.1), we obtain the quasi-steady-state model:

$$\dot{\bar{x}} = f(\bar{x}, \bar{\phi}(\bar{x}), 0). \tag{7.8}$$

Because z, whose velocity $\dot{z} = g(x, z, \varepsilon)/\varepsilon$, could become large when $\varepsilon \to 0$, it converges to a root of (7.1) rapidly.

The Boundary-Layer-Model. Singular perturbations cause a multi-time-scale behavior of dynamics systems by the presence of both slow and fast transients in the system. The slow response or the "quasi-steady-state" is approximated by the reduced model, while the discrepancy between the response of the reduced model and that of the full model is the fast transient. To analyze this fast transient characteristics, we will look at it closely by changing time scale.

The boundary-layer model can be obtained by the following steps:

Step 1: Performing a change of variables as follows:

$$\hat{z} = z - \bar{z} \tag{7.9}$$

and a change of the time base by introducing a new time scale variable τ. Given an initial value at $t = t_0$, the new time variable

$$\tau = \frac{t - t_0}{\varepsilon}, \tag{7.10}$$

is "stretched," which means that if $\varepsilon \to 0$, $\tau \to \infty$ even for fixed t only slightly larger than t_0. The slowly varying variables x and t are treated as constant with respect to the fast time base.

Step 2: Substituting (7.9) and (7.10) into the second equation of (7.1), we obtain the boundary-layer-model

$$\frac{d\hat{z}(\tau)}{d\tau} = g(x^0, \hat{z}(\tau) + \bar{z}(t_0), 0) \tag{7.11}$$

Here the new variable $\hat{z}$ is the deviation of the fast variable from its quasi steady state $\bar{z} = \bar{\phi}(\bar{x})$.

We have obtained the slow model (7.8) and fast model (7.11) respectively. Now we are ready to provide the results in stability analysis, which is based on Hassan K. Khalil's theorem in [119].

7.2 Stability Analysis

In this section we show that with proper controllers and observers that have been designed, the closed-loop system of ADRC is stable. Singular perturbation theory [98] is used to analyze the system. Based on the analysis, we construct a Lyapunov function to prove the stability property of the slow and fast subsystems.

7.2.1 The Error Dynamics of ESO

The plant defined by (4.24) can be represented in a matrix form as follows:

$$\begin{cases} \dot{x} = Ax + Bu + E\eta \\ y = Cx \end{cases} \tag{7.12}$$

where

$$A = \begin{bmatrix} 0 & 1 & 0 & \cdots & 0 \\ 0 & 0 & 1 & \cdots & 0 \\ \vdots & \vdots & \vdots & \ddots & \vdots \\ 0 & 0 & 0 & \cdots & 1 \\ 0 & 0 & 0 & \cdots & 0 \end{bmatrix}_{(n+1)\times(n+1)} \quad B = \begin{bmatrix} 0 \\ 0 \\ \vdots \\ b \\ 0 \end{bmatrix}_{(n+1)\times 1} \quad E = \begin{bmatrix} 0 \\ 0 \\ \vdots \\ 0 \\ 1 \end{bmatrix}_{(n+1)\times 1} \quad C = \begin{bmatrix} 1 \\ 0 \\ \vdots \\ 0 \\ 0 \end{bmatrix}^T_{1\times(n+1)}$$

The corresponding ESO is designed based on the plant above as follows:

$$\begin{cases} \dot{z} = Az + Bu + l(y - \hat{y}) \\ \hat{y} = Cz \end{cases} \tag{7.13}$$

where l is the observer gain vector to be selected.

Define the estimation error vector of ESO as

$$\tilde{e} = x - z \tag{7.14}$$

Subtracting (7.13) from (7.12), the error dynamics of the LESO is as follows

$$\dot{\tilde{e}} = (A - lC)\tilde{e} + E\eta \tag{7.15}$$

For the purpose of parameterization and the stability analysis, we introduce the following change of coordinates,

$$\begin{cases} \tilde{e}_1 = \omega_o \xi_1 \\ \vdots \\ \tilde{e}_n = \omega_o^n \xi_n \\ \tilde{e}_{n+1} = \omega_o^{n+1} \xi_{n+1} \end{cases} \tag{7.16}$$

Equation (7.16) can also be equally written as

$$\tilde{e} = \begin{bmatrix} \omega_o & 0 & 0 & \cdots & 0 \\ 0 & \omega_o^2 & 0 & \cdots & 0 \\ \vdots & \vdots & \omega_o^i & \vdots & \vdots \\ 0 & 0 & 0 & \ddots & 1 \\ 0 & 0 & 0 & \cdots & \omega_o^{n+1} \end{bmatrix} \xi = \Lambda \xi \tag{7.17}$$

where $\tilde{e} = [\tilde{e}_1, \tilde{e}_2, \ldots, \tilde{e}_{n+1}]^T$, $\xi = [\xi_1, \xi_2, \ldots, \xi_{n+1}]^T$, and ω_o is a scaling factor, which has specific meaning. $\Lambda = \text{diag}\ [\omega_o, \omega_o^2, \cdots, \omega_o^{n+1}]$, $\Lambda^{-1} = \text{diag}\ [\omega_o^{-1}, \omega_o^{-2}, \cdots, \omega_o^{-(n+1)}]$. Substitute (7.17) into (7.15), and we can get

$$\Lambda\dot{\xi} = (A_e - lC)\Lambda\xi + E\eta \tag{7.18}$$

Since matrix Λ is a diagonal matrix and invertible, equation (7.18) could be transformed as follows:

$$\dot{\xi} = \Lambda^{-1}(A_e - lC)\Lambda\xi + \Lambda^{-1}E\eta \tag{7.19}$$

With the parameterized observer gain l is defined as

$$l = \left[\beta_1\omega_o, \beta_2\omega_o^2, \cdots, \beta_n\omega_o^n, \beta_{n+1}\omega_o^{n+1}\right]^T \tag{7.20}$$

we can transfer (7.19) to the following form

$$\dot{\xi} = \omega_o A_z \xi + \omega_o^{-(n+1)} E\eta \tag{7.21}$$

where $A_z = \begin{bmatrix} -\beta_1 & 1 & 0 & \cdots & 0 \\ -\beta_2 & 0 & 1 & \cdots & 0 \\ \vdots & \vdots & \vdots & \ddots & \vdots \\ -\beta_n & 0 & 0 & \cdots & 1 \\ -\beta_{n+1} & 0 & 0 & \cdots & 0 \end{bmatrix}$

7.2.2 The Error Dynamics of the Plant

The plant in (4.21) can also be rewritten in the following form

$$\begin{cases} \dot{x} = A_1 x + B_1 u + B_f f(\cdot) \\ y = Cx \end{cases} \tag{7.22}$$

where

$$A_1 = \begin{bmatrix} 0 & 1 & 0 & \cdots & 0 \\ 0 & 0 & 1 & \ddots & \vdots \\ \vdots & \ddots & \ddots & \ddots & 0 \\ 0 & 0 & \cdots & 0 & 1 \\ 0 & 0 & \cdots & 0 & 0 \end{bmatrix}_{n\times n} \quad B_1 = \begin{bmatrix} 0 \\ 0 \\ \vdots \\ 0 \\ b \end{bmatrix}_{n\times 1} \quad B_f = \begin{bmatrix} 0 \\ 0 \\ \vdots \\ 0 \\ 1 \end{bmatrix}_{n\times 1} \quad C = \begin{bmatrix} 1 \\ 0 \\ \vdots \\ 0 \\ 0 \end{bmatrix}^T_{1\times n}$$

For the tracking problem, let us define the desired track state vector as

$$x_r = [y_r, \dot{y}_r, \cdots, y_r^{(n-1)}]^T \tag{7.23}$$

and define the tracking error vector as follows:

$$e = x - x_r = [e_1, e_2, \cdots, e_n]^T \tag{7.24}$$

Then the error dynamics of the tracking problems is as follows:

$$\dot{e} = A_1 e + B_1 u + B_f f(\cdot) \tag{7.25}$$

As described in Section 4.3, the control law is designed as

$$u = \frac{1}{b}[-z_{n+1} + u_0] \tag{7.26}$$

This reduced the plant to approximate a nth order integral plant

$$y^{(n)} = (f(\cdot) - z_{n+1}) + u_0 \approx u_0 \tag{7.27}$$

The control law is designed as follows:

$$\begin{aligned} u_0 &= k_1(y_r - z_1) + k_2(\dot{y}_r - z_2) + \cdots + k_n(y_r^{(n)} - z_n) \\ &= k_1\left[y_r - (x_1 - \tilde{e}_1)\right] + k_2[\dot{y}_r - (x_2 - \tilde{e}_2)] + \cdots + k_n[y_r^{(n-1)} - (x_n - \tilde{e}_n)] \\ &= k_1(y_r - x_1) + k_1\tilde{e}_1 + k_2(\dot{y}_r - x_2) + k_2\tilde{e}_2 + \cdots + k_n(y_r^{(n-1)} - x_n) + k_n\tilde{e}_n \\ &= -k_1 e_1 + k_1\tilde{e}_1 - k_2 e_2 + \cdots - k_n e_n + k_n\tilde{e}_n \end{aligned} \tag{7.28}$$

From equation (7.14), we conclude that

$$z_{n+1} = f(\cdot) - \tilde{e}_{n+1} \tag{7.29}$$

Substitute (7.28) and (7.29) into (7.26), and we can get the control input as

$$u = \frac{1}{b}[-Ke + K_f \Lambda \xi - f(\cdot)] \tag{7.30}$$

where $K = [k_1, k_2]^T$,which can be designed to make $A_f = A_1 - B_1 K$ the Hurwitz matrix, and $K_f = [k_1, k_2, 1]^T$.

Substitute controller defined by (7.30) into error dynamics (7.25), the error dynamics of the closed-loop system is as follows:

$$\dot{e} = A_f e + B_1 K_f \Lambda \xi \tag{7.31}$$

Dynamics of the Combined Closed-loop System

Combining the closed-loop tracking error dynamics (7.31) and observer error dynamics (7.21), we obtain

$$\begin{cases} \dot{e} = A_f e + B_f K_f \Lambda \xi, \\ \dot{\xi} = \omega_o A_z \xi + \omega_o^{-(n+1)} E \eta. \end{cases} \tag{7.32}$$

As the closed-loop system dynamics, (7.32) is thereby serve as the starting point for the next step of the stability analysis.

7.2.3 Stability Analysis

The main objective of this section is to study stability characteristics of ADRC. In particular, we wish to determine conditions for stability of the closed-loop error dynamics described by (7.32). This is guided by the insight that the observer dynamics, the second equation in (7.32), is usually much faster than that of the state feedback. The task of analysis is made easier if we separate the fast dynamics from the slow one, and this is a common practice in singular perturbation theory.

In order to apply singular perturbation theory to the stability analysis of the closed-loop error dynamics, we need to reformulate the error dynamics in (7.32) to the standard singular perturbation system as described in (7.2). This is achieved by defining $\varepsilon = 1/\omega_o$, which results in

$$\begin{cases} \dot{e} = A_f e + B_f K_f \Lambda \xi \\ \varepsilon \dot{\xi} = A_z \xi + \varepsilon^{n+2} E \eta \end{cases} \tag{7.33}$$

Clearly, (7.33) is now a standard singularly perturbed system. We apply some existing theorems on stability conditions of the singularly perturbed systems to analyze (7.33). In particular, we introduce the following theorem which proves to be especially useful in the later studies.

Theorem 2. *Consider the singularly perturbed system [119]*

$$\begin{cases} \dot{x} = f(x, z, \varepsilon, t) \\ \varepsilon \dot{z} = g(x, z, \varepsilon, t) \end{cases} \tag{7.34}$$

Assume that the following assumptions are satisfied for all $(t, x, \varepsilon) \in [0, \infty) \times B_r \times [0, \varepsilon_0]$

1). $f(0, 0, \varepsilon, 0) = 0$ *and* $g(0, 0, \varepsilon, 0) = 0$.

2). The equation $g(0, 0, \varepsilon, t) = 0$ *has an isolated root* $z = h(x, t)$ *such that* $h(0, t) = 0$.

3). The function f, g, h, *and their derivatives up to the second order are bounded for* $z - h(x, t) \in B_\rho$.

4). The origin of the reduced system $\dot{x} = f(x, h(x, t), 0, t)$ *is exponentially stable.*

5). The origin of the boundary-layer system $\frac{dy}{d\tau} = g(x, y + h(x, t), 0, t)$ *is exponentially stable, uniformly in* (x, t).

Then, there exists $\varepsilon^* > 0$ *such that for all* $\varepsilon < \varepsilon^*$, *the origin of (7.34) is exponentially stable.*

Applying Theorem 2 to (7.33), we obtain our first main result in stability analysis. Before proceeding to derive Theorem 2, we assume that the following conditions are satisfied for system (4.21).

Condition 1: It is assumed that $f(\cdot)$ and its derivative $\eta(\cdot)$ are locally Lipschitz in their arguments and bounded within the domain of interest. In addition, the initial conditions are assumed such that $f(\cdot)|_{t=0}$=0, and $\eta(\cdot)|_{t=0} = 0$.

Condition 2: It is assumed that the desired output and its derivatives up to $(n + 2)nd$ order are bounded, such that $|y_r^{(i)}| \leq \gamma$.

Theorem 3. *Consider the ADRC error dynamics in (7.33). Let Condition 1 and Condition 2 hold for (4.21), then there exists an* $\varepsilon^* > 0$ *such that for all* $\varepsilon < \varepsilon^*$*, the origin of (7.33) is exponentially stable.*

Proof: In order to apply Theorem 2, we need to show is that (7.33) meets all five assumptions of Theorem 2. Comparing (7.33) and (7.34), it is obvious that

$$f = A_f e + B_f K_f \Lambda \xi \tag{7.35}$$

$$g = A_z \xi + \varepsilon^{n+2} E \eta \tag{7.36}$$

By the definitions of f, g and Condition 1, one can easily see that Assumptions 1 is satisfied.

For Assumption 2, we need to separate the slow and fast model from the original system defined by (7.33) and follow the procedures described in [119]. To obtain the quasi-steady-state model, let $\varepsilon = 0$, and solve the algebraic equation:

$$A_z \xi + \varepsilon^{(n+2)} E \eta = 0 \rightarrow \bar{\xi} = \phi(\bar{e}, t) = 0 \tag{7.37}$$

Obviously, $\bar{\xi}$ is an isolated root for (7.37), and Assumption 2 is therefore satisfied.

To check Assumption 3, we need to show that function f, g, ϕ and their partial derivatives are bounded. Since e and ξ vanish at the origin for all $\varepsilon \in [0, \varepsilon_0]$, they are Lipschitz in ε linearly in the state (e, ξ). By Conditions 1 and 2: both $\eta(\cdot)$ and $\dot{\eta}(\cdot)$ are bounded, we have

$$\|B_f K_f \Lambda \xi\| \leqslant L_1 \|\xi\| \tag{7.38}$$

$$\|\eta\| \leqslant L_2(\|e\| + \|\xi\|) \tag{7.39}$$

$$\|\dot{\eta}\| \leqslant L_3(\|\dot{e}\| + \left\|\dot{\xi}\right\|) \tag{7.40}$$

where L_1, L_2 and L_3 are positive constants. Hence, we now exam the expressions of f, g, ϕ and their partial derivatives are bounded:

$$f = A_f e + B_f K_f \Lambda \xi \leqslant A_f \|e\| + L_1 \|\xi\| \tag{7.41}$$

$$\dot{f} = A_f \dot{e} + B_f K_f \Lambda \dot{\xi} \leqslant A_f \|\dot{e}\| + L_1 \left\|\dot{\xi}\right\| \tag{7.42}$$

$$g = A_z \xi + \varepsilon^{n+2} E\eta \leqslant A_z \|\xi\| + \varepsilon^{n+2} \|E\eta\| \leqslant A_z \|\xi\| + \varepsilon^{n+2} E L_2(\|e\| + \|\xi\|) \tag{7.43}$$

$$\dot{g} = A_z \dot{\xi} + \varepsilon^{n+2} E\dot{\eta} \leqslant A_z \left\|\dot{\xi}\right\| + \varepsilon^{n+2} E L_3(\|\dot{e}\| + \left\|\dot{\xi}\right\|) \tag{7.44}$$

$$\phi(\bar{e}, t) = 0. \tag{7.45}$$

Therefore, we conclude that Assumption 3 is satisfied.

Substitute (7.37) into the first equation of (7.33), we obtain the quasi-steady-state model as follows:

$$\dot{e} = A_f e \tag{7.46}$$

Since A_f is a Hurwitz matrix, it is obvious that Assumption 4 holds.

The boundary layer system, which is the fast dynamics, is obtained by introducing a time scale of

$$\tau = t/\varepsilon \tag{7.47}$$

As $\varepsilon \to 0$, substitute (7.47) into the second equation of (7.33), we obtain

$$\frac{d\xi}{d\tau} = A_z(\tau)\xi(\tau). \tag{7.48}$$

This is the fast dynamics of (7.33). Since A_z is a Hurwitz matrix, it is obvious that Assumption 5 holds.

Note that all the assumptions are satisfied. By Theorem 2, the origin of (7.33) is exponentially stable. Q.E.D.

Remarks

By using singular perturbation approach, we separate the original system into two subsystems: the slow subsystem or quasi-steady state system and the fast subsystem or boundary-layer system. We can then study the subsystems independently.

Under the assumption of $\varepsilon = 0$, the observer error and the tracking error of the system are exponentially stable. Since it is impossible for the ESO to have $\varepsilon = 0$, it is necessary to find a positive value of ε for which the stability properties are valid. For this purpose, we want to establish the stability properties of the singularly perturbed system (7.33) for small ε. We need to show that, under mild assumption that for sufficient small ε, any weighted sum of Lyapunov functions of the reduced and boundary-layer system is exponentially stable.

Theorem 2 shows proof that there exists a certain ε^* that can guarantee the origin of (7.33) is exponentially stable. Since (7.33) is a linear system, Theorem 6 can be used to find the upper bonds of ε.

Before showing the new result in Theorem 6, we first state Theorem 4 and Theorem 5 in [119].

Theorem 4. *Let $x = 0$ be an equilibrium point for the nonlinear system*

$$\dot{x} = f(t, x) \tag{7.49}$$

where $f : [0, \infty) \times D \to R^n$ is continuous differentiable, $D = \{x \in R^n | \, \|x\| < r\}$ and the Jacobian matrix $[\partial f / \partial x]$ is bounded on D uniformly in t.

Let k, λ and r_0 be positive constant with $r_0 < r/k$, and define $D_0 = \{x \in R^n | \, \|x\| < r_0\}$. Assume that the trajectories of the system satisfy

$$\|x(t)\| \leq k \, \|x(t_0)\| \, e^{-\lambda(t-t_0)}, \forall x(t_0) \in D_0, \forall t \geq t_0 \geq 0 \tag{7.50}$$

then there is a function $V : [0, \infty) \times D_0 \to R$ that satisfies the inequalities

$$c_1 \|x\|^2 \leq V(t, x) \leq c_2 \|x\|^2 , \tag{7.51}$$

$$\frac{\partial V}{\partial t} + \frac{\partial V}{\partial x} f(t, x) \leq -c_3 \|x\|^2 , \tag{7.52}$$

$$\left\| \frac{\partial V}{\partial x} \right\| \leq c_4 \|x\| , \tag{7.53}$$

for some positive constants c_1, c_2, c_3 and c_4. Moreover, if $r = \infty$ and the origin is globally exponentially stable, then $V(t, x)$ satisfies the aforementioned inequalities on

R^n. Furthermore, if the system is autonomous, $V(t,x)$ can be chosen independent of t.

Theorem 5. *The system shown below is considered to be slowly varying*

$$\dot{x} = f(x,u) \tag{7.54}$$

where $x \in R^n$ and $u \in \Gamma \subset R^m$ for all $t \geq 0$.

Suppose $f(x,u)$ is locally Lipschitz on $R^n \times \Gamma$ for every $u \in \Gamma$, the equation (7.54) has a continuously differentiable isolated root. To analyze the stability properties of the frozen equilibrium point $x = h(\alpha)$, we shift it to the origin via the change of variables $z = x - h(\alpha)$ to obtain the equation

$$\dot{z} = f(x + h(\alpha), \alpha) \stackrel{def}{=} g(z,\alpha) \tag{7.55}$$

Now, consider the system (7.55), suppose $g(z,\alpha)$ is continuously differentiable and the Jacobian matrices $[\partial g/\partial z]$ and $[\partial g/\partial z]$ satisfy

$$\left\| \frac{\partial g}{\partial z}(z,\alpha) \right\| \leq L_1, \left\| \frac{\partial g}{\partial \alpha}(z,\alpha) \right\| \leq L_2 \|z\| \tag{7.56}$$

for all $(z,\alpha) \in D \times \Gamma$ where $D = \{z \in R^n | \, \|z\| < r\}$.

Let k, γ, and r_0 be positive constants with $r_0 < r/k$, and define $D_0 = \{z \in R^n | \, \|z\| < r_0\}$. Assume that the trajectories of the system satisfy

$$\|z(t)\| \leq k \|z(0)\| e^{-\gamma t}, \forall z(0) \in D_0, \alpha \in \Gamma, \forall t \geq 0, \tag{7.57}$$

then there is a function $W : D_0 \times \Gamma \to R$ that satisfies (7.58) through (7.61). Moreover, if all the assumptions hold globally in z, then $W(z,\alpha)$ is defined and satisfies (7.58) through (7.61) on $R^n \times \Gamma$

$$b_1 \|z\|^2 \leq W(z,\alpha) \leq b_2 \|z\|^2, \tag{7.58}$$

$$\frac{\partial W}{\partial z} g(z,\alpha) \leq -b_3 \|z\|^2, \tag{7.59}$$

$$\left\| \frac{\partial W}{\partial z} \right\| \leq b_4 \left\| z \right\|, \tag{7.60}$$

$$\left\| \frac{\partial W}{\partial \alpha} \right\| \leq b_5 \left\| z \right\|, \tag{7.61}$$

for all $z \in D = \{z \in R^n | \, \|z\| < r\}$ *and* $\alpha \in \Gamma$*, where* $b_i, i = 1, \ldots, 5$ *are positive constants independent of* α*.*

Theorem 6. *Consider the singular perturbed system (7.33), and assume that Condition 1 and Condition 2 hold for (4.21), then there exist an upper bound of* ε^**, such that*

$$\varepsilon^* \leq \min \left(\sqrt[n+1]{\left[2(1-d)c_3 - c_4 L_1(1-d)\right] / d b_4 L_2}, \frac{d b_3}{c_4 L_1 (1-d)}, \sqrt[n+1]{\frac{1}{3} \frac{c_4 L_1 (1-d)}{d b_4 L_2}} \right)$$

where $b_i (i = 1, \ldots, 4)$*,* $c_i (i = 1, \ldots, 4)$*,* L_1*, and* L_2 *are nonnegative constants,* $0 < d < 1$*. Then for all* $\varepsilon \leq \varepsilon^*$*, the origin of (7.33) is exponentially stable.*

Proof: By Theorem 4, there is a Lyapunov function $V(e)$ for the reduced system that satisfies

$$c_1 \left\| e \right\|^2 \leq V(e) \leq c_2 \left\| e \right\|^2, \tag{7.62}$$

$$\frac{\partial V}{\partial x} A_f e \leq -c_3 \left\| e \right\|^2, \tag{7.63}$$

$$\left\| \frac{\partial V}{\partial e} \right\| \leq c_4 \left\| e \right\|, \tag{7.64}$$

for some positive constants $c_i, i = 1, \ldots, 4$ and for $e \in B_{r0}$ with $r_0 \leq r$.

By Theorem 5, there is a Lyapunov function $W(\xi)$ for the boundary layer system that satisfies

$$b_1 \left\| \xi \right\|^2 \leq W(\xi) \leq b_2 \left\| \xi \right\|^2, \tag{7.65}$$

$$\frac{\partial W}{\partial \xi} A_z \xi \leq -b_3 \left\| \xi \right\|^2, \tag{7.66}$$

$$\left\| \frac{\partial W}{\partial \xi} \right\| \leq b_4 \left\| \xi \right\|, \tag{7.67}$$

for some positive constants $b_i (i = 1, \ldots, 4)$ and for $\xi \in B_{\rho_0}$ with $\rho_0 \leq \rho$.

Since e and ξ vanish at the origin for all $\varepsilon \in [0, \varepsilon_0]$, they are Lipschitz in ε linearly in the state (e, ξ). In particular,

$$\|B_f K_f \Lambda \xi\| \leq L_1 \|\xi\| \tag{7.68}$$

$$\|E\eta\| \leq L_2 (\|e\| + \|\xi\|) \tag{7.69}$$

where L_1 and L_2 are two positive constants.

We set

$$V_{cl}(e, \xi) = (1-d)V(e) + dW(\xi) \tag{7.70}$$

as a Lyapunov function candidate for system (7.33), where d is a weighting variable, $0 < d < 1$. Using the properties of functions and the estimates from (7.62) to (7.69), one can verify that the derivative of (7.70) along the trajectories of (7.33) satisfies the following inequalities:

$$\begin{aligned}
\dot{V}_{cl} &= (1-d)\frac{\partial V}{\partial e}(A_f e + B_f K_f \Lambda \xi) + d\frac{\partial W}{\partial \xi}(\frac{1}{\varepsilon}A_z \xi + E\eta) && (7.71)\\
&= (1-d)\frac{\partial V}{\partial e}A_f e + (1-d)\frac{\partial V}{\partial e}B_f K_f \Lambda \xi + d\frac{\partial W}{\partial \xi}\frac{1}{\varepsilon}A_z \xi + d\frac{\partial W}{\partial \xi}E\eta && (7.72)\\
&\leq -(1-d)c_3\|e\|^2 + (1-d)c_4\|e\| L_1 \|\xi\| - \frac{d}{\varepsilon}b_3\|\xi\|^2 \\
&\quad +db_4\|\xi\| \left[L_2(\|e\| + \|\xi\|)\right] && (7.73)\\
&\leq -(1-d)c_3\|e\|^2 - \frac{d}{\varepsilon}b_3\|\xi\|^2 + db_4\varepsilon^{n+1}L_2\|\xi\|^2 \\
&\quad + \left(c_4 L_1(1-d) + db_4\varepsilon^{n+1}L_2\right)\|e\|\,\|\xi\| && (7.74)\\
&\leq -(1-d)c_3\|e\|^2 + \left[db_4\varepsilon^{n+1}L_2 - \frac{d}{\varepsilon}b_3\right]\|\xi\|^2 \\
&\quad + \left(c_4 L_1(1-d) + db_4\varepsilon^{n+1}L_2\right)\left(\frac{\|e\|^2 + \|\xi\|^2}{2}\right) && (7.75)\\
&\leq \left[-(1-d)c_3 + \frac{1}{2}c_4 L_1(1-d) + \frac{1}{2}db_4\varepsilon^{n+1}L_2\right]\|e\|^2 \\
&\quad + \left[\frac{3}{2}db_4\varepsilon^{n+1}L_2 - \frac{d}{\varepsilon}b_3 + \frac{1}{2}c_4 L_1(1-d)\right]\|\xi\|^2 && (7.76)\\
&\leq -\mu_1\|e\|^2 - \mu_2\|\xi\|^2 && (7.77)
\end{aligned}$$

where $\begin{cases} \mu_1 = (1-d)c_3 - \frac{1}{2}c_4L_1(1-d) - \frac{1}{2}db_4\varepsilon^{n+1}L_2 \\ \mu_2 = \left[\frac{d}{\varepsilon}b_3 - \frac{1}{2}c_4L_1(1-d) - \frac{3}{2}db_4\varepsilon^{n+1}L_2\right] \end{cases}$

From (7.77), in order to get the desired $v_{cl} \leq 0$, we need to make both μ_1 and μ_2 be positive.

First let $\mu_1 \geq 0$, we can obtain:

$$\begin{aligned} &\mu_1 = (1-d)c_3 - \frac{1}{2}c_4L_1(1-d) - \frac{1}{2}db_4\varepsilon^{n+1}L_2 \geq 0 \\ &\Rightarrow \varepsilon_1^* \leq \sqrt[n+1]{[2(1-d)c_3 - c_4L_1(1-d)]\,/db_4L_2}. \end{aligned} \tag{7.78}$$

Then let $\mu_2 \geq 0$, we can obtain:

$$\begin{aligned} &\mu_2 = \left[\frac{d}{\varepsilon}b_3 - \frac{1}{2}c_4L_1(1-d) - \frac{3}{2}db_4\varepsilon^{n+1}L_2\right] \geq 0 \\ &\Rightarrow \begin{cases} \frac{d}{\varepsilon}b_3 - \frac{1}{2}c_4L_1(1-d) \geq \frac{1}{2}c_4L_1(1-d) \\ \frac{1}{2}c_4L_1(1-d) \geq \frac{3}{2}db_4\varepsilon^{n+1}L_2 \end{cases} \\ &\Rightarrow \varepsilon_2^* \leq \min\left(\frac{db_3}{c_4L_1(1-d)}, \sqrt[n+1]{\frac{1}{3}\frac{c_4L_1(1-d)}{db_4L_2}}\right) \end{aligned} \tag{7.79}$$

Based on the selection of ε_1^* and ε_2^*, it will be guaranteed that

$$\dot{V}_{cl} \leq -\min(\mu_1, \mu_2)\left[\|e\|^2 + \|\xi\|^2\right] \tag{7.80}$$

which completes the proof. Q.E.D.

Example

Take an example of the exit velocity loop dynamics in equation (5.4)

$$\dot{v}_e(t) = \frac{1}{J}(-B_f v_e(t) + R^2(t_r - t_c(t)) + RK_e u_e(t) - R^2\delta_e(t)) \tag{7.81}$$

It is a first-order system, and the general dynamics in terms of $f(\cdot)$ is expressed as follows

$$\dot{y}(t) = f(\cdot) + \frac{RK_e}{J}u_e(t) \tag{7.82}$$

where $f(\cdot) = \frac{1}{J}(-B_f v_e(t) + R^2(t_r - t_c(t)) - R^2\delta_e(t))$.

From the error dynamics described in section 7.2.1 and 7.2.2, A_f and A_z are expressed as follows

$$A_f = A_1 - B_1 K = -bK, A_z = \begin{bmatrix} -\beta_1 & 1 \\ -\beta_2 & 0 \end{bmatrix} = \begin{bmatrix} -2 & 1 \\ -1 & 0 \end{bmatrix} \tag{7.83}$$

Since A_f and A_z are both linear Hurwitz matrix, we define a Lyapunov function $V(e) = e^T P e$ for the reduced system, where P is the positive definite solution of the Lyapunov equation $A_f^T P + P A_f = -I$, where I is a corresponding identity matrix.

Similarly, we define a Lyapunov function $W(\xi) = \xi^T Q \xi$ for the boundary-layer system, where Q is the positive definite solution of the Lyapunov equation $A_z^T Q + Q A_z = -I$, where I is a corresponding identity matrix.

We solve Lyapunov function on Matlab and obtain the P and Q matrix as follows: $P = \frac{1}{2bK} = 0.707$, $Q = \begin{bmatrix} 0.5 & -0.5 \\ -0.5 & 1.5 \end{bmatrix}$. Based on P and Q matrix, we determine that $b_3 = 1, b_4 = 2$, $c_3 = 1, c_4 = 1/2$, $L_1 = 1, L_2 = 3 \times 10^4$, and choose d=1/2. Finally, we are able to calculate ε as follows:

$$\varepsilon = \min\left[\sqrt{\frac{2\times(1-1/2)-1/2\times1\times(1-1/2)}{1/2\times3.414\times30000}}, \frac{1/2\times1}{1/2\times1\times(1-1/2)}, \sqrt{\frac{1}{3}\frac{1/2\times1\times(1-1/2)}{1/2\times3.414\times30000}}\right] = 0.0004033.$$

Therefore, we obtain the lower bound of the observer bandwidth as $\omega_o = 1/\varepsilon = 2479.5$.

Remarks

(1). Theorem 6 is an extension of Theorem 3, in which equation (7.78)-(7.80) determine the upper bound of ε. Since $\varepsilon = 1/\omega_o$, it means that the lower bound of observer bandwidth ω_o can be obtained based on Theorem 6.

(2). The ESO in the fast time scale τ is faster than the dynamics of the plant and the controller, we are able to make the estimated state converge to the real state faster. This explains why ESO can actively reject the disturbance, since the extended state can estimate the unknown dynamics very well.

(3). The derived lower bound of the observer bandwidth is larger than the real tuning parameter, because it was derived by Lyapunov functions, which are very conservative.

The above results show that for the closed-loop system, when controlled by ESO and ADRC control law presented in (7.32), achieves exponentially asymptotic convergence of the tracking errors.

7.3 Summary

We presents in this chapter a singular perturbation approach to analyze the stability characteristics of the closed-loop error dynamics based on the active disturbance rejection control (ADRC) for nonlinear time-invariant plant. The closed-loop error dynamics is first formulated into a standard singular perturbation system. Then we analyze the resulting singular perturbation system to provide a necessary condition of the stability characteristics of the original error dynamics. We found that there exists a small ε that guarantees that the origin of the error dynamics is exponentially stable. Since the decomposed singular perturbation systems are linear, we can further the study to obtain an upper bound for ε by applying Khalil's theorem in ([119]). Our result shows that parameter ε is reversely proportional to the bandwidth of the controller and it is bounded by a upper limit of ε. This has significant practical meaning because it will be very helpful for the real control system design.

CHAPTER VIII

CONCLUSION AND FUTURE WORK

8.1 Conclusion

The problem of web winding system, both single elements of an accumulator and large-scale systems, have been investigated in this dissertation.

Firstly, the mathematical tools and assumptions for modeling of web winding systems are reviewed. Based on these assumptions and mathematical laws, the general mathematical model of web winding system is derived. It is observed that the existing web winding system control literature is not extensive. Thus an in-depth literature review of web winding system with a highlight of system modeling, control structures and control strategies, tension observer techniques, and other related aspects has been conducted thoroughly.

Secondly, from literature review, nearly all controllers proposed have been either too complicated to implement or costly to tune for a given system. Furthermore, one of the challenges of web winding systems control is the unexpected disturbances that can propagate through the system and affect both tension and velocity loops. To solve these issues, we presented a unique active disturbance rejection control strategy for a class of tension and velocity regulation problems found in accumulators in web processing lines. Simulation results show remarkable disturbance rejection capability of the proposed control scheme in coping with large dynamic variations commonly seen in web tension applications.

Thirdly, another complication in web winding system stems from its large-scale, coupled interconnections nature. This motivates the research in formulating a novel robust decentralized control strategy. Web winding system is a strongly coupled system. While the literature has taken some advantage of the intuitive decoupling present in the system, it has not been exploited to its fullest extent. Hence, we have reformulated the web winding system as a large-scale decentralized control problem. A literature review of both large-scale systems and accordingly decentralized control strategies are reviewed first, then the decentralized web winding system control is discussed in detail. All subsystem nonlinearities and interactions between adjunct subsystems are regarded as perturbations, to be estimated by an augmented state observer. The proposed decentralized control strategy was implemented on a 3-tension-zone web winding processing line. Simulation results show that the proposed control method has better tension and velocity regulation results than industrial PID controller.

The core technology that has been applied to web winding system is active disturbance rejection control strategy. Therefore, an extensive literature review of existing disturbance rejection control strategies, both passive and active disturbance rejection control, have been investigated.

ADRC has been demonstrated and exhibited excellent results both in simulation and real applications in many benchmark problems and practical industrial applications. However, the stability and convergence have not been rigorously addressed previously. Therefore, a systematic analysis of the stability of the close-loop system is essential. A novel approach to the stability analysis of the close-loop system by singular perturbation theory is creatively proposed to solve this issue. Finally, it is shown that the exponential stability is assured for the dynamic system if the observer bandwidth is higher than the given lower bound of the bandwidth of the controller.

The major accomplishments in this work are as follows:

- Extensive state-of-the-art review of web winding system, including system modeling, tension control, tension estimation, existing control techniques, and the challenges in terms of control.

- Literature review of large-scale decentralized control problems and specific applications in decentralized control of web winding systems.

- Literature review of disturbance rejection control in terms of passive and active rejection mechanism. Advantages and disadvantages of each strategy have been fully investigated.

- The velocity and tension regulation problems are reformulated as a disturbance rejection problem, opening a new direction in research.

- Active disturbance rejection control strategy is evaluated and employed for a class of tension and velocity regulation problems found in accumulators. The coupled tension and velocity loops are easily decoupled by ADRC, which is demonstrated in a web processing line.

- Demonstrated that ADRC is not a formula, instead it is an idea. ADRC has been originally proposed to deal with disturbance rejection problems. In this dissertation, the ADRC idea is creatively applied in the decentralized control framework, where the unknown dynamics of the interactions between each subsystem are treated as disturbances to each subsystem. Again, this opens up a new research direction in a well-established field: decentralized control.

- Formulated and implemented a novel robust decentralized control strategy and demonstrated its application in large-scale web winding systems.
- Stability characteristics of ADRC for nonlinear, uncertain, and time-varying plant are analyzed. A novel reformulation of the stability problem is proposed, leading to the application of a class of mathematical analysis techniques.

8.2 Future Work

ADRC has been applied to both accumulator and large scale web winding system in simulation. Future work would be an experimental validation for these results.

The decentralized control problem is still a hot research topic nowadays. There are still many research areas in this direction, such as how to deal with fault tolerant control for large scale decentralized control problems.

ADRC is not omnipotent; it has its limitations, one of which is to deal with time-delay problems. Therefore, one of the possible directions is to solve this problem.

This dissertation has demonstrated ADRC absolutely is not a formula. New directions and research ideas should rest on this philosophy and expand the current results. Future research could be to focus on the following directions:

- Noise is the limitation to the perfect result of ADRC. To improve the performance of ADRC, one direction of ADRC research could be focus on applying wavelets or other filtering methods to get cleaner input signals to the ESO, thus improving the limits of the observer bandwidth.

- ADRC can be applied to minimum phase system without any "zero dynamics". How about non-minimum phase system with unstable "zero-dynamics"? There are some open issues on how ADRC applies to these systems.

- In some situations, minimum control effort is the main concern. ADRC is very aggressive in achieving excellent performance and eliminating the disturbance; however, it also costs a large amount of control effort. If f is well estimated, the control effort would be much smaller, thus achieving the smaller control effort.

BIBLIOGRAPHY

[1] K. J. Astrom, and T. Hagglund, *PID Controllers: Theory, Design, and Tuning,* International Society for Measurement and Control, 1995.

[2] J. N. R. Sandell, P. Varaiya, M. Athans, and M. G. Saronov, "Survey of decentralized control methods for large scle systems," *IEEE Transactions on Automatic Control,* April 1978, vol. 23, pp 108-128.

[3] D. D. Sljak, *Decentralized control of complex systems,* New York: Academic Press, 1991.

[4] D. P. Campbell, *Dynamic Behavior of the Production Process,* John Wiley and Sons, Inc., New York, First edition, 1958.

[5] D. R. Roisum, *The Mechanics of Winding,* TAPPI Press, 1994.

[6] D. R. Roisum, *The Mechanics of Web Handling,* TAPPI Press, 1998.

[7] K. P. Grenfell, "Tension control on paper-making and converting machinery," *IEEE 9th Annual Conference on Electrical Engineering in the Pulp and Paper Industry,* Boston, MA, June 1963, pp. 20-21.

[8] G. E. Young, and K. N. Reid, "Lateral and longitudinal dynamic behavior and control of moving webs," *Transactions of the ASME, Journal of Dynamic Systems, Measurement and Control,* 1993, Vol. 115, pp. 309-317.

[9] H. W. Swift, "Power transmission by belts: An investigation of fundamentals," *Proceedings of Institute of Mechanical Engineers,* 1928, Vol. 115, pp. 659-743.

[10] D. King, "The mathematical model of a newspaper press," *Newspaper Techniques,* December, 1969, pp. 3-7.

[11] D. P. Whitworth, and M. C. Harrison, "Tension variations in pliable material in production machinery," *Applied Mathematical Modeling,* 1983, Vol. 7, pp. 189-196.

[12] G. Brandenburg, "New mathematical models for web tension and register error," *Proceedings of the Third International IFAC Conference on Instrumentation and Automation in the Paper, Rubber, and Plastics Industry,* Brussels, Belgium, 1976, pp. 185-190.

[13] J. J. Shelton, "Dynamics of web tension control with velocity or torque control," *Proceedings of the 1986 American Control Conference,* Seattle, WA , 1986, pp. 1423-1427.

[14] M. J. Grimble, "Tension controls in strip processing lines," *Metals Technology,* Oct. , 1976, pp. 446-453.

[15] B. T. Boulter, "The Effect of Speed Loop Bandwidths and Line-speed on System Natural Frequencies in Multi-Span Strip Processing Systems," *IEEE IAS Annual Meeting* , August, 1997.

[16] W. Liu and E. J. Davison, "Servomechanism controller design of web handling systems," *IEEE Trans. On Control Systems,* Vol. 1l, No. 4, July, 2003, pp. 555-564.

[17] F. Lynch, S. A. Bortoff, and K. Robenack, "Nonlinear tension observers for web machines," *Automatica* , 2004, Vol. 40, pp. 1517-1524.

[18] H. Koc, D. Knittel, M. D. Mathelin, and G. Abba, "Modeling and robust control of winding systems for elastic webs," *IEEE Trans. on Control Systems Technology,* Vol. 10, No. 2, March 2002.

[19] W. Wolfermann, "Tension control of webs, a review of the problems and solutions in the present and future," *Proceedings of the Third International Conference on Web Handling,* June 1995, pp. 198-229.

[20] P. Lin and M. S. Lan, "Effects Of PID gains for controller with dancer mechanism on web tension," *Proceedings of the Second International Conference on Web Handling,* Stillwater, Oklahoma, 1993, pp. 66-76.

[21] K. N. Reid, K. H. Shin, and K. C. Lin, "Variable-gain control Of longitudinal tension in a web transport system", AMD-Vol. 149, *Web Handling, ASME*, 1992, pp. 87-100.

[22] S. Jee, S. Kim and K. H. Shin, "Adaptive fuzzy control of tension variations due to the eccentric unwinding roll in multi-span web transport systems," *Proceedings of ASME Dynamic System and Control Division,* Vol. 67, 1999, pp. 877-882.

[23] K. Okada, and T. Sakamoto, "An adaptive fuzzy control for web tension control system," *Proc. IEEE International Symposium on Industrial Electronics,* 1998, pp. 1762-1767.

[24] F. L. Luo, and C. Wen, "Multi-page mapping artificial network algorithm used for constant tension control," *Expert System with Applications,* Vol. 13, No. 4, 1997, pp. 307-315.

[25] C. Wang, and Y. Z. Wang, "Research on precision tension control system based on neural network," *IEEE Transaction on Industrial Electronics* Vol. 51, No. 2, 2004, pp. 381-386.

[26] A. Angermann, M. Aicher, and D. Schroder, "Time-optimal tension control for

processing plants with continuous moving webs," *Proc. 35th Annual Meeting-IEEE Industry Applications Society,* Rome, Oct. 1999.

[27] P. R. Pagilla, S. S. Garimella, L. H. Dreinhoefer, and E. O. King, "Dynamics and control of accumulators in continuous strip processing lines," *IEEE Transactions on Industry Applications,* Vol. 37, 2001, pp. 934-940.

[28] H. Koc, D. Knittel, M. D. Mathelin, and G. Abba, "Robust gain-scheduled control of winding systems," *IEEE Conf. Decision and Control,* Sidney, Australia, Dec. 2000.

[29] P. R. Pagilla, I. Singh and R. V. Dwivedula, "A study on control of accumulators in web processing lines," *Journal of Dynamic Systems, Measurement, and Control,* 2004, Vol. 126, pp. 453-461.

[30] M. D. Baumgart, and L. Y. Pao, "Robust Lyapunov-based feedback control of nonlinear web-winding systems," *Proceedings of IEEE Conference on Decision and Control,* June 2003.

[31] D. Knittel, E. Laroche, and H. Koc, "Tension control for winding systems with two-degrees-of-freedom H_∞ controllers," *IEEE Trans on Industry Applications,* Vol. 39, No. 1, June 2003, pp. 113-120.

[32] P. R. Pagilla, R.V. Dwivedula, Y. Zhu, and L. P. Perera, "Periodic tension disturbance attenuation in web processing lines using active dancers," *ASME Journal of Dynamic Systems, Measurement, and Control,* September 2003, Vol. 125, No. 3, pp. 361-371.

[33] K. H. Shin, "Distributed control of tension in multi-span web transport systems," Ph.D. thesis, Oklahoma State University, Stillwater, Oklahoma, May 1991.

[34] K. H. Shin, *Tension control,* TAPPI Press, 2000.

[35] S. H. Wang and E. J. Davison, "On the stabilization of decentralized control systems," *IEEE Transactions on Automatic Control,* 1973, Vol. 18, pp. 473-478.

[36] B. D. Anderson and J. B. Moore, "Time-varying feedback laws for decentralized control," *IEEE Transactions on Automatic Control,* 1981, Vol. 26, pp. 1133-1138.

[37] P. P. Khargonekar and A. B. Ozguler, "Decentralized control and periodic feedback," *IEEE Transactions on Automatic Control,* April 1994, Vol. 39, pp. 877-882.

[38] P. A. Ioannou, "Decentralized adaptive control of interconnected systems," *IEEE Transactions on Automatic Control,* 1986, Vol. 31, No. 4, pp. 291-298.

[39] L. Shi and S. K. Singh,"Decentralized adaptive controller design for large-scale systems with higher order interconnections," *IEEE Transactions on Automatic Control,* 1992, Vol. 37, No. 8, pp. 1106-1118.

[40] S. Jain and F. Khorrami, "Decentralized adaptive control of a class of large-scale interconnected nonlinear systems," *IEEE Transactions on Automatic Control,* 1997, Vol. 42, No. 2, pp. 177-186.

[41] B.M. Mirkin and P. O. Gutman,"Decentralized output-feedback control of linear state delay systems," *IEEE Transactions on Automatic Control,* September 2003, Vol. 48, pp. 1613-1619.

[42] P. R. Pagilla and H. Zhong, "Semi-globally stable decentralized control of a class of large-scle interconnected nonlinear systems," *Proceedings of the American Control Conference,* 2003.

[43] P. R. Pagilla, "Robust decentralized control of large-scale interconnected systems: General interconnections," *Proceedings of the American Control Conference,* 1999, Vol. 6, pp. 4527-4531.

[44] M. Ikdea, *Decentralized control of large scale systems, Three decades of mathematical system theory,* Springer-Verlag, 1989, pp. 219-242.

[45] N. Viswanadham and A. Ramakrishna, "Decentralized estimation and control for interconnected systems," *Large Scale Systems,* 1982, Vol. 3, pp. 255-266.

[46] M. Aldeen and J. F. Marsh, "Decentralized observer-based control scheme for interconnected dynamical systems with unknown inputs," *IEE Proceedings on Control Theory and Applications,* Sept. 1999, Vol. 146, pp. 349-357.

[47] N. Abdel-Jabbar, C. Kravaris, and B. Carnahan, "A partially decentralized state observer and its parallel computer implementation," *Industrial and Engineering Chemistry Research,* 1998, Vol. 37, pp. 2741-2760.

[48] Z. P. Jiang, "Decentralized and adaptive nonlinear tracking of large-scale systems via output feedback," *IEEE Transactions on Automatic Control,* 2000, Vol. 45, pp. 2122-2128.

[49] K. S. Narendra and N. O. Oleng, "Exact output tracking in decentralized adaptive control systems," *IEEE Transactions on Automatic Control,* 2002, Vol. 47, no. 2, pp. 390-395.

[50] D. D. Siljak, D. M. Stipanovic, and A. I. Zecevic, "Robust decentralized turbine/governor control using linear matrix inequalities," *IEEE Transactions on Power Systems,* August 2002, Vol. 17, pp. 715-722.

[51] B. M. Mirkin and P. O. Gutman, “Decentralized output-feedback control of linear state delay systems,” *IEEE Transactions on Automatic Control,* September 2003,Vol. 48, pp. 1613-1619.

[52] P. R. Pagilla and Y. Zhu, “A decentralized output feedback controller for a class of large-scale interconnected nonlinear systems,” *ASME Journal of Dynamic Systems, Measurement, and Control,* 2005, Vol. 127, no. 1, pp. 167-172.

[53] D. T. Gavel and D. D. Siljak, “Decentralized adaptive control: Structural conditions for stability,” *IEEE Trans. Automat. Control.,* April 1989, Vol. 34, pp. 413-426.

[54] L. Shi and S. K. Singh, “Decentralized adaptive controller design for large scale systems with higher order interconnections,” *IEEE Trans. Automat. Control.,* Aug. 1992, Vol. 37, pp. 1106-1118.

[55] C. Wen, “Decentralized adaptive regulation,” *IEEE Trans. Automat. Contr.,* Oct. 1994, vVol. 39, pp. 2163-2166.

[56] C. Wen, “Indirect robust totally decentralized adaptive control of continuous time interconnected systems,” *IEEE Trans. Automat. Control.,* June 1995, Vol. 40, pp. 1122-1126.

[57] J. T. Spooner and K. M. Passino, “Adaptive control of a class of decentralized nonlinear systems,” *IEEE Trans. Automat. Control,* Feb. 1996, Vol. 41, pp. 280-284.

[58] S. Jain and F. Khorrami, “Decentralized adaptive control of a class of large scale interconnected nonlinear systems,” *IEEE Trans. Automat. Control,* Feb. 1997, Vol. 42, pp. 136-154.

[59] Z. P. Jiang, “Decentralized and adaptive nonlinear tracking of large-scale systems via output feedback,” *IEEE Trans. Automat. Control,* Nov. 2000, Vol. 45, pp. 2122-2128.

[60] Z. P. Jiang, “New results in decentralized adaptive control with output-feedback,” *Proc. 38th Conf. Decision Control,* Phoenix, AZ, 1999, pp. 4772-4777.

[61] M. Makoudi and L.Radouane, “Robust decentralized adaptive control for non-minimum phase systems with unknown and/or time varying delay,” *Automatica,* Volume 35, Number 8, August 1999, pp. 1417-1426.

[62] C. L. Hwang, and H. Y. Lin, “A fuzzy decentralized variable structure tracking control with optimal and improved robustness designs: theory and applications,” *IEEE T. Fuzzy Systems*, 2004, Vol. 12, no. 5, pp. 615-630.

[63] J. T. Spooner, and K. M. Passino, “Decentralized adaptive control of nonlinear systems using radial basis neural networks,” *IEEE Transactions on Automatic Control,* Nov. 1999, Vol. 44, no. 11, pp. 2050-2057.

[64] N. L. Hovakimyan, E. B. Yang, and A. J. Calise, “Coordinated decentralized adaptive output feedback control of interconnected systems,” *IEEE Transactions on Neural Networks,* Jan. 2005, Vol. 16, no. 1, pp. 185- 194.

[65] F. Da, and W. Song, “Fuzzy neural networks for direct adaptive control,” *IEEE Transactions on Industrial Electronics,* June 2003, Vol. 50, no. 3, pp. 507- 513.

[66] A. J. Van der Schaft, “L_2-gain analysis of nonlinear systems and nonlinear state feedback H_∞ control,” *IEEE Trans.Automatic control*, 1992, Vol 37, pp. 770-784.

[67] D. C. Jiang, and Z. P. Jiang, "H_∞ almost disturbance decoupling with stability for uncertain nonlinear systems," *Proceedings of the fourth European Control Conference,* Brussels, Belgum, 1997.

[68] G. Zhai, K. Yasuda, and M. Ikeda, "Decentralized H_∞ control of large-scale systems via output feedback," *Proceedings of the 32nd IEEE Conference on Decision and Control,* San Antonio, Texas, 1993, pp. 1652-1658.

[69] Y. Guo, D. J. Hill and Y. Wang, "Nonlinear decentralized control of large-scale power systems," *Automatica,* 2000, Vol. 36, No. 9, pp. 1275-1289.

[70] W. J. Wang, and Y. H. Chen, "Decentralized robust control design with insufficient number of controllers," *International Journal of Control,* 1996, Vol. 65, pp. 1015-1030.

[71] S. L. Xie, L. H. Xie, and W. Lin, "Global H_∞ control for a class of interconnected nonlinear systems," *Preprints of the 14th IFAC world congress,* Beijing, China, 1999, pp. 73-78.

[72] S. J. Khorrami, "Decentralized adaptive control of a class of large-scale interconnected nonlinear systems," *IEEE Transactions of Automatic Control,* 1997, Vol. 42, No. 2, pp. 136-151.

[73] S. L. Xie,, and L. H. Xie, "Decentralized global robust stabilization of a class of large-scale interconnected minimum-phase nonlinear systems," *Proceedings of the 37th IEEE Conference on Decision and Control,* 1998, pp. 1482-1487.

[74] X. Liu, and G. Huang, "Global decentralized robust stabilization for interconnected uncertain nonlinear systems with multiple inputs," *Automatica,* 2001, Vol. 37, pp. 1435 -1442.

[75] Y. S. Liu and X. Y. Li, "Decentralized robust adaptive control of nonlinear systems with unmodeled dynamics," *IEEE Transactions on Automatic Control,* May 2002, Vol. 47, No. 5, pp. 848-856.

[76] Z. H. Guana, G. Chen, X. H. Yu, and Y. Qian, "Robust decentralized stabilization for a class of large-scale time-delay uncertain impulsive dynamical systems," *Automatica,* 2002, Vol. 38, pp. 2075-2084.

[77] Y. Zhang, C. Wen, and Y. C. Soh, "Robust decentralized adaptive stabilization of interconnected systems with guaranteed transient performance," *Automatica,* 2000, Vol. 36, pp. 907-915.

[78] S. S. Stankovic, X. B. Chen, M. R. Matauek, and D. D. Iljak, "Stochastic inclusion principle applied to decentralized automatic generation control," *International Journal of Control,* 1999, Vol. 72, pp. 276-288.

[79] A. Yousuff, "Application of inclusion principle to mechanical systems," *Proceedings of ACC*, 1988, Atlanta, Georgia, pp. 1516-1520.

[80] X. B. Chen, and S. Stankovic, "Decomposition and decentralized control of systems with multi-overlapping structure," *Automatica,* 2005, Vol. 41, pp. 1765-1772.

[81] W. Wolfermann and D. Schroeder, "New decentralized control in processing machines with continuous moving webs," *Proceedings of the Third International Conference on Web Handling,* Stillwater, Oklahoma, 1995, pp. 96-115.

[82] K. H. Shin, K. N. Reid and S. O. Kwon, "Non-interacting tension control in a multi-span web transport system," *Proceedings of the Third International Conference on Web Handling,* Stillwater, Oklahoma, 1995, pp. 312-325.

[83] T. Sakamoto, and Y. Izumihara, "Decentralized control strategies for web tension control system," *Proc. IEEE International Symposium on Industrial Electronics,* 1997, pp. 1086-1089.

[84] T. Sakamoto, "Decentralized controller design of web tension control system in terms of interactions," *Proc. IEEE International Symposium on Industrial Electronics,* 1999, pp. 1466-1471.

[85] T. Sakamato and Y. Izumihnra, "Decentralized control strategies for web tension control system", *Proc. IEEE International Symposium on Industrial Electronics,* 1997, pp. 1086-1089.

[86] P. R. Pagilla, "Robust decentralized control of large-scale interconnected systems: general interconnections," *Proceedings of ACC,* June 1999, San Diego, pp. 4527-4531.

[87] A. Benlatreche, D. Knittel, and E. Ostertag, "Robust decentralized control strategies for large-scale web handling systems," *Proc. of IFAC Symposium on Large-Scale Systems,* Osaka, Japan, 2004.

[88] S. Stankovic, M. Stanojevic, and D. Siljak, "Decentralized overlapping control of a platoon of vehicles," *IEEE Trans. Contr. Syst. Technol.,* Sept. 2000, Vol. 8, pp. 816-831.

[89] M. Ikeda, and D. D. Siljak, "Overlapping decentralized control with input, state, and output inclusion," *Control Theory and Advanced Technology,* June 1986, Vol. 2, No. 2, pp. 155-172.

[90] T. Sakamoto, "PI Control of web tension control system based on overlapping decomposition," *Proc. IEEE Nordic Workshop on Power and Industrial Electronics,* 1998, pp. 158-163.

[91] T. Saknmota and S.Tannka, “Overlapping decentralized controller design for web tension control system,” *Trans IEE of Japan,* Vol. 18, No.11, Nov. 1998, pp. 1272-1278.

[92] F. Claveau, P. Chevrel, M. Yagourbi, and D. Kittel, “Decentralized control for winding system: which incidence on reach performance,” *Proc. of the IEEE Mediterranean Conferences,* 2003, pp. 1021-1026.

[93] J. Han, “Nonlinear design methods for control systems,” *Proc. of the 14th IFAC World Congress*, 1999.

[94] A. Radke, and Z. Gao, “A Survey of state and disturbance observers for practitioners,” *Proc. Of the American Control Conference, ACC/IEEE*, Minneapolis, Minnesota, June 14-16, 2006.

[95] C. Johnson, “Accommodation of External Disturbances in Linear Regulator and Servomechanism Problems,” *IEEE Trans. Autonm. Control,* Vol. 16, No. 6, pp. 635-644, 1971.

[96] E. Schrijver and J. V. Dijk, “Disturbance Observers for Rigid Mechanical Systems: Equivalence, Stability, and Design,” *Journal of Dynamic Systems, Measurement, and Control,* December 2002, Vol. 124, pp. 539-548.

[97] K. Yang, “On the Tracking Performance Improvement of Optical Disk Drive Servo Systems Using Error-Based Disturbance Observer,” *IEEE Transactions on Industrial Electronics,* Feb. 2005, Vol. 52, No. 1, pp. 270- 279.

[98] S. Kwon, W. K. Chung and Y. Youm, “A novel robust tracking controller based on hierarchical perturbation compensation,” *Proceedings of the American Control Conference,* 2001, Vol. 1, pp. 541-546.

[99] S. Kwon, W.K. Chung, “A Discrete-Time Design and Analysis of Perturbation Observer for Motion Control Applications,” *IEEE Tran. on Control Systems Technology,* 2003, Vol. 11, No. 3, pp. 399-407.

[100] J. Cheong, Y. Youm, and W.K. Chung, “Joint tracking controller for multi-link flexible robot using disturbance observer and parameter adaptation scheme,” *Journal of Robotic Systems*, 2002, Vol. 19, No. 8, pp. 401-417.

[101] T. Umeno, and Y. Hori, “Robust speed control of DC servo motors using modern two degrees-of-freedom controller design,” *IEEE Trans. Ind. Election.*, 1991, Vol. 38, pp. 363-368.

[102] C. B. Choi, C. H. Lim, “Model-based disturbance attenuation for CNC machining centers in cutting process,” *IEEE/ASME Trans. on Mechatronics*, 1999, Vol. 4, No. 2, pp. 157-168.

[103] S. Kwon,and W. K. Chung, “A discrete-time design and analysis of perturbation observer for motion control applications,” *IEEE Tran. on Control Systems Technology,* 2003, Vol. 11, No. 3, pp. 399-407.

[104] A. Tornambe, and P. Valigi, “A decentralized controller for the robust stabilization of a class of MIMO dynamical systems,” *ASME, Journal of Dynamic Systems, Measurement, and Control,* June 1994, Vol. 116, No. 2, pp. 293-304.

[105] Y. Guan, and M. Saif, “A novel approach to the design of unknown input observer,” *Automatic Control, IEEE Trans*, May 1991, Vol. 36, No. 5, pp. 632-635.

[106] G. Tian, *Reduced-order extended state observer and frequency response analysis,* Masters Thesis, Cleveland State University, 2007.

[107] C. E. Garcia, and M. Morari, "Internal model control: A unifying review and some new results," *Industrial Engineering of Chemical Proceedings Design and Development,* 1982, Vol. 21, No. 2, pp. 308-323.

[108] K. Y. Toumi and O. Ito, "A time delay controller for systems with unknown dynamics," *Trans. ASME, J. Dyn. Syst. Meas. Control*, Mar. 1990, Vol. 112, No. 1, pp. 133-142.

[109] K. Y. Toumi and S. T. Wu, "Input/output linearization using time delay control," *Trans. ASME, J. Dyn. Syst. Meas. Control*, Mar. 1992, Vol. 114, No. 1, pp. 10-19.

[110] Q. Zheng, L.Q. Gao, and Z. Gao, "On estimation of plant dynamics and disturbance from input-output data in real time, " *IEEE Multi-conference on Systems and Control*, Singapore, Oct. 1-3, 2007.

[111] Y. Huang, and J. Han, "Disturbance rejection and tracking design via the SSR approach for second order uncertain systems," *Journal of Systems Science and Mathematical Sciences,* 1999, Vol. 12(Suppl), pp. 96-103.

[112] C. J. Kempf and S. Kobayashi, "Disturbance observer and feed-forward design for a high-speed direct-drive positioning table," *IEEE Trans. Control Systems Tech.*, September 1999, Vol. 7, No. 5, pp. 513-526.

[113] R. Bickel and M. Tomizuka, "Passivity-based versus disturbance observer based robot control: equivalence and stability," *Journal of Dynamic Systems, Measurement, and Control*, March 1999, Vol. 121, pp. 41-47.

[114] Y. Choi, K. Yang, W.K. Chung, H.R. Kim, and I.H. Suh, "On the robustness and performance of disturbance observers for second-order systems," *IEEE Trans. Automatic Control*, February 2003, Vol. 48, No. 2, pp. 315-320.

[115] B. K. Kim, H. T. Choi, W. K. Chung, and I. H. Suh, "Analysis and design of robust motion controllers in the unified framework," *Journal of Dynamic Systems, Measurement, and Control*, June 2002, Vol. 124, pp. 313-321.

[116] R. Miklosovic and Z. Gao, "A robust two-degree-of-freedom control design technique and its practical application," *Proc. of the IEEE Industrial Application Society World Conference,* Oct. 3-7, 2004.

[117] F. Nardi, N. Hovakimyan, and A. Calise, "Decentralized control of Large-Scale systems using Single Hidden Layer Neural Networks," *Proceedings of the 2001 American Control Conference,* 2001, Vol. 4, No. 4, pp. 3122-3127.

[118] P. Kokotovic, H. K. Khalil, and J. O. Reilly, *Singular perturbation methods in control analysis and design,* SIAMM, 1986.

[119] H. K. Khalil, *Nonlinear systems (Third Edition),* Prentice Hall, NJ, 2002.

[120] H. Noura, and T. Bastogne, "Tension optimal control of a multivariable winding process," *Proceedings of the American Control Conference,* Albuquerque, New Mexico, June 1997, pp. 2499-2503.

[121] Y. Hou, Z. Gao, F. Jiang, and B. T. Boulter, "Active disturbance rejection control for web tension regulation," *Proc. IEEE Conference on Decision and Control,* Vol. 5, Dec. 2001, pp. 4974 - 4979.

[122] P. D. Mathur, and W. C. Messner, "Controller development for a prototype high-speed low-tension tape transport," *IEEE Transactions on Control Systems Technology,* 2006, Vol. 4, pp. 534-542.

[123] E. J. Davison, "Multivariable tuning regulators: The feed-forward and robust control of a general servomechanism problem," *IEEE Trans. Automat. Contr.,* Jan. 1976, Vol. 21, pp. 35-47.

[124] D. Schroder and W. Hoger, “Adaptive state space control for axial winders,” *IFAC 10th Triennial World Congress,* 1987, pp. 115-120.

[125] P. R. Pagilla and N. Siraskar, “Robust decentralized controllers for large-scale interconnected systems: applications to web handling systems,” *Current Trends in Nonlinear Systems and Control,* December. 2005, Springer-Verlag, pp. 387-406.

[126] P. R. Pagilla, N. Siraskar and R. V. Dwivedula, “Decentralized control of web processing lines,” *IEEE Conf. on Control Applications,* 2005, Toronto, Canada, pp. 940-945.

[127] J. Han, “A class of extended state observers for uncertain systems,” *Control and Decision*, 1995, Vol. 10, No. 1, pp. 85-88(In Chinese).

[128] J. Han, “Nonlinear state error feedback control,” *Control and Decision*, 1995, Vol. 10, No. 3, pp. 221-225 (In Chinese).

[129] J. Han, “Auto-disturbance rejection control and its applications,” *Control and Decision*, 1998. Vol. 13, No. 1, pp. 19-23 (In Chinese).

[130] Z. Gao, “Active disturbance rejection control: a paradigm shift in feedback control system design,” *Proc. of the 2006 American Control Conference*, 2006, pp. 2399-2405.

[131] B. C. Kuo, *Automatic Control Systems*, Prentice Hall, 7th ed. 1995.

[132] Z. Gao, S. Hu, and F. Jiang, “A novel motion control design approach based on active disturbance rejection,” *Proceedings of IEEE Conference on Decision and Control*, Vol. 5, Dec. 2001, pp. 4877 - 4882.

[133] F. Goforth, "On motion control design and tuning techniques," *Proc. of the 2004 American Control Conference,* June 2004, Boston, Vol. 1, pp. 716 - 721.

[134] W. Zhou, and Z. Gao, "An active disturbance rejection approach to tension and velocity regulations in web processing lines," *IEEE Multi-conference on Systems and Control,* Singapore, October 2007.

[135] R. Miklosovic and Z. Gao, "A dynamic decoupling method for controlling high performance turbofan engines," *Proc. of the 16th IFAC World Congress,* July 2005.

[136] Q. Zheng, L. Dong, and Z. Gao, "Control and time-varying rotation rate estimation of vibrational MEMS gyroscopes," *IEEE Multi-conference on Systems and Control,* Singapore, October 2007.

[137] Z. Zhou, Q. Zheng, and Z. Gao, "Active disturbance rejection control of chemical processes," *IEEE Multi-conference on Systems and Control,* Singapore, October 2007.

[138] Y. X. Su, B. Y. Duan, C.H. Zheng, Y. F. Zhang, G. D. Chen, and J. W. Mi, "Disturbance-rejection high-precision motion control of a Stewart platform," *IEEE Transactions on Control System Technology,* May 2004, Vol. 12, No. 3, pp. 364 - 374.

[139] Z. Gao "Scaling and parameterization based controller tuning," *Proc. of the 2003 American Control Conference,* Vol. 6, June 2003, pp. 4989 - 4996.

[140] Z. Gao, Y. Huang, and J. Han, "An alternative paradigm for control system design," *Proc. of IEEE conference on Decision and Control*, Vol. 5, Dec. 2001, pp. 4578 - 4585.

[141] I. S. Choi, J. A. Rossiter, P. J. Fleming, "A MPC design for the looper and tension control in a hot strip mill," *UK Control,* Sept. 2004, University of Bath, pp. 99-105.

[142] B. T. Boulter and Z. Gao,"A novel approach for on-line self-tuning web tension regulation", *Proceedings of IEEE Conference on Control Applications,* 1995, pp. 91-98.

[143] E. J. Davison and B. M. Scherzinger, "Perfect control of the robust servomechanism problem," *IEEE Trans. Autom. Control,* Aug. 1987, Vol. 32, No. 8, pp. 689-702.

[144] P. R. Pagilla, E. O. King, L.H. Dreinhoefer, and S.S. Garimella, "Robust observer-based control of an aluminum strip processing line," *IEEE Transactions on Industry Applications,* 2000, Vol. 36, pp. 865-870.

[145] S. H. Song and S. K. Sul, "A new tension controller for continuous strip processing line," *IEEE Ind. Applicat. Conf.,* 1998, Vol. 3, pp. 2225-2230.

[146] K. C. Lin, M. C. Tsai, and Z. W. Wang, "Observer-based web tension control with inertia compensation," *Int. Conf. Metratronic Technology,* Taiwan, R.O.C., 1998, pp. 355-360.

[147] K. C. Lin, "Observer-based tension feedback control with friction and inertia compensation," *IEEE Trans. on Control Systems Technology,* Jan. 2003, Vol. 11, No. 1, pp. 109-118.

[148] I. Hoshino, Y. Okamura, and H. Kimura, "Observer-based multivariable tension control of aluminum hot rolling mills," *Proc. 35th Conf. Decision Control,* Kobe, Japan, December 1996, pp. 1217-1222.

[149] W. Schlosser, and W. Hoger, "Adaptive state space control for axial winder," *Proceedings of the IFAC 10th Triennial World Congress,* Munich, Germany, 1987, pp. 115-120.

[150] W. Wolfermann, and D. Schroder, "Application of decoupling and state space control in proceeding machines with continuous moving webs," *Proceedings of the IFAC 10th Triennial World Congress,* Munich, Germany, 1987, pp. 103-108

[151] W. Wolfermann, "Sensorless tension control of webs," *Proceedings of the Fourth International Conference on Web Handling,* Oklahoma, 1997.

[152] W. Wolfermann and D. Schroeder, "New decentralized control in processing machines with continuous moving webs," *Proceedings of the Second International Conference on Web Handling IWEB2,* Stillwater, Oklahoma, 1993.

[153] T. Patri,W. Wolfermann and D. Schroder, "The usage of decentralized observer in continuous moving webs," *IEEE Control Systems Magazine,* Feb. 2001, pp. 147-154.

[154] G. Ellis, and D. Motion, *Observers in control systems: a practical guide*, Academic Press, 2002.

[155] K. J. Astrom and B. Wittenmark, *Adaptive control,* Reading, MA: Addison-Wesley, 1989.

[156] K. Zhou, and J. C. Doyle, *Essentials of robust control*, NJ: Prentice-Hall, 1997.

[157] P. A. Ioannou and J. Sun, *Robust adaptive control*, Upper Saddle River, NJ: Prentice-Hall, 1996.